ENERGY LABORATORY

MASSACHUSETTS INSTITUTE OF TECHNOLOGY

THE USE OF BURNABLE POISON TO IMPROVE
URANIUM UTILIZATION IN PWRs

W. T. Loh
M. J. Driscoll
D. D. Lanning

THE USE OF BURNABLE POISON TO IMPROVE

URANIUM UTILIZATION IN PWRs

by

W. T. Loh
M. J. Driscoll
D. D. Lanning

Department of Nuclear Engineering

and

Energy Laboratory

Massachusetts Institute of Technology

Cambridge, Massachusetts 02129

NOTICE

Printed in the United States of America

Available from:

Distribution

R. Crowther
Project Manager
General Electric Company
175 Curtner Company
San Jose, California 95125

Dr. Peter M. Lang, Chief
LWR Branch
Division of Nuclear Power Development
US Dept. of Energy, Mail Stop B-107
Washington, D.C. 20545 (5 copies)

N. L. Shapiro
Manager, Advanced Design Projects
Combustion Engineering, Inc.
1000 Prospect Hill Road
Windsor, CT 06-95

W. L. Orr
Manager of Product Development Support
Nuclear Fuel Division
Westinghouse Electric Corp.
P.O. Box 355
Pittsburgh, PA 15230

Dr. Richard B. Stout
Nuclear Fuels Engineering Dept.
Exxon Nuclear
2101 Horn Rapids Road
Richland, W 99352

V. Uotinen
Project Manager
The Babcock & Wilcox Co.
P.O. Box 1260
Lynchburg, VA 24505

ABSTRACT

A methodology based on the linear reactivity model of core behavior has been developed and employed to evaluate fuel management tactics for improving uranium utilization in Pressurized Water Reactors in a once-through fuel cycle mode on a consistent basis. A major focus has been on the benefit of using burnable poison in conjunction with low-leakage fuel management schemes. Key features in the methodology, such as power weighting of batch reactivity values and correlation of neutron leakage effects with peripheral assembly power, were verified against results generated using detailed state-of-the-art computer analyses. A relation between batch power fraction and batch reactivity was derived from a $1\frac{1}{2}$-group diffusion theory model, and similarly validated. These prescriptions have been used in two ways: to develop analytical models which allow quick scoping calculations; and, programmed into a code, to facilitate more rigorous applications.

The methodology has been applied to evaluate fuel management schemes of contemporary interest, such as the use of burnable poison to shape the power history profile, the use of low-leakage fuel loading patterns, and extended cycle length/burnup, and combinations of these individual schemes.

It was found that shaping of the power history profile in a low-leakage assembly pattern by means of burnable poison, even after accounting for the anticipated residual poison reactivity penalty, has the potential of increasing PWR discharge burnup, and hence uranium utilization by roughly 1%. The overall improvement in uranium utilization for a low-leakage loading over that for the current out-in/scatter scheme, was about 3.6% for current cycle lengths (3-batch, discharge burnup $\sim$ 30,000 MWD/MT), and approximately 11.1% for extended cycle operation (3-batch, discharge burnup $\sim$ 50,000 MWD/MT).

ACKNOWLEDGEMENTS

TABLE OF CONTENTS

TABLE OF CONTENTS (continued)

TABLE OF CONTENTS (continued-3)

TABLE OF CONTENTS (continued-4)

LIST OF FIGURES

LIST OF FIGURES (continued)

LIST OF FIGURES (continued-3)

LIST OF FIGURES (continued-4)

LIST OF TABLES

LIST OF TABLES (continued)

LIST OF TABLES (continued-3)

CHAPTER 1

INTRODUCTION

1.1 FOREWORD

There has been considerable interest of late in the
achievement of higher fuel burnup in light water reactors due
to a convergence of motivating factors: a desire to improve
uranium utilization, particularly in view of the slower than
anticipated implementation of fuel reprocessing and the de-
layed development of breeder reactors (due in part to a concern
in some quarters over the attendent commerce in weapons-usable
materials); and the interest by utilities in extending the
length of the burnup cycle to increase plant capacity factor,
reduce replacement energy costs, alleviate the impending short-
age of spent fuel storage space, and decrease staff effort on
reload licensing activities. In response to these concerns
the U.S. Department of Energy (DOE) and the nuclear industry
have collaborated to evaluate and prove-out modifications in
LWR fuel design and fuel management strategy to permit the
attainment of high burnup. MIT has participated in this program,
sponsored by the DOE and its precursor, the Energy Research and
Development Administration (ERDA), initially as part of the
effort in support of the NASAP (Nonproliferation Alternative
Systems Assessment Program) and INFCE (International Nuclear
Fuel Cycle Evaluation) assessments, but most recently as part

of the DOE's LWR Technology Program for Improved Uranium Utilization.

Recent MIT work, including that reported here, has been concerned with the self-consistent evaluation of ways to facilitate the realization of high burnup and high neutron economy. A major focus of the present effort is on development of an optimum strategy for the use of a generalized burnable poison to alleviate the power peaking which typically characterizes high burnup assembly designs and core arrangements.

The present work is an extension of prior efforts at MIT [G-1, F-1, C-1, K-1, S-2], and, as with other recent efforts here and elsewhere, is limited to readily backfittable innovations applicable to the once-through mode of fueling. While cost of energy is the ultimate objective function for optimization, the subsidiary goal of improving natural uranium utilization will often suffice, since yellowcake accounts for on the order of half of the levelized lifetime fuel cycle cost projected for LWR's scheduled for startup in the mid-1980's [G-2].

The applications examined in this report are limited to PWRs since these reactors have captured two-thirds of the U.S. and one-half of the world markets for large central station nuclear units. Moreover the closely-related BWR accounts for the remaining one-third of the U.S. roster, and one-quarter of the world's. In addition the PWR has become the reactor of choice for many countries which originally selected other

types, such as the USSR, and very recently the United Kingdom, and for other nations just embarking on a nuclear power program, such as mainland China.

1.2 BACKGROUND AND PREVIOUS WORK

Over the past twenty years the discharge burnup of LWR fuel has risen steadily at a rate of nearly 1000 MWD/MT per year -- due in part to the inherently lower burnup of startup batches, but also to a growing emphasis on the attainment of higher steady state burnups [T-1]. The average of current performance specifications is approximately 31,000 MWD/MT. Steady state burnup can be related directly to uranium utilization efficiency. This parameter will be defined here as the total amount of electric energy produced per unit of natural uranium used [D-2]:

$$U \left(\frac{kWh}{lb\ U_3O_8} \right) = 9.231 \frac{(x_F - x_W)\, \eta B_{dis}}{(x_P - x_W)} \tag{1.1}$$

where η is the net thermodynamic efficiency of the plant, MWe/MWth, which averages ~ 0.32 for LWR's

B_{dis} is the discharge burnup (MWD/MT)

x_F is natural uranium feed enrichment, wt %

x_P is the reload batch enrichment, wt %

and x_W is the enrichment plant tails assay enrichment which typically is ~ 0.2 wt %.

Thus the goal of higher burnup is a long standing one and great progress has been made, even if not widely heralded. The current focus on this goal should help insure continuance

of this historical trend.

Numerous studies completed over the last few years have shown that uranium utilization can be improved by a variety of strategies: extending burnup, subdividing the core into a larger number of staggered-reload batches, adopting low-leakage fuel reload arrangements, incorporating axial blankets, reoptimizing the lattice water-to-fuel ratio, introducing mechanical spectral shift, pin pulling and bundle reconstitution using smaller fuel assemblies, and by practicing routine coastdown. Table 1.1 summarizes the uranium conservation tactics envisioned for PWRs on a once-through fuel cycle and the potential ore savings estimated for each strategy. It must be pointed out that the total percentage savings in U_3O_8 are not directly additive, but cumulative amounts in the range of 15% (near-term) to 40% (long term) are projected.

The most effective near-term means of improving uranium utilization are to increase the discharge burnup, incorporate a larger number of in-core fuel batches and employ a modified (so-called "low-leakage") fuel management scheme, such as in-out-in, which reduces core neutron leakage. A substantial reduction, in the range of 10 to 20%, in yellowcake consumption can be achieved, if the discharge exposure of the fuel is increased to about 50,000 MWD/MT and the number of staggered in-core batches to five, as compared to current PWR designs and fuel management strategy, which use a three-batch out-in fuel management scheme and typically have discharge burnups of about 30,000 MWD/MT. Higher discharge burnup permits an

TABLE 1.1   POTENTIAL IMPROVEMENTS IN URANIUM UTILIZATION
FOR PWRs ON A ONCE-THROUGH FUEL CYCLE

OPTION	$\frac{\text{NAT}_U}{\text{SAVINGS}}$ (%)	REFERENCES	COMMENTS
1. Extended Burnup and Increased Number of Batches	∿15	F-1,S-3, M-1,M-2	5-batch core with discharge burnup of ∿55,000 MWD/MT; risk of premature fuel failure must be considered
2. Low-Leakage Fuel Management	∿ 3	M-1,S-3, S-4	Must cope with power peaking problem; if burnable poison is used, residual poison may negate savings
3. Axial Blankets	∿ 2	K-1,M-1, S-3	Aggravates axial power peaking; may require poison or enrichment zoning
4. Re-Optimizing Lattice Fuel-to-Moderator Ratio	2-3	R-1	For high burnup cores; depends on specifics of current core design
5.(a) Continuous Mechanical Spectral Shift	10-15	S-2	May not be practical from an engineering standpoint
5.(b) D_2O Spectral Shift	10-15	C-3,G-2	D_2O is expensive
6. Mid-Cycle Pin Pulling and Bundle Reconstruction	∿10	S-2,R-1	Potential thermal-hydraulic problems; reduces plant capacity factor
7. Routine Preplanned Coastdown	∿ 7	F-1,M-1, S-3,M-2, D-3	If coastdown to economic breakeven is considered instead of to the optimum, the uranium savings can be approximately doubled (as is the duration of coastdown)

annual refueling schedule to be maintained even with a lower fuel reload fraction. This will reduce the number of spent fuel assemblies discharged at the end of a cycle as well as over the lifetime of the plant and, therefore, decrease the requirement for shipping, handling, storage and disposal of spent fuel. There are other benefits offered by extended burnup. Separative work requirements are reduced and since there is less net plutonium production per unit of energy generated and a larger buildup of long-lived fission products and higher plutonium isotopes in the discharged fuel, the incentive for diversion will also be reduced.

The major disadvantages associated with this option are the increased potential for premature fuel failure at higher burnup, and the almost inevitable increase in power peaking. The main concerns relating to fuel failure at higher exposure in current LWR fuel are pellet-clad interaction, fuel-rod internal pressure due to fission gas release, changes in the structure and dimensions of the fuel and both internal and external cladding corrosion. Currently, extended burnup fuel-rod performance is being evaluated in several DOE-sponsored irradiation programs [L-1]. To date these projects have achieved assembly average burnups exceeding 40,000 MWD/MT, and burns to about 55,000 MWD/MT are currently being conducted [C-2]. In another program, fuel assemblies capable of achieving batch burnups in excess of 50,000 MWD/MT have been fabricated, and are in the process of being tested [A-1]. Data from these programs can provide the basis for further

improvements in fuel design and the required assurance to both vendors and utilities that high burnup fuel is ready for routine use.

As already noted, one disadvantage associated with the extended burnup option lies in the higher power peaking encountered (by about 10%) compared to that associated with current designs and fuel managements schemes [C-2]. This problem is attributable to the higher enrichment (hence reactivity) of the reload fuel. The large difference between the reactivity of the fresh fuel and fuel that has already received several cycles of exposure leads to correspondingly large differences in assembly power between the fresh and exposed batches, as well as large local flux and power gradients. This motivates the use of burnable poisons to suppress the local power, either by the insertion of discrete rods of lumped burnable poisons, or by admixture of burnable poison with the uranium dioxide fuel itself. Burnable poisons are also required to keep soluble boron concentrations at the beginning of cycle (BOC) sufficiently low to obtain an acceptable (slightly negative) moderator temperature coefficient of reactivity.

Higher discharge burnup also facilitates the implementation of a longer cycle (18 instead of 12 months) while keeping the number of feed assemblies the same. The basic incentive for this tactic is that one refueling outage is eliminated every three years, which permits a higher plant capacity factor, and thus significant savings in replacement power costs.

More efficient use of utility system outage maintenance teams
can also be anticipated (including for example, lower life-
time radiation exposure and more tolerant scheduling con-
straints), and the increase in time between the reload licen-
sing submittals will also result in potential savings in
analysis and licensing costs [B-1]. This fuel management
scheme employs reload fuel enrichments ranging from 3.6 w/o
to 4.2 w/o to attain discharge burnups ranging from 36,000
MWD/MT to 45,500 MWD/MT [B-2]. Again burnable poison will be
required to limit the concentration of soluble boron at BOC
so that the moderator temperature coefficient of reactivity
will be negative.

In the low-leakage fuel management scheme, fresh fuel
assemblies are dispersed among older fuel assemblies in the
core interior while once or twice burned low-reactivity fuel
is placed on the core periphery in order to reduce radial
neutron leakage from the core, in contrast to current PWR
out-in/scatter fuel management strategy in which fresh fuel
is loaded on the core periphery for the purpose of flattening
the radial power profile. Ideally, by implementing this fuel
management option, a further reduction in uranium requirements
can be realized ($\sim$ 3%), because of the lower radial neutron
leakage and because of the higher importance weighting of the
high-reactivity fuel present in the core interior at the end
of the cycle. However, when fresh fuel is placed in the core
interior, severe power peaking problems can occur. This can
be overcome by incorporating burnable poison into the fresh

fuel assemblies to limit the power density in these assemblies.

Leakage of neutrons from the core can be further reduced by employing axial blankets, comprised of natural or depleted uranium, at the top and bottom of the active core. This has the potential of improving uranium utilization since neutrons which would otherwise leak into the reflector and be lost through parasitic absorption, are captured instead in the fertile blanket material, producing additional fissile material. Studies [K-1, M-1, S-3] have shown that ore savings of about 3% can be achieved, but at the expense of a slightly higher axial power peaking factor. This problem can be solved using axial enrichment zoning and/or zoned axial poison.

All current LWRs have core lattice designs that were optimized under the assumption that spent fuel reprocessing and the recycling of recovered uranium and plutonium would be the normal mode of operation, under which circumstance high burnup is not as attractive. As a result, the lattices in use today may be slightly undermoderated (low water-to-fuel ratio). Hence a reactivity increment can be realized when the lattice is made a little wetter (for example, through the use of annular fuel or by decreasing the fuel rod diameter), thereby reducing the fissile inventory required to maintain criticality at the end of cycle, which translates into lower reload enrichment and yellowcake consumption. A wetter lattice, however, tends to have a less negative moderator temperature coefficient, particularly at BOC, and again one is led to use burnable poison in place of soluble poison.

There are other concepts which have the potential of improving uranium utilization: spectral shift through variation of coolant voids or inlet temperature, mechanical spectral shift (variation in lattice pitch), D_2O spectral shift, pin pulling and bundle reconstitution, using smaller fuel assemblies and routine pre-planned coastdown at the end of cycle. Although some of these options cannot be readily back-fitted into current PWR designs, end-of-cycle coastdown or stretchout is already being practiced by a number of utilities [Q-1]. In this technique, insertion of positive reactivity to keep the reactor critical after the normal full power end of life has been reached is accomplished by reducing the coolant (and hence fuel) temperature to take advantage of the negative temperature (doppler) coefficient and/or by reducing the reactor power level (thus reducing both the xenon poisoning and fuel temperature), thereby extending the cycle length. In normal reactor operation, optional end-of-cycle coastdown has been used to obtain cycle flexibility; for example, should other units experience forced outages, refueling can be delayed through coastdown. Routine pre-planned coastdown on the other hand has the objective of lowering fuel cycle cost and minimizing uranium usage. This can be realized by reducing the feed enrichment enough to retain the original cycle length. However, either the plant capacity factor or its thermodynamic efficiency are below average in the latter stages of coastdown and the duration of the coastdown must thus be optimized. Utilities planning to adopt this technique routinely must

therefore weigh the above factors (U_3O_8 savings versus re-placement power cost) to suit their needs.

The benefits, and indeed the perceived necessity, of using burnable poisons in conjunction with the different methods of improving uranium utilization in PWRs is clearly indicated by the preceding discussion, where burnable poisons were employed for power peaking control, criticality control and moderator temperature coefficient adjustment. However, it will be shown in the present work that there is still another dimension to the use of burnable poison: obtaining higher discharge burnup, and therefore better uranium utilization, through optimum power-shaping (i.e., creation of an improved power history trajectory). Important qualifications to this new aspect such as the effect of different reload patterns and the amount and effect of residual poison are addressed in chapters four and five of this report.

1.3 RESEARCH OBJECTIVES

In the many options available to improve uranium utilization and in particular, those which are retro-fittable to present generation PWRs, it is necessary to incorporate burnable poisons into the fuel assemblies to control power distribution (hence, holding power peaking below prescribed limits) and to keep the concentration of soluble poison at BOC sufficiently low to obtain an acceptable moderator temperature coefficient of reactivity. In this context, the identification of the objective of the present work becomes obvious, that is,

to evaluate the use of burnable poisons as a means to facili-
tate implementation of the improved design/management strate-
gies discussed in the preceding section.

An evaluation of the benefits of burnable poisons can
obviously be done on a case-by-case basis with the use of
full-fledged state-of-the-art computer capabilities. The
amount of detail involved makes this approach economically
unappealing -- at least in preliminary scoping analyses. It
also discourages generalization and the identification of
global strategies. Moreover, it may prove to be difficult to
make comparisons on an "all-else-being-equal" basis since this
approach allows too much flexibility -- abetting the introduc-
tion of other changes which obscure the effect under study.
On the other hand, too simplified a method may overlook small,
but worthwhile improvements (or deleterious effects). To
achieve the assigned goal of evaluating the use of burnable
poisons on a strategic level, a simple model which has a
sound theoretical basis will be developed. In a way, the
model is an extension as well as a refinement of screening
methods previously developed at MIT [S-2], which were found
to be capable of evaluating the effects of small changes in
core design and fuel management schemes on a consistent basis.
The present methodology, although evolved from the linear
reactivity model of core behavior, utilizes an improved ver-
sion which has a better theoretical basis, and one which is
more thoroughly benchmarked against results generated with
detailed state-of-the-art computer analyses.

Although many aspects of PWR core design and fuel manage-
ment are addressed in the present work, the most important
subtask was to determine the optimum (maximum discharge burn-
up) power history trajectory of a fuel batch obtainable using
burnable poison and to debit the compensatory penalty in dis-
charge burnup caused by residual poison. These results will
provide core designers with a clearer picture of the "best
attainable" poison performance against which specific designs
can be evaluated.

1.4 ORGANIZATION OF REPORT

The work presented in this report is organized as follows.
Chapter two provides an outline of the state-of-the-art com-
puter codes used in this research together with the reactor
system and lattice model employed in the calculations. A
short discussion on the selection of burnable poisons and the
characteristics of candidate poisons is also included in this
chapter.

Chapter three deals with the linear reactivity model
(LRM) of core behavior. Significant improvements in and addi-
tions to LRM methodology are presented. Key features of the
extended LRM methodology such as leakage, and power sharing
among fuel batches are discussed. A power split relation is
derived using "group-and-one-half" diffusion theory, to supp-
lant the purely empirical relations used by prior authors.
Application of the LRM to obtain analytical estimates of the
discharge burnup for a variety of reactivity-burnup histories

concludes the chapter.

In Chapter Four, the methodology is extended to compute discharge burnup numerically, using a computer code, DISBURN, developed for this purpose. Some important features of the code will be presented. The code will also be applied to evaluate various fuel management strategies, and the analytical results obtained in Chapter Three are compared and normalized to more precise numerically computed results.

Finally, the economic impact of using burnable poison with regard to the residual poison penalty and the radial power flattening effect of burnable poison are briefly discussed.

Chapter Five summarizes the present study: the development of the methodology and the results obtained therefrom. Recommendations for future work are also made.

Several Appendices are included containing data supporting the work reported in the main text. A listing of the code DISBURN together with a sample problem run are included here.

CHAPTER 2

METHODS AND MODELS

2.1 INTRODUCTION

In-core fuel management analysis relies heavily upon reactor physics calculations. The major objective of these neutronic calculations is the accurate prediction of pertinent core parameters such as reactivity, reaction rates (thus, power density) and isotopic compositions at all in-core locations and at all time. Equipped with this information, plant operators and reactor designers can make appropriate management decisions pertaining to the operation and design of the reactor plant. Although well developed and sophisticated computer codes are available to perform very detailed and thus very accurate neutronic analyses of the reactor core (using hundreds of energy groups, thousands of spatial mesh intervals and very small time increments), technical and economic constraints such as the size of today's computers and the cost associated with running long programs forbid exclusive reliance on such efforts. Fortunately, less comprehensive state-of-the-art computer programs and methodology can often provide acceptably accurate results for the purposes of reactor fuel management. Even further, simple models of the type developed in the present work can provide results which are useful on a global scale, at the sacrifice of local detail.

The computer programs employed in the present work were primarily the LEOPARD and PDQ-7 codes. They were used either individually or in combination to generate results against which the models developed and deployed in this research are tested. These codes were, and still are in widespread use [A-2, C-4, S-5], and they have been benchmarked against extensive experimental data. Moreover, previous workers at MIT: namely, Fujita [F-1], Correa [C-1] and Sefcik [S-2] have accumulated extensive experience with these same codes, and have shown that for applications similar to those of present concern, the codes are sufficiently accurate. A brief description of these well-documented codes will be presented in this chapter.

Recent interest in the use of burnable poisons to facilitate the implementation of improved uranium utilization tactics has accelerated the development of more powerful computational techniques, such as transport and collision probability methods. This progress is due in part to the cumulative increase in computer memory and speed realized over the past decade. Besides being able to handle highly shielded absorbers in lumped form or admixed with the fuel, codes employing transport and collision probability methods can also deal simultaneously with a number of adjacent cells within an assembly (for example, fueled cells, water holes, control rod channels, etc.). A representative example is Combustion Engineering's DIT program [J-1]. The Electric Power Research Institute (EPRI) has, under its Advanced Recycle Methodology

Program (ARMP), several computer codes of similar capabilities: EPRI-CELL, CPM and MICBURN [E-1]. In the present work we are interested in the generic behavior of burnable poisons, rather than the specific details which such codes provide. Hence we will only review typical results published by others to establish overall patterns of reactivity behavior in assemblies containing burnable poison.

2.2 COMPUTER CODES

In this section, a brief description of the computer codes used in the present work, LEOPARD and PDQ-7, will be given.

The LEOPARD code [B-3] calculates the spectrum and neutron multiplication factor, and generates few group (2 or 4) cross sections for a LWR unit fuel cell or a supercell (cell plus an extra region). The unit cell consists of fuel, gap, metallic cladding and moderator, and, in the case of a supercell, an extra region representing fuel assembly water holes, control rod sheaths, spacer grids and inter-assembly water gaps [see Fig. 2.1]. The code can also perform zero dimensional depletion calculations in which the neutron spectrum (and appropriate few group cross sections) are recomputed after each depletion time step. The microscopic cross section library for the version of LEOPARD used in this work (EPRI-LEOPARD) is derived from the ENDF/B-IV data set and only geometrical dimensions, temperatures, pressures, material compositions and the corresponding number densities, and burnup

Water Gap

Spacer Grids

Extra Region

Control
Rod
Sheath

Fuel

Clad

Moderator

Fuel Assembly

LEOPARD
Supercell

Moderator

Clad

Fuel
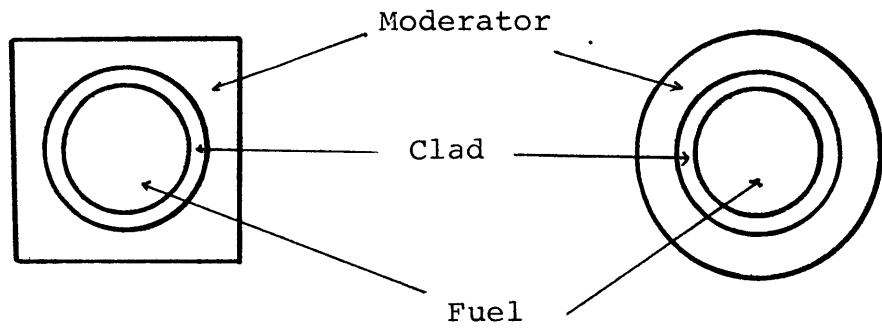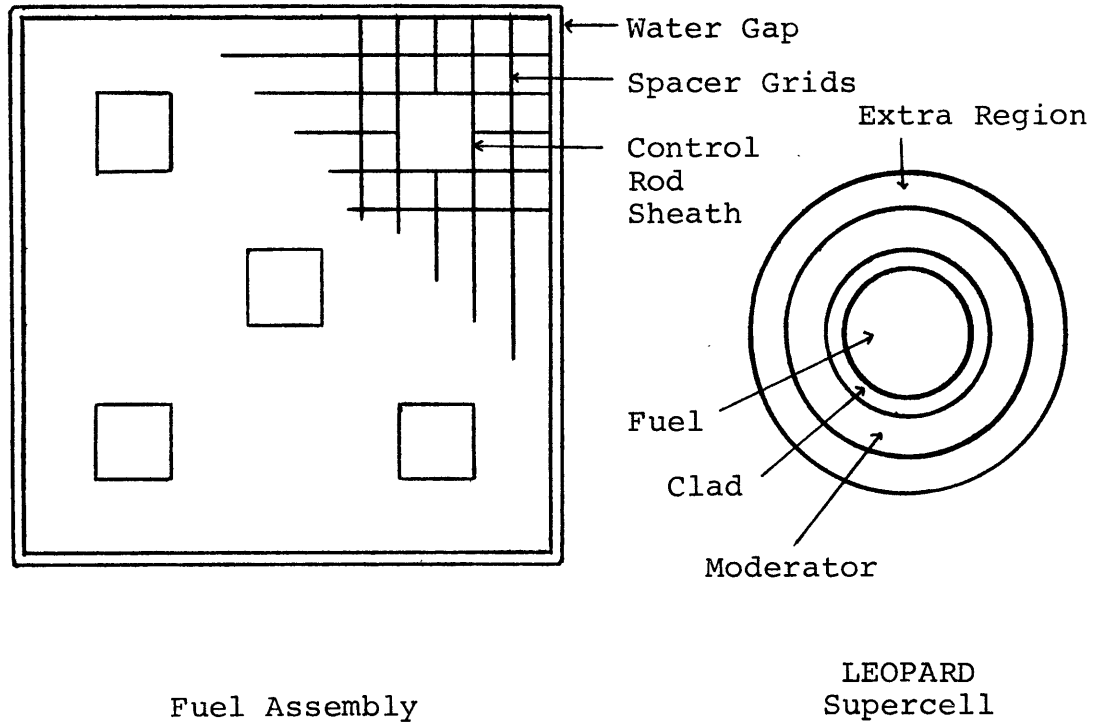
Fig. 2.1 LEOPARD Geometrical Representation

time-steps (for depletion calculations) are required as user
input by the code.

The LEOPARD code uses the MUFT [B-4] subprogram to cal-
culate the fast and empithermal region spectrum (in 54 groups)
while SOFOCATE [A-3] handles the thermal spectrum (with 172
energy groups) using the Wigner-Wilkin treatment. As both
MUFT and SOFOCATE execute homogeneous medium calculations,
the cell heterogeneity is corrected for through the use of
fast advantage factors, thermal disadvantage factors and an
iteratively adjusted resonance self-shielding factor. The
code also permits optional use of the Mixed Number Density
(MND) approach [B-5], which employs a boundary condition of
neutron activation continuity rather than flux continuity.

An option is provided in LEOPARD to adjust the cross
section of the single non-saturating fission product used in
the code to allow for differences in fuel type by inputing a
scaling factor. In the present research, a value of 0.84
[M-3] was used for typical PWR uranium oxide fuel and a value
of 1.26 was employed in cases involving plutonium enriched
fuel [S-6].

The LEOPARD code and its companion cross section library
have been extensively benchmarked at MIT by Garel [G-3] and
Correa [C-1]. Garel has tested the code against critical and
exponential experiments for 63 cases of slightly-enriched-
uranium (U-235/U-238) light water lattices and 42 plutonium-
enriched uranium oxide light water cases. On the other hand
Correa concentrated his work on tight pitch U-233/ThO$_2$,

Pu/ThO$_2$ and U-235/UO$_2$ lattices. Table 2.1 summarizes the
results obtained by these two previous workers at MIT. For
lattices of interest to the present work (that is, U-235/UO$_2$
lattices with and without soluble boron), the $|\overline{\Delta k}|$ was found to
be ± 0.012. This result is sufficiently accurate for the type
of work we are interested in here. Finally, in a recent study
an assessment was made of LEOPARD and two other newer codes,
and LEOPARD was found to be in better agreement with experi-
mental results than the other codes [L-2].

The PDQ-7 code [C-5] solves the multigroup diffusion
equations in one, two or three dimensions. The eigenvalue
solution to the equations can be obtained in rectangular,
cylindrical, spherical or hexagonal geometry. Although this
code allows up to five energy groups, only two energy groups
were used in the present work; no depletion calculations were
done using the code.

In PDQ-7 the diffusion equation is solved by discretizing
the energy variable and finite-differencing (central) the
spatial part of the equation over a constant (or variable)
mesh interval. The one dimensional equations are solved
using the Gauss elimination technique and the two dimensional
equations are solved using a single-line cyclic semi-iterative
procedure. For three dimensional problems, a block Gauss-
Seidel procedure is used. However, only two dimensional
analyses were done in the present work.

The calculational flow path linking the LEOPARD and PDQ-7
codes is shown in Fig. 2.2. The LEOPARD code can be used to

TABLE 2.1 SUMMARY OF LEOPARD BENCHMARK COMPARISONS

FUEL:	U-233/ThO$_2$[1]	U-235/ThO$_2$[1]	U-235/UO$_2$[1]	U-235/U[1]	U-235/UO$_2$[2]	Pu/UO$_2$[2]
ε(w/o)	3.00	3.78-6.33	3.00-4.02	0.7-1.5	1.3-4.1	1.5-6.6
F/M	0.01-1.00	0.11-0.78	0.23-2.32	0.15-1.69	0.1-1.3	0.1-0.9
(H+D)/U-238 (or/Th-232)	3.4-403.	4.7-36.	1.31-14.6	0.8-5.7	2.9-1.3	3.5-39.0
ϕ_1/ϕ_2	0.3-21.	1.7-23.	2.4-50.	1.3-12.	1.6-12.	1.2-20.
D$_2$O(%)	0.-99.34	0.-81.96	0.-89.14	---	---	---
Boron(PPM)	---	---	---	---	0.-3400.	---
$\bar{k}$	1.003	1.009	0.998	1.006	1.003	1.018
$\pm\Delta k$	0.012	0.016	0.006	0.011	0.012	0.014
# of cases	16	16	26	82	63	42

(1) Reference C-1

(2) Reference G-3
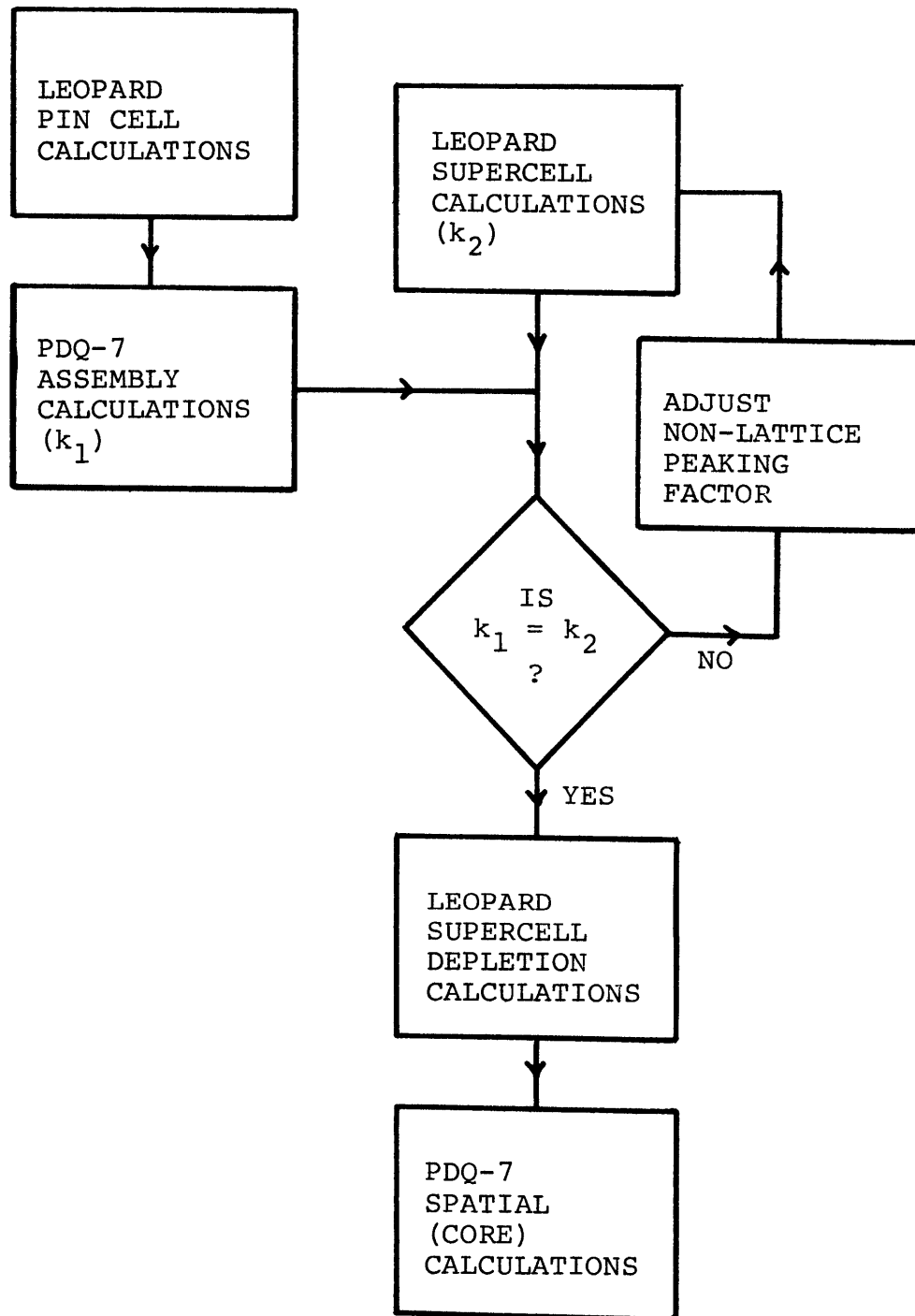
Fig. 2.2 Calculational Flow Path

carry out simulated full-assembly calculations by correctly
specifying the non-lattice fraction ('extra' region of the
supercell) and its corresponding non-lattice power peaking
factor. Fig. 2.2 shows how this is done, by adjusting the
non-lattice peaking factor to match PDQ-7 whole-assembly
calculations.

2.3 REACTOR MODELS AND LATTICES

In the present work it was considered essential, in the
interests of realism, to have a specific reactor design to
serve as a reference case in the establishment of relevant
design parameters. The Maine Yankee PWR system was selected
because of the fact that it is a large modern PWR (designed
by Combustion Engineering, Inc.) which is currently operating
and, more importantly, the reactor fuel design characteristics
and other information vital to this study were readily avail-
able in publicly available information supplied by the Yankee
Atomic Electric Co., which manages the operation of the
reactor. Although the information in this report is referred
to as deriving from "Maine Yankee," it should not be consi-
dered as representing that actual system in its present or
projected operating configuration, but as an idealization
thereof. It should also be noted that the results in this
report have not been either reviewed or approved by the
Yankee organization. Table 2.2 briefly summarizes the
Maine Yankee reactor's key core parameters, and Tables 2.3
and 2.4 list the geometrical dimensions, the thermodynamic

TABLE 2.2   MAINE YANKEE REACTOR CORE PARAMETERS [S-7]

ITEM	VALUE	UNITS
Rated Thermal Power	2630	MWth
Rated Electric Power	840	MWe
Fuel Management	3-batch, out-in/scatter	
Equilibrium Discharge Burnup	33,000	MWD/MT
Power Density	80.85	kw/liter
Initial System Pressure	2250.0	psia
Average Linear Heat Rate (102% of Nominal)	6.35	kw/ft.
Nominal Coolant Bulk Temperature	576.4	°F
Fuel Rod Array	14 x 14	
Fuel Rod Pitch	0.580	inches
Pellet OD	0.3765	inches
Clad Material	Zircaloy-2	
Clad OD	0.440	inches
Clad ID	0.384	inches

TABLE 2.3   VOLUME FRACTIONS OF VARIOUS MAINE YANKEE
            SUPERCELL CONSTITUENTS

REGION

CONSTITUENT	Pellet	Clad[1]	Moderator	Extra
UO_2	1.0000	0.0	0.0	0.0
Zircaloy-2	0.0	0.907475	0.012124	0.087651
Light Water	0.0	0.0	0.986144	0.912349
Chromium	0.0	0.0	0.000330	0.0
Nickel	0.0	0.0	0.000909	0.0
Manganese	0.0	0.0	0.000006	0.0
Iron	0.0	0.0	0.000478	0.0
Carbon	0.0	0.0	0.000001	0.0
Aluminum	0.0	0.0	0.000008	0.0

(1)   Volume fractions do not add to unity due to the
      presence of the fuel-clad gap in this region.

TABLE 2.4   REQUIRED DIMENSIONAL, THERMODYNAMIC AND NEUTRONIC PARAMETERS USED
FOR THE MAINE YANKEE SUPERCELL

PARAMETER	VALUE	PARAMETER	VALUE
"Resonance" Temperature (°F)	1232.0	Non-Lattice Fraction	0.115166
Pellet Temperature (°F)	1232.0	H_2O Pressure (Psia)	2250.0
Clad Temperature (°F)	630.4	H_2O Density (g/cc)	1.0*
Moderator Temperature (°F)	576.4	Fuel Theoretical Density Fraction	0.92
Geometrical Buckling (cm^{-2})	7.319×10^{-5}	Power Density (Watts/cm^3)	80.8574
Non-Lattice Peaking Factor	1.16	Fission Product Absorption Cross-Section Scale Factor	0.84
Pellet Outer Radius (in)	0.18825		
Clad Outer Radius (in)	0.220		
Clad Inner Radius (in)	0.1920		
Pitch (in)	0.580		
Power (fraction of full power)	1.0		

* The code adjusts the density to correspond to the specified moderator temperature

and the neutronic parameters required to describe this reactor in a LEOPARD supercell calculation, that is, a simulated full-assembly calculation.

2.4 BURNABLE POISON MODELING

Incorporation of burnable poison into the fuel assemblies for the purpose of facilitating the implementation of certain uranium utilization improvement techniques (for example, extended burnup and/or low-leakage fuel management schemes) can be done in two ways: homogeneously mixing the burnable poison with the uranium oxide fuel; or in the heterogeneous form of poison pins placed in fuel rod locations (lattice shims) or in control rod guide tubes (water-hole shims). There are advantages and disadvantages associated with both methods of incorporating the burnable poison within the fuel assemblies, and these two options are both in use.

The selection of material for burnable poisons and the way in which they can be incorporated within the fuel lattice are governed by several considerations: acceptable total reactivity worth, depletion rate, good corrosions resistance in water, resistance to radiation damage, ease of fabrication, compatibility with clad and/or fuel, manufacturability, material cost, etc. From a neutronic standpoint, the ideal burnable poison should have a depletion characteristic such that relatively uniform depletion of the poison throughout the operating cycle is maintained and complete destruction of the high cross section isotopes occurs just before the end of

cycle. This would compensate for the linear loss in reactivity of the freshly-loaded fuel as a function of burnup, and leave a negligible shim residual at the end of cycle. The amount of residual poison present at EOC is of concern since the discharge burnup (hence, the uranium utilization) can be significantly affected.

Researchers [F-2, L-3] over the past several years have studied a number of elements, particularly those with high microscopic thermal absorption cross sections (> 10^3 barns), as potential candidates for burnable poisons. The two elements which are considered leading candidates for use as burnable poison in PWRs are boron and gadolinium. Extensive experience with these elements has been accumulated over many years of reactor operation: boron in the form of B_4C has been employed as control material in both PWRs and BWRs, boron in alumina or a pyrex-type glass has been used to poison startup cores, and gadolinium burnable poison (in the form of Gd_2O_3 mixed with UO_2 fuel) has been used in BWRs. In recent years, the DOE and the nuclear industry have embarked on a number of programs which include gadolinium and boron burnable poison design development, demonstration of high burnup poison fuel for PWRs, analytical modeling of burnably-poisoned fuel burnup, poisoned fuel pin/assembly modeling, comparison of analytical and experimental results, and the like.

Preliminary studies [H-3] have shown that gadolinia admixed with UO_2, and boron in the form of borosilicate rods, deplete at a relatively uniform rate (i.e., with an essentially

linear reactivity vs. exposure characteristic) over an operating cycle, and leave a small residual at the end of cycle. Figures 2.3 and 2.4 show typical curves of the reactivity versus burnup behavior of burnable-poison-load PWR fuel assemblies. For the purpose of this work, a simple depletion model of a generalized burnable poison, consistent with such results, will be adopted: that is, a poison material is postulated which burns out at a uniform rate over a cycle and leaves a small residual at the EOC. Figure 2.5 illustrates this model. An important subtask of this work is to determine the optimum shape (slope and intercept) of the reactivity-burnup trace with respect to maximization of fuel burnup.

2.5 CHAPTER SUMMARY

In this chapter a brief description was presented of the computer codes (LEOPARD and PDQ-7) employed in the present research. The manner in which the codes are linked together in computations performed for this work was also outlined. The LEOPARD code was determined to be sufficiently accurate for the type of work to be done here. The Maine Yankee reactor system was chosen as the reference system because it is a modern, operating PWR, and information pertaining to this system was readily available. Finally, a simple generic depletion model of burnable poison (consistent with results obtained from more sophisticated computer calculations) in a fuel assembly was defined.
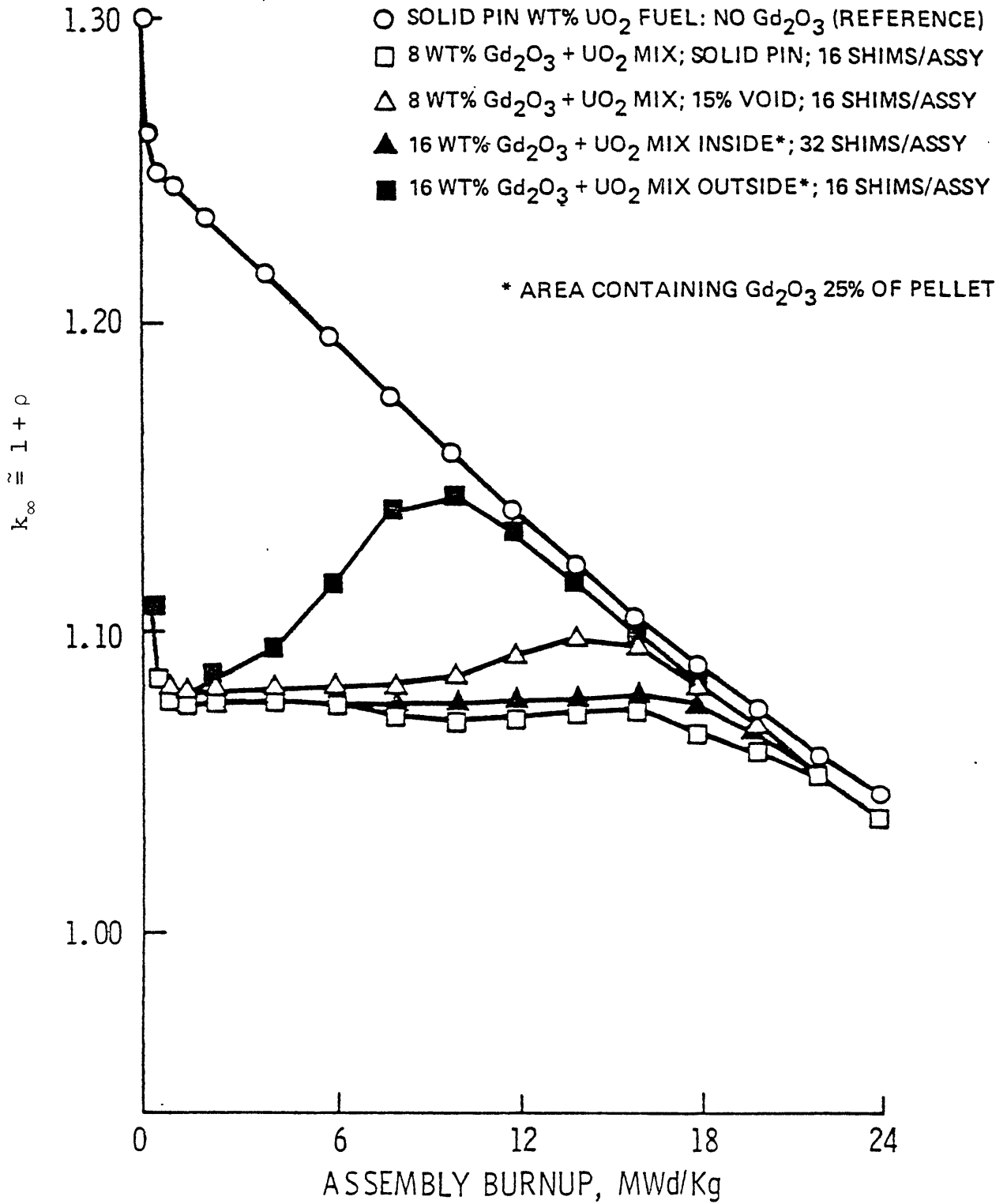
Fig. 2.3 k_∞ versus Burnup for Gadolinia-Poisoned Assemblies
(From Ref. [H-3]
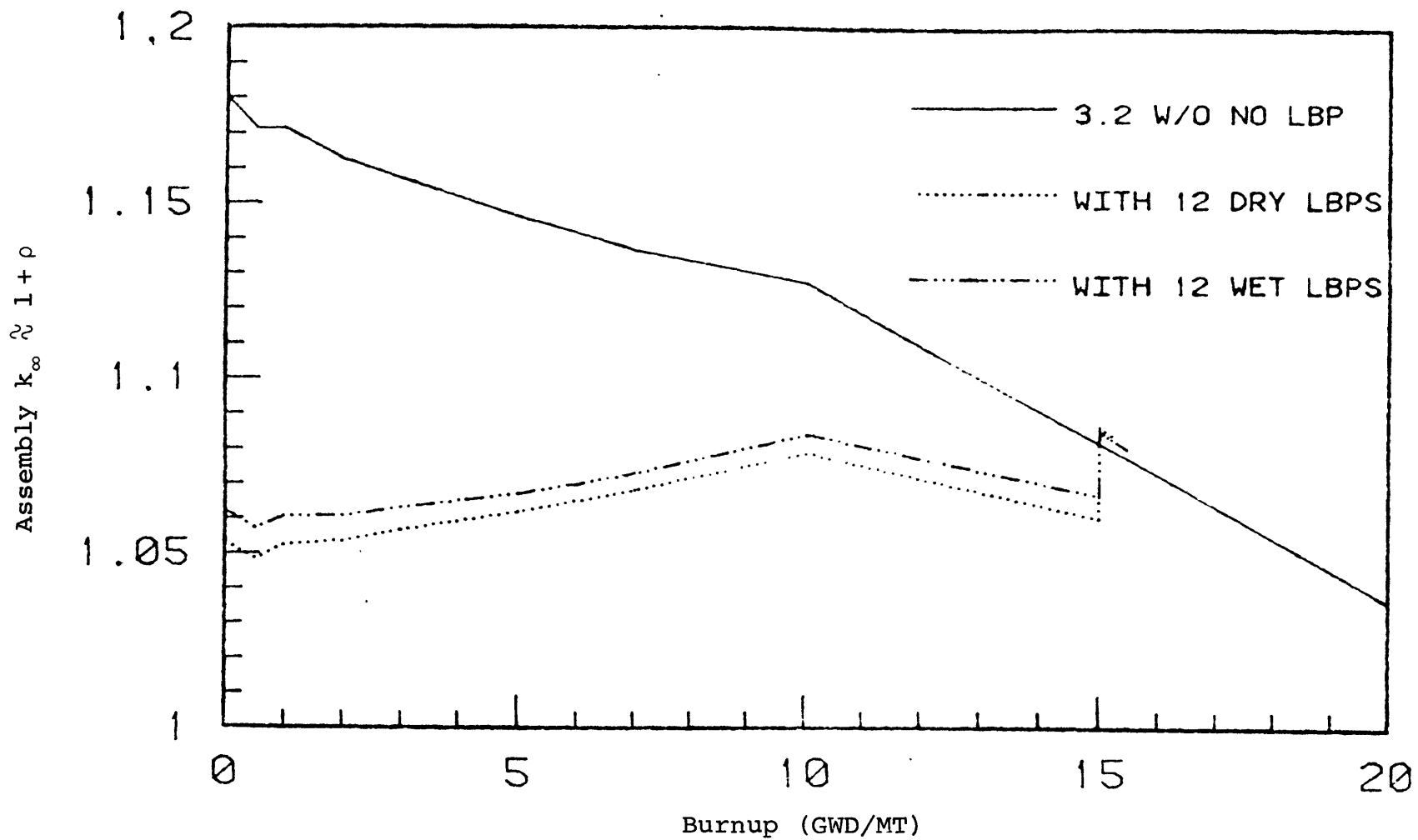
Fig. 2.4 k_∞ versus Burnup for Boron-Poisoned Assemblies (From Ref. [H-4])
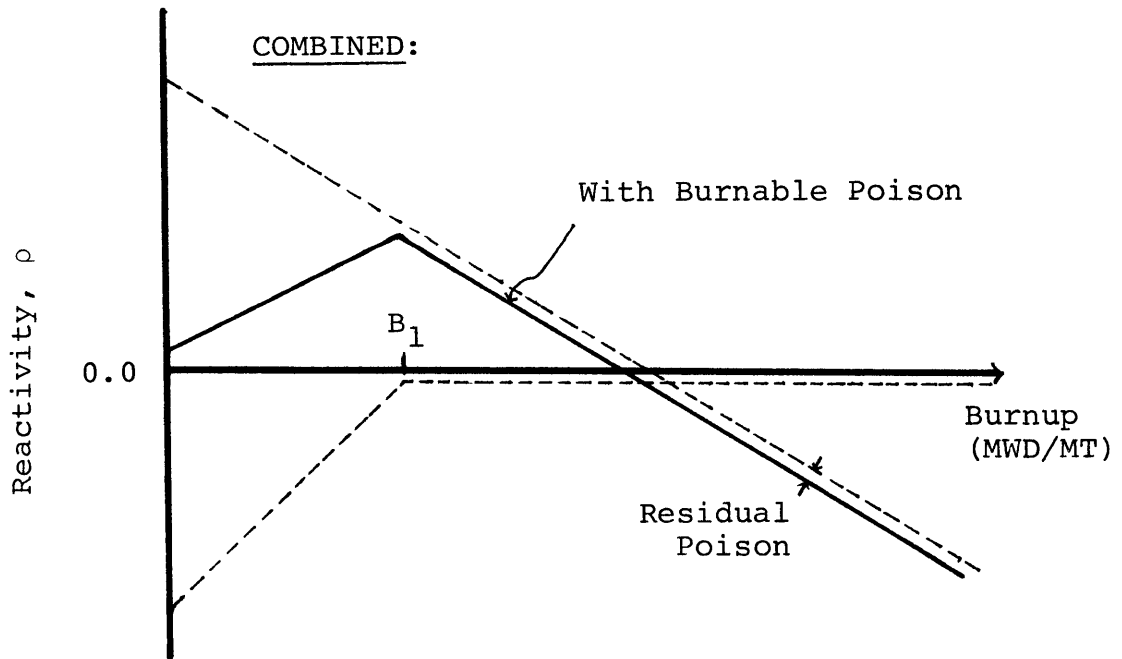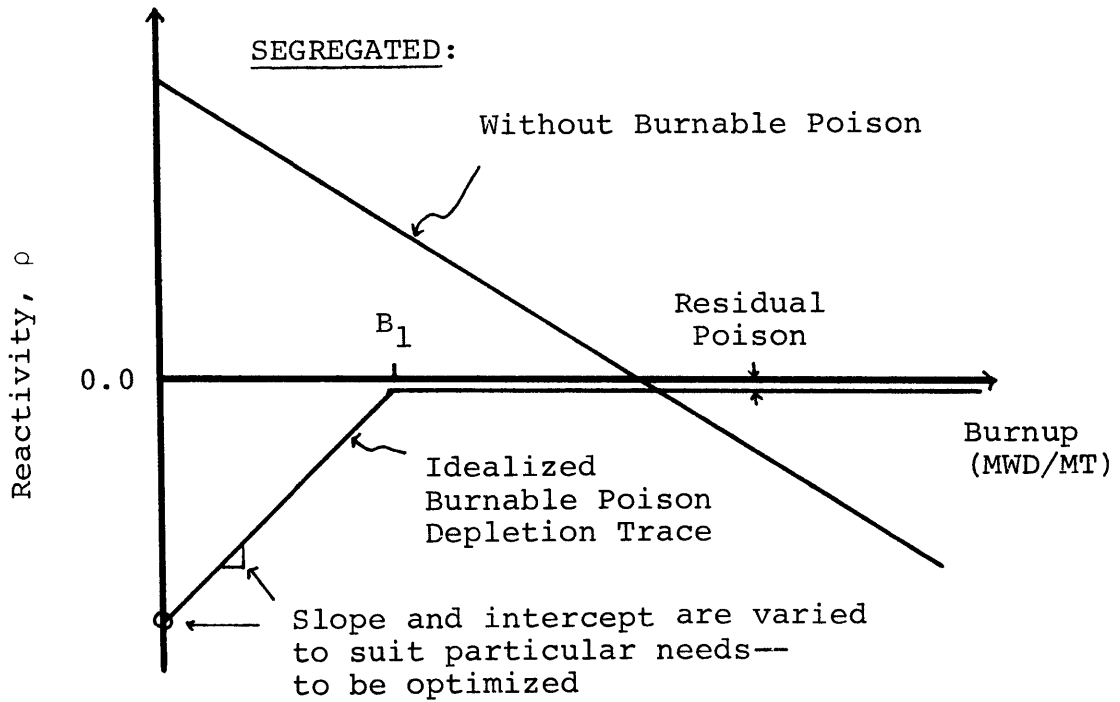
Fig. 2.5 Generic ρ versus Burnup Trace for
Assembly with Burnable Poison

CHAPTER 3

LINEAR REACTIVITY MODEL METHODOLOGY

3.1 INTRODUCTION

The linear reactivity model (LRM) is based on the obser-
vation that the reactivity, ρ, of a PWR fuel assembly (em-
bedded in a lattice of similar assemblies) decreases linearly
as a function of burnup. With this model one can determine
in-core fuel management parameters such as the reactivity
contribution of a fuel assembly or batch of assemblies after a
certain in-core residence time. Having this information the
cycle and discharge burnups of the fuel can be computed.
Elementary versions of this approach have been employed for
approximate analyses and pedagogical purposes for some time
now. Since greater accuracy is required in the present work,
other important, and newer additions to the methodology will
be included here: power weighting of the reactivity, and ex-
plicit treatment of the core leakage in the radial direction.
Since both of these key features have been discussed in some
detail in prior MIT work by Sefcik [S-2], only a brief summary
description will be given in this chapter. More attention
will be given to the final component in the LRM methodology,
the relation used to estimate the sharing of power among in-
core fuel batches. Prior empirical prescriptions will be re-
placed by one derived from the "group-and-one-half" model of

neutron behavior. Verification of this relation for both interior and peripheral fuel assemblies will be presented.

Finally, an analytical model permitting computation of the discharge burnup for various cases of fuel management schemes of contemporary interest will be developed.

3.2 THE LINEAR REACTIVITY MODEL

The eigenvalue (λ) obtained by solving the neutron diffusion equation for a core lattice is, on a physical basis, the neutron multiplication factor (k) of that assembly. It has been observed that the k of a typical PWR fuel assembly/lattice, with fuel enrichment in excess of roughly 2.0 w/o, varies, approximately, linearly with burnup [G-3]. However, the reactivity (ρ) of the fuel assembly/lattice, defined as

$$\rho = \frac{k-1}{k} = 1 - \frac{1}{k} \tag{3.1}$$

has been found to be a much more linear function of burnup than k. In fact, Sefcik [S-2] has shown that for the Maine Yankee supercell reference lattice with enrichment variations ranging from 1.5 w/o U-235 to 4.34 w/o U-235, the linear least squares curve-fits of ρ versus burnup (150-50,000 MWD/MT) gave an average coefficient of determination (R^2) of 0.995 (i.e., only 0.5% of the variance is not accounted for by the correlation) compared to an average R^2 value of 0.9898 for linear fit of k versus burnup. Figure 3.1 shows the plots of ρ versus burnup for the Maine Yankee supercell with
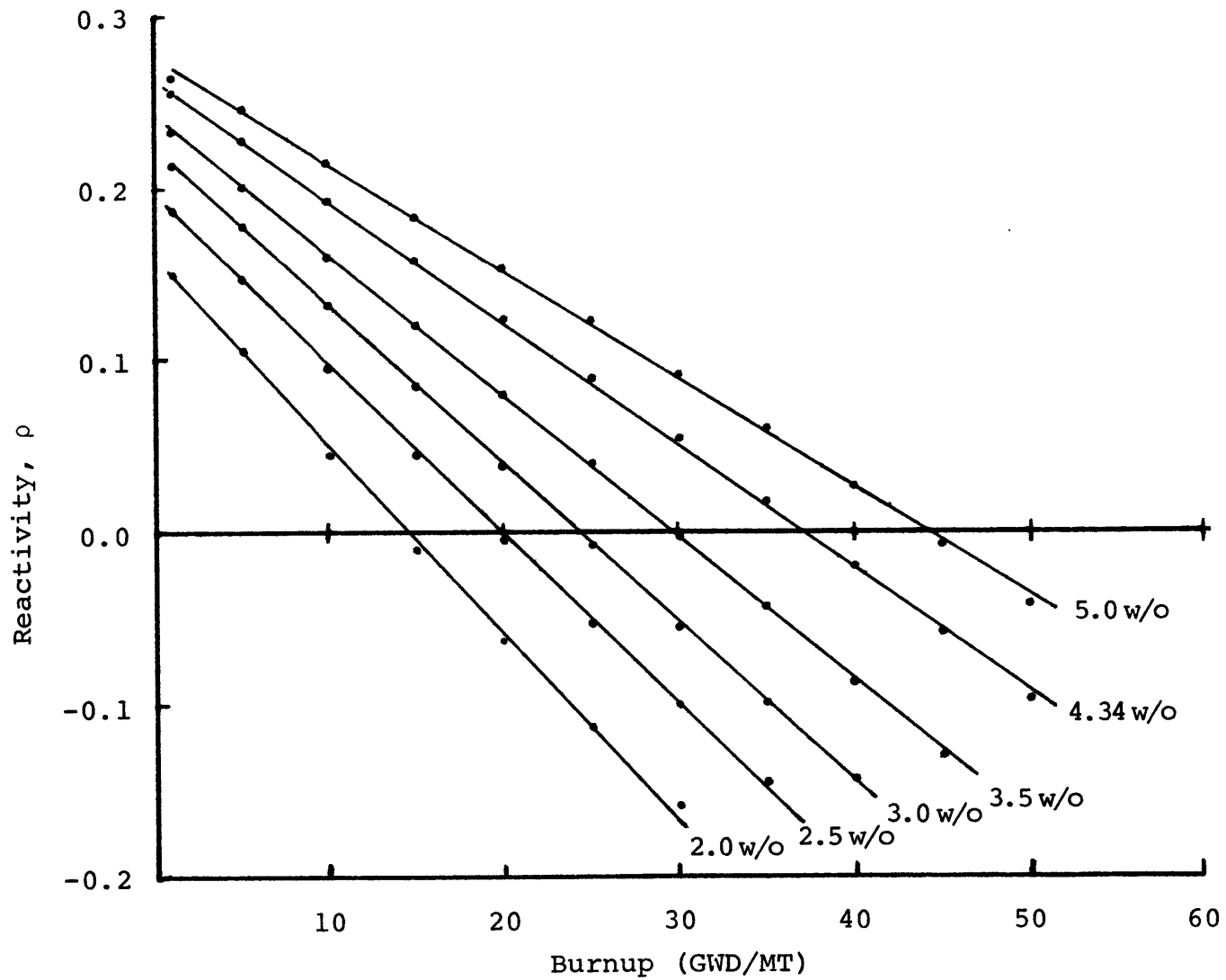
Fig. 3.1 Reactivity versus Burnup for the Main Yankee Super-
cell with Different Fuel Enrichments

different fuel enrichments. Although not shown in the figure,
there is a sharp drop in the reactivity during the first 150
MWD/MT for each curve due to the buildup of the xenon and
samarium fission product poisons to their saturation levels.
Omitting this initial transient, then, for a particular curve,
we can write,

$$\rho = \rho_o - AB \tag{3.2}$$

where ρ_o is the extrapolated beginning of life reactivity
(i.e., at B=0),

A is the slope of the curve, $(MWD/MT)^{-1}$,

and   B is the burnup, MWD/MT.

In a simple application of the linear reactivity model rele-
vant to the present work, the discharge burnup $(B_{dis,n})$ of an
n-batch core under steady-state refueling conditions will be
determined as follows. Neglecting leakage for the moment,
and assuming that the core has a fixed thermal power rating
and there is equal power sharing among the fuel batches (of
fixed size), the freshest batch will be burned to $(B_{dis,n})/n$
at the end of cycle, the next older batch to $(2B_{dis,n})/n$, etc.
The system reactivity of the combination of the fuel batches
is obtained by algebraic averaging of the EOC reactivity of
each batch,

$$\rho_1 = \rho_{on} - A \cdot \frac{(B_{dis,n})}{n}$$

$$\rho_2 = \rho_{on} - A \cdot \frac{(2B_{dis,n})}{n} \qquad (3.3)$$

$$\begin{array}{ccc}
| & | & | \\
| & | & | \\
| & | & | \\
| & | & |
\end{array}$$

$$\rho_n = \rho_{on} - A \cdot \frac{(nB_{dis,n})}{n}$$

- -

System reactivity $\rho_{sys} = \frac{1}{n} \sum_{i=1}^{n} \rho_i = \frac{1}{n}\left(n\rho_{on} - A \cdot (B_{dis,n})\right.$

$$\left. \cdot \frac{n(n+1)}{2n}\right) \qquad (3.4)$$

At the EOC, $\rho_{sys} = 0$ (reactivity-limited EOC condition), and Eq. (3.4) can be rearranged to give

$$B_{dis,n} = \left(\frac{2n}{n+1}\right) \frac{\rho_{on}}{A} \qquad (3.5)$$

For a one-batch (n=1) core, the discharge burnup is given by

$$B_{dis,1} = \frac{\rho_{ol}}{A} \qquad (3.6)$$

When the one-batch core has the same discharge burnup as the n-batch core ($B_{dis,1} = B_{dis,n}$), the reload reactivity (hence, reload enrichment) of the latter will be lower than that of the former:

$$\rho_{on} = \left(\frac{n+1}{2n}\right) \rho_{ol} \qquad (3.7)$$

Or alternatively, if the reload reactivity is the same

$(\rho_{on} = \rho_{ol})$, an n-batch core can be driven to a higher burnup:

$$B_{dis,n} = \left(\frac{2n}{n+1}\right) B_{dis,1} \tag{3.8}$$

The above results (Eqs. 3.5 to 3.8) were obtained based on the linearity of the $\rho(B)$ trace of a fuel lattice. However, the EOC reactivity balance approach of Eq. (3.3) can be extended to evaluate the discharge or cycle burnup of a reactor core whose fuel lattice/assembly reactivity varies non-linearly with burnup (for example, the natural uranium fuel of the heavy water moderated CANDU reactor). This is discussed in Appendix A. Similarly, the approach can be employed to compute the burnup of fuel batches in subsequent cycles following different types of perturbation from the steady state condition, such as changes in cycle length due to an early un-scheduled shutdown of the reactor or due to coastdown, and changes in reload enrichment or batch fraction [D-2]. In the present work, however, the focus will remain on the steady state or equilibrium cycle of the reactor.

3.2.1 ρ VERSUS BURNUP CURVES FOR DIFFERENT FUEL TYPES

In the preceding section a case has been made for the use of the linear reactivity model for current PWR fuel (i.e., UO_2 slightly enriched with U-235). While the present study deals exclusively with this fuel in a once-through fueling mode, it is of interest to inquire whether the LRM is applicable to

other fuel types in similar lattices, since the commercialization of spent-fuel reprocessing will lead to the use of other fissile isotopes (U-233, Pu-239 and Pu-241) and the other major fertile species, Th-232, in LWR fuel. The results will also provide valuable insight into the nature of the physical properties contributing to or detracting from the linearity of $\rho(B)$.

Several Maine Yankee supercell depletion calculations using all possible combinations of fissile and fertile materials were performed. The isotopic compositions of the fissile material used in these computations corresponds to those one would obtain from the reprocessing of current LWR spent fuel. Table 3.1 gives the compositions of these fissile constituents. Figures 3.2 and 3.3 show the reactivity versus burnup curves for the different fuel types, and Table 3.2 gives the coefficients of determination (R^2) for the linear least squares curve-fits of the $\rho(B)$ traces, and other relevant parameters. Except for the Pu/ThO$_2$ system the results confirm the validity of applying the LRM methodology to different fuel types. For Pu/ThO$_2$ the methods of appendix A could be used to improve the accuracy of the linear model or to show that it is precise enough for a given application.

The departure from linearity of the Pu/ThO$_2$ system $\rho(B)$ trace can be attributed to the "Phoenix Effect" which involves the conversion of fertile Pu-240 by neutron capture into fissile Pu-241. Plutonium discharged from a typical PWR has a high concentration of Pu-240 (here, approximately 26% by

TABLE 3.1   ISOTOPIC COMPOSITION OF PLUTONIUM- AND
            U-233-ENRICHED FUEL

FUEL TYPE	ISOTOPE	WEIGHT FRACTION
1. Plutonium Enriched:	Pu-239	0.5422
	Pu-240	0.2596
	Pu-241	0.1394
	Pu-242	0.0588
2. U-233 Enriched:*	U-233	0.9064
	U-234	0.0808
	U-235	0.0128

---

* U-236 is neglected

TABLE 3.2 RESULTS OF LINEAR CURVE-FITTING OF THE ρ(B) TRACES
FOR THE DIFFERENT FUEL TYPES

FUELS:	$U-233/UO_2$	$U-235/UO_2$	Pu/UO_2	$U-233/ThO_2$	$U-235/ThO_2$	Pu/ThO_2
Fissile Enrichment (ε w/o)	3.15	3.00	3.08	2.94	3.23	3.34
Extrapolated BOL Reactivity, (ρ_o)	0.30609	0.22340	0.09450	0.22003	0.11586	0.06566
Slope (A, MWD/MT^{-1})	-9.299E-6	-9.266E-6	-3.883E-6	-1.074E-5	-6.394E-6	-3.270E-6
R^2	0.999987	0.999968	0.998288	0.998959	0.999483	0.975308
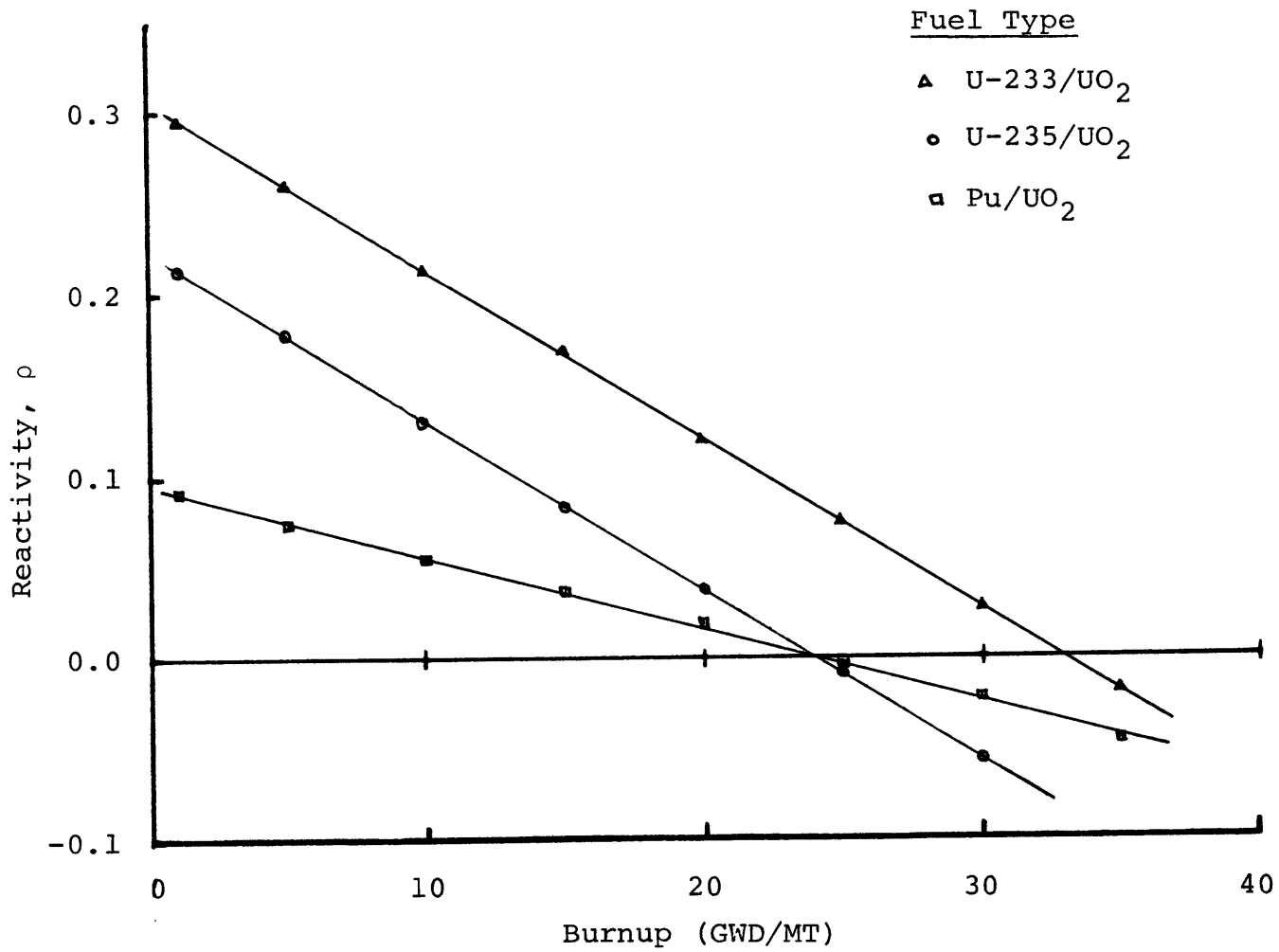
Fig. 3.2   Reactivity versus Burnup for Various Fissile
            Materials in UO_2
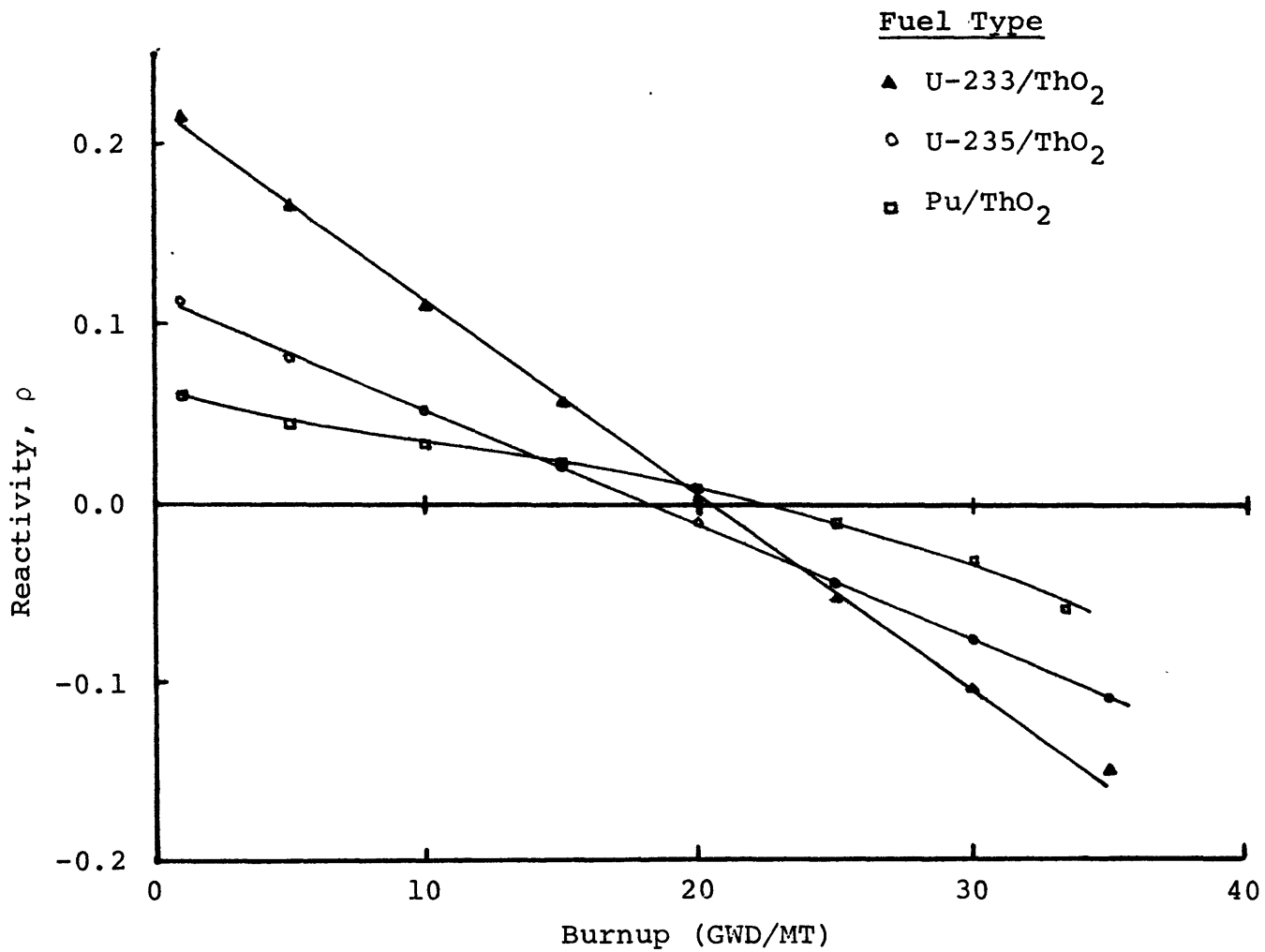
Fig. 3.3 Reactivity versus Burnup for Various Fissile
Materials in ThO_2

weight. The Pu-240 isotope has a large, sharp resonance at 1.05 eV and thus behaves like a self-shielded burnable poison to thermal neutrons. The production of the high-worth fissile isotope Pu-241, coupled with the depletion of the "burnable poison" Pu-240, provides extra reactivity which effectively 'flattens' the $\rho(B)$ trace of the Pu/ThO$_2$ system [H-2]. The above explanation for the non-linear behavior of the Pu/ThO$_2$ system $\rho(B)$ trace was confirmed by making a similar supercell depletion calculation using pure Pu-239 as the fissile material. The resulting reactivity versus burnup curve was much "steeper" and much more linear (with $R^2 = 0.995$).

3.2.2 A CONTRIBUTION TO THE DEBATE AS TO WHY $\rho(B)$ IS LINEAR

Although researchers in the field of PWR nuclear fuel management have recognized the linearity of the $\rho(B)$ curve for a core lattice/assembly and have made good use of this empirical observation, no physical explanation has been advanced to account for this phenomenon. Through the process of induction, an attempt is made here to better understand the cause for this linear behavior.

For the U-235/UO$_2$ lattice system, a major reactivity penalty comes from the accumulation of fission products with burnup. The reactivity loss due to fission product buildup is given by (using a one-group model)

$$\rho_{FP} = \frac{C_{FP}}{\nu F} \qquad (3.9)$$

where   F   is the fission rate which, for constant power level

operation, is approximately, a constant,

$$= [N_{25}\sigma_f^{25} + N_{49}\sigma_f^{49}] \cdot \phi$$

and C_{FP} is the capture rate in the fission products

$$= N_{FP} \cdot \sigma_c^{FP} \cdot \phi$$

But $N_{FP} \simeq 2F \cdot t$ (3.10)

where $F \cdot t$ is the total fissions, and the relatively small

effect of fission product transmutation is neglected

[A-4].

Therefore, the reactivity loss due to fission products is

given by,

$$\rho_{FP} = \frac{2F \cdot t \cdot \sigma_c^{FP} \cdot \phi}{\nu F}$$

$$= \left(\frac{2\sigma_c^{FP}}{\nu} \right) \cdot \phi \cdot t$$

$$\simeq (\text{constant}) \cdot \phi \cdot t \qquad (3.11)$$

Since, as is well known, ϕ increases with time (to maintain

a constant power level as fissile fuel depletes), we would ex-

pect ρ_{FP} to increase at a greater than linear rate with t.

But, the results from LEOPARD calculations, as shown in Fig. 3.4, indicate that there is a continuous readjustment of the spectrum by the lattice to produce changes in the spectrum-averaged cross sections (and to a lesser extent, ν), such that the loss in reactivity due to fission products, ρ_{FP}, is caused to be a linear function of time (burnup). This prompts the speculative suggestion that an underlying physical principle may govern the behavior of neutrons in a steady state LWR lattice parallel to Le Chatelier's principle in physical chemistry! In any event, the linearity is a fortunate convergence of several complicated adjustments in lattice neutronics—not readily explained in simplistic terms: as already noted, the same effect is observed in other fuel types, ruling out the attribution of this linear behavior to some unique properties of a particular fissile/fertile species.

3.3 OTHER KEY FEATURES OF LRM METHODOLOGY

To improve the accuracy of the linear reactivity model, some of its constraining conditions had to be relaxed. Equal power sharing among fuel batches and the neglect of neutron leakage from the reactor core, are perhaps the only two important assumptions made in the previous derivations, which do not reflect the actual behavior of pressurized water reactor cores. In this section the correct algorithm for combining the reactivity of fuel batches in a core, to account for unequal power sharing characteristics of these batches will be formulated, and leakage of neutrons from the reactor core will

Burnup (GWD/MT)

Reactivity Loss due to Fission Product Buildup, ρ_{FP}

Fuel Type

• Pu/UO$_2$

▲ U-233/UO$_2$

▽ Pu/ThO$_2$

+ U-235/ThO$_2$

○ U-235/UO$_2$

□ U-233/ThO$_2$
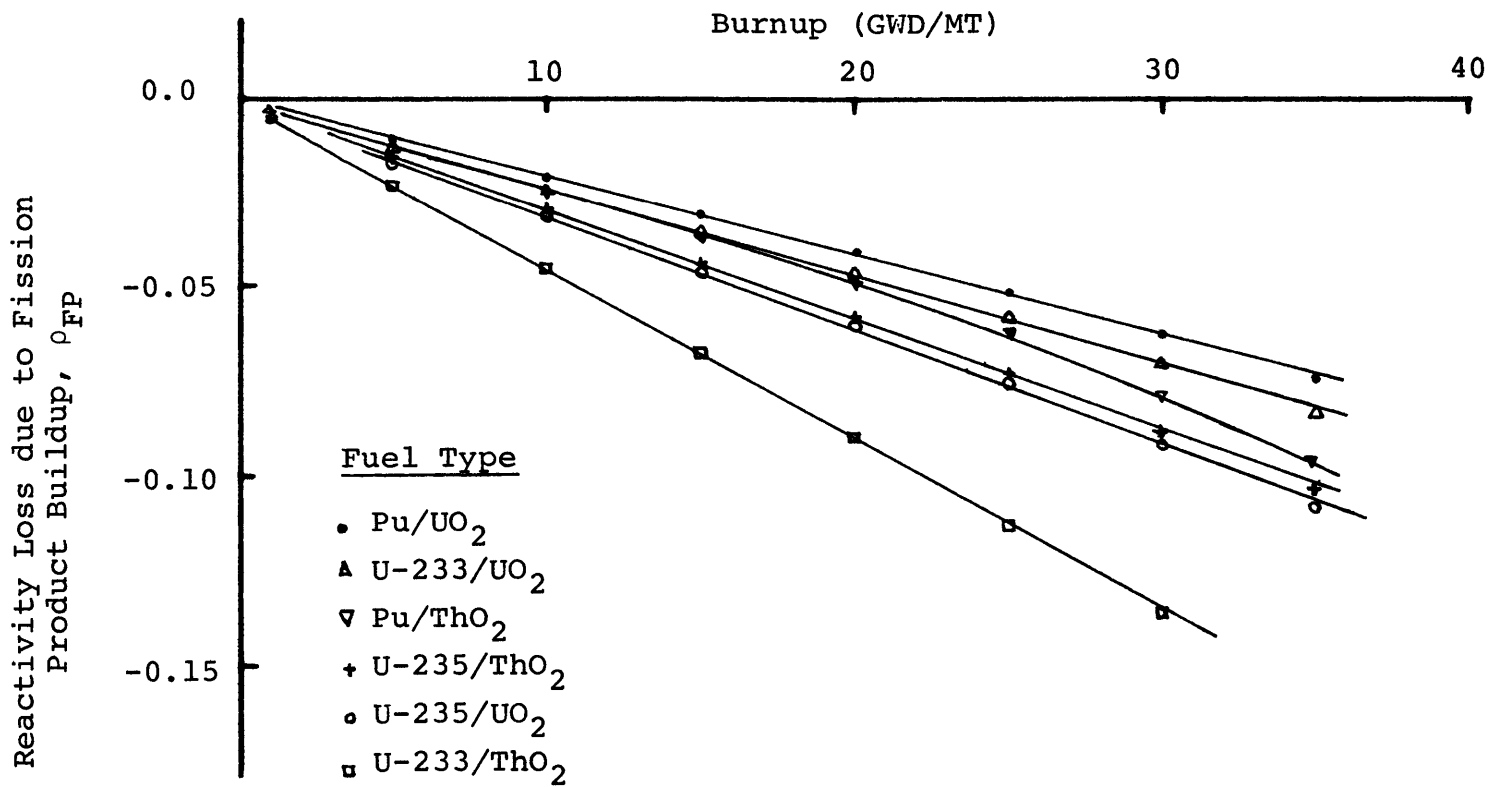
Fig. 3.4 Reactivity Loss Due to Fission Product Buildup versus
Burnup for Different Fuel Types

also be included in the methodology.

3.3.1 POWER WEIGHTING

The equal power sharing approximation assumes that the total thermal power in the reactor core, at any time, is contributed by all the fuel batches (of the same size) in equal proportion. But, intuitively we expect a fresh batch of fuel (of higher reactivity worth) to run at a higher power level than an older fuel batch. The first step in accounting for this added realism is to develop a power-reactivity weighting algorithm.

Consider a large reactor core with no leakage of neutrons and having n fuel regions (assemblies or batches). The reactivity of an individual fuel region, i, can be defined in terms of the neutron production rate by fission, νF_i, and neutron destruction rate by absorption, A_i

$$\rho_i = \frac{\nu F_i - A_i}{\nu F_i} \tag{3.12}$$

The system reactivity is thus,

$$\rho_{sys} = \frac{\sum_{i=1}^{n} (\nu F_i - A_i)}{\sum_{i=1}^{n} \nu F_i} \tag{3.13}$$

Using Eq. (3.12) to eliminate A_i in Eq. (3.13) yields:

$$\rho_{sys} = \frac{\sum_{i=1}^{n} \nu F_i \rho_i}{\sum_{i=1}^{n} \nu F_i} \tag{3.14}$$

We now assume that the average amount of thermal power generated is directly proportional to the total fission neutron production rate, and that this quantity does not vary significantly with the burnup status (i.e., composition) of the fuel. This assumption is valid if the ratio of the average energy released per fission (κ) to the average number of neutrons released per fission (ν) is a constant. Figure 3.5 shows that the variation of (κ/ν) with burnup is very slight in Maine Yankee supercell depletion calculations. Hence:

$$\rho_{sys} = \frac{\sum_{i=1}^{n} q_i \rho_i}{\sum_{i=1}^{n} q_i} \tag{3.15}$$

where q_i is the thermal power associated with fuel region i. Total core power Q is given by

$$Q = \sum_{i=1}^{n} q_i \tag{3.16}$$

If we define the normalized thermal power fraction f_i as

$$f_i = \frac{q_i}{\sum_{i=1}^{n} q_i} = \frac{q_i}{Q} \tag{3.17}$$

such that

$$\sum_{i=1}^{n} f_i = 1 \tag{3.18}$$
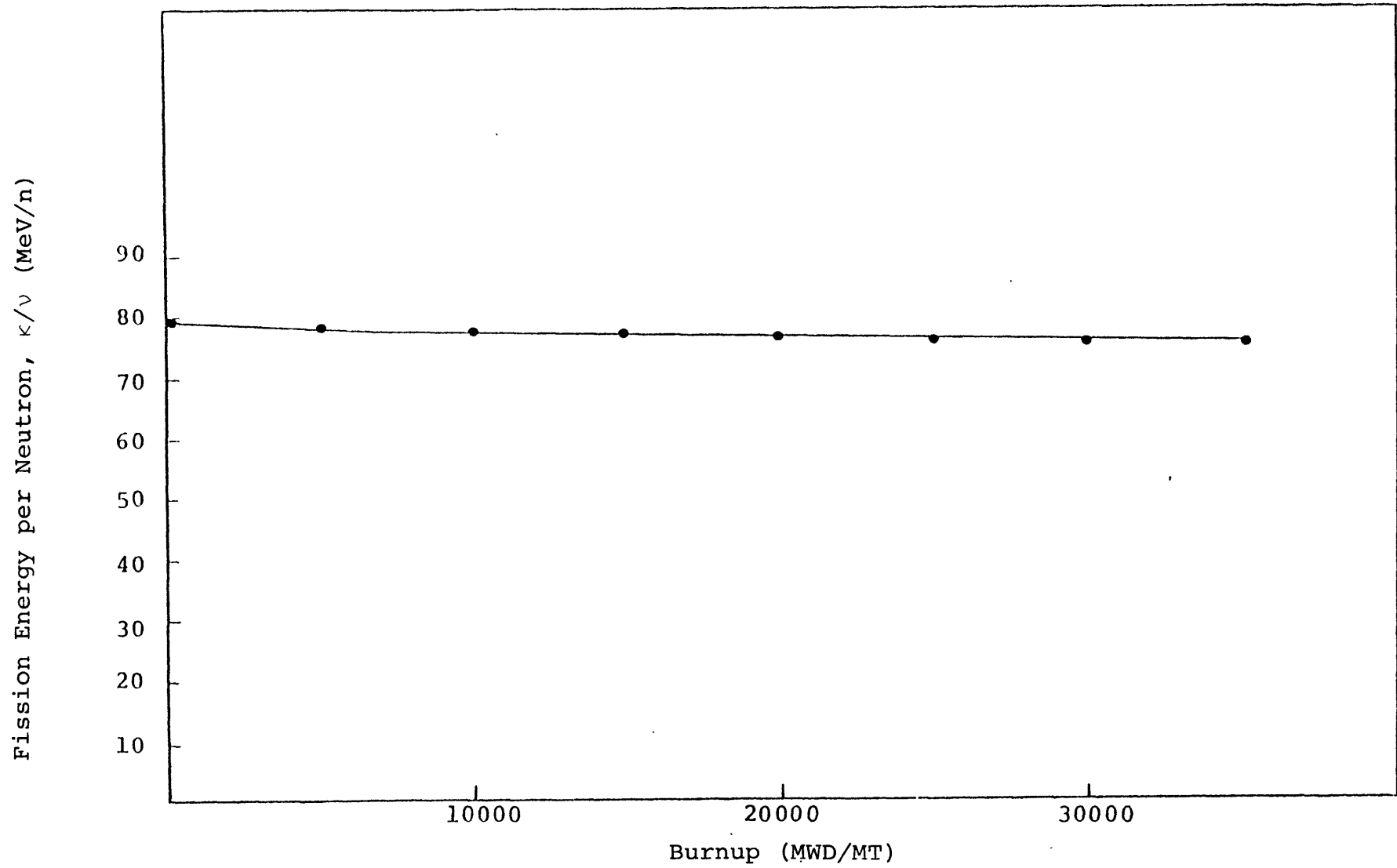
Fig. 3.5 Average Energy Release per Fission Neutron (κ/ν) as a Function of Fuel Burnup [S-2]

then Eq. (3.15) can be rewritten:

$$\rho_{sys} = \sum_{i=1}^{n} f_i \rho_i \qquad (3.19)$$

Sefcik [S-2] has tested this equation (expressed in terms of the neutron multiplication factor, k) against PDQ-7 results generated for a two-region (i=2), zero current boundary condition problem. Good agreement ($\Delta k_{sys} < 0.4$ %) was found between the eigenvalues calculated using Eq. (3.19) and those computed by the PDQ-7 code, supporting the use of Eq. (3.19) for present purposes. The approximate value of this relation should be noted, however: in addition to assuming K/ν is invariant, the preceding development implies that the infinite medium reactivity also characterizes assemblies surrounded by non-identical neighbors -- an inexact prescription because of inevitable changes in the neutron spectrum, particularly near the assembly periphery. The consequences of power weighting can now be realized by redoing the reactivity balance for an n-batch, steady state core. Assuming that the cycle burnup for a given batch, i, is proportional to its average power level $\bar{f}_i$:

$$\rho_1 = \rho_o - AB_{dis}\bar{f}_1$$

$$\rho_2 = \rho_o - AB_{dis}(\bar{f}_1 + \bar{f}_2) \qquad (3.20)$$

$$\vdots \qquad \vdots$$

$$\rho_n = \rho_o - AB_{dis}(\bar{f}_1 + \bar{f}_2 + \ldots + \bar{f}_n)$$

At the end of cycle (reactivity-limited condition), and assuming that the corresponding thermal power fraction of batch i is given by f_i:

$$\rho_{sys} = 0 = \sum_{i=1}^{n} f_i \rho_i \qquad (3.21)$$

Expanding the equation, we get

$$\rho_{sys} = 0 = \rho_o - AB_{dis}\left[\sum_{i=1}^{n} \sum_{j=1}^{i} f_i \bar{f}_j\right] \qquad (3.22)$$

or

$$B_{dis} = \frac{\rho_o}{A\left[\sum_{i=1}^{n} \sum_{j=1}^{i} f_i \bar{f}_j\right]} \qquad (3.23)$$

The term with a double summation in the denominator (designated as the "cycle schedule index" (CSI) by Sefcik [S-2] reduces to $\left(\frac{n+1}{2n}\right)$ if we assume that the power fractions for the batches remain constant over a cycle

$$f_i = \bar{f}_i \qquad (3.24)$$

and that there is equal power sharing among the batches

$$f_i = f_{i+1} \qquad i = 1, 2, \ldots, n-1 \qquad (3.25)$$

In addition, it can be shown that the condition of equal

power sharing as expressed in Eq. (3.25) results in the minimum value of the CSI when Eq. (3.24) is also imposed and hence the "maximum" discharge burnup. Although the preceding development suggests the objective of achieving a uniform burnup rate, it should be pointed out that this goal is not attainable in practice. A fresh fuel batch having large positive reactivity inherently tends to have higher power, and hence cycle burnup, than those older fuel batches having low or negative reactivity. Fortunately, because Eq. (3.24) is not necessarily true, the use of burnable poison for power/ reactivity suppression can lead to higher discharge burnups than the flat power result. This is discussed in the next chapter.

It is important to note that the effects of unequal power sharing are not large; for example, the difference in discharge burnup between a $(\frac{1}{3}, \frac{1}{3}, \frac{1}{3})$ set of f_i and a $(\frac{1}{2}, \frac{1}{3}, \frac{1}{6})$ pattern is only 4 %.

Finally, it should be noted that the f_i appear in a dual role: as the parameters determining the cycle-by-cycle burnup history of a given batch, and as the parameters defining the power level of all batches in the core during a given cycle. The CSI accounts for the effect of non-uniform core power distribution among the fuel batches. This index will be expressed more explicitly once the appropriate functional dependence of f_i on ρ_i is established.

3.3.2 LEAKAGE OF NEUTRONS

Accounting for neutron leakage from a reactor core is an important improvement to the linear reactivity model since approximately 3 % to 4 % of the neutrons are lost via leakage in a normal pressurized water reactor operated with a conventional out-in/scatter fuel management scheme. This will allow a more accurate determination of the core reactivity (and hence, the discharge burnup) using the LRM approach.

The neutrons leaking from the core are parasitically absorbed in the structures surrounding the core (such as the core barrel, thermal shields, grids, etc.). The absorption of neutrons in the ex-core regions can be incorporated into the system reactivity expression by introducing the term A_R which is defined as the neutron absorption rate in the non-fuel, ex-core regions. The system reactivity of a steady state core having n fuel regions (assemblies/batches) can therefore be written as:

$$
\rho_{sys} = \frac{\left[\sum_{i=1}^{n} (\nu F_i - A_i) \right] - A_R}{\sum_{i=1}^{n} \nu F_i}
$$

$$
= \left[\sum_{i=1}^{n} f_i \rho_i \right] - \frac{A_R}{\sum_{i=1}^{n} \nu F_i} \tag{3.26}
$$

where νF_i and A_i are the neutron production rate by fission and the neutron absorption rate in the fuel region i, respectively; ρ_i is the reactivity of fuel region i, and f_i is

its thermal power fraction. The term $\dfrac{A_R}{\sum\limits_{i=1}^{n} \nu F_i}$ is associated

with leakage and thus can be characterized as the leakage

reactivity, ρ_L. Equation (3.26) can therefore be written as:

$$\rho_{sys} = \left[\sum_{i=1}^{n} f_i \rho_i\right] - \rho_L \tag{3.27}$$

and the corresponding discharge burnup:

$$B_{dis} = \frac{\rho_o - \rho_L}{A\left[\sum\limits_{i=1}^{n}\sum\limits_{j=1}^{i} f_i \bar{f}_j\right]} \tag{3.28}$$

If A_R is the total ex-core absorption rate, then ρ_L will inc-
lude the radial as well as the axial leakage of neutrons from
the core. However, for the purpose of this research, the
radial and the axial component of the leakage reactivity are
assumed to be "decoupled," i.e., separable -- changes in one
will not affect the other.

Neutrons leaking from the core are primarily those of the
fast group (since thermal leakage is approximately an order
of magnitude smaller) and this leakage is essentially depen-
dent upon the shape of the source. If we consider a fuel
region of total length 2L with a source shape which is sym-
metrical about the centerline/origin, then the leakage reacti-
vity (fraction of neutrons leaking out of the edge of the
fuel region) is given by:

$$\rho_L = \frac{\int_0^L J(x,L)\ \psi(x)\ dx}{\int_0^L \psi(x)\ dx} \qquad (3.29)$$

where $\psi(x)$ is the source shape and the neutron current at L (the edge) due to a source at x

$$J(x,L) = \frac{-\ Dd\phi(x,L)}{dx} \qquad (3.30)$$

The flux kernel (flux at L due to source at x) $\phi(x,L)$ is given by (plane geometry approximation):

$$\phi(x,L) = \frac{M}{2D}\ exp\ [-\ \frac{(L-x)}{M}] \qquad (3.31)$$

where   D is the coefficient of diffusion, and M^2 is the migration area.

Equation (3.29) can thus be written as

$$\rho_L = \frac{\int_0^L \frac{1}{2}\ exp\ [-\ \frac{(L-x)}{M}]\ \psi(x)\ dx}{\int_0^L \psi(x)\ dx} \qquad (3.32)$$

However, the treatment of leakage developed thus far is only applicable to the leakage of neutrons in the axial direction since the source shape in this direction is readily characterized throughout the in-core residence of the fuel. On the other hand, the radial source shape is more complex, varying with the fuel loading pattern. Therefore a different approach is taken to account for radial leakage, as will be discussed later in this section.

In a PWR core, the axial source shape is cosine $[\psi(x) = \psi_o \cos\left(\frac{\pi x}{2L}\right)]$ at the beginning of life and flat with drooping ends $[\psi(x) \simeq \psi_o \left(1 - \exp\{-\frac{(L-x)}{M}\}\right)]$ by the end of a typical in-core cycle. Since the reactivity balance of greatest interest is at end of cycle (EOC) the EOC source shape should be employed to evaluate the leakage reactivity in the axial direction. Thus

$$\rho_L = \frac{\int_o^L \frac{1}{2} \exp\left[-\frac{(L-x)}{M}\right] \cdot \psi_o[1-\exp\{-\frac{(L-x)}{M}\}] \ dx}{\int_o^L \psi_o[1-\exp\{-\frac{(L-x)}{M}\}] \ dx}$$

$$\simeq \frac{1}{4[(\frac{L}{M})-1]} \tag{3.33}$$

Using representative values for a PWR of the core half-height, L = 175.0 cm, and the migration length, M = 7.5 cm, the axial leakage reactivity is approximately 0.0112.

Closer inspection of the flux kernel indicates that the leakage effect is most prominent in the last few migration (diffusion) lengths of the fuel material. This implies that, in the context of a core, neutrons leaking from it are predominantly from within two or three migration lengths of the core periphery. This suggests an approach for handling radial leakage, that is, the the correlation of radial leakage reactivity with core assembly peripheral power since PWR assemblies are approximately 2M $\simeq$ 15 cm wide. We can thus express the radial leakage reactivity as:

$$\rho_L = \alpha \, f_{per} \qquad (3.34)$$

where f_{per} is the cumulative power fraction of the peripheral assemblies

and α is a constant which depends upon the particulars of a given reactor design.

The correlation expressed by Eq. (3.34) agrees well with the results of PDQ-7 calculations for a CE System 80 PWR, as shown in Fig. 3.6 [K-2]. Similar analyses were done by Sefcik [S-2] for the Maine Yankee reactor, again using PDQ-7 static computations. Here, by successively shuffling four fuel batches in the core between the periphery and the interior, the peripheral power was varied. Fresh fuel loaded on the core periphery produces the highest power fraction, whereas cycle four fuel on the core periphery gives the lowest power fraction case. The results are shown in Fig. 3.7.

3.4 POWER SPLIT RELATION AMONG BATCHES

In the preceding section, the power-weighting scheme for combining the reactivity of fuel batches in a core, and prescriptions accounting for neutron leakage were incorporated into the LRM methodology. However, the remaining component necessary for the implementation of the LRM methodology in a complete and rigorous fashion is the power sharing relationship among the fuel batches in the PWR core. Although the power fractions of the fuel regions (assemblies/batches) can be determined using detailed computer analysis, a simple
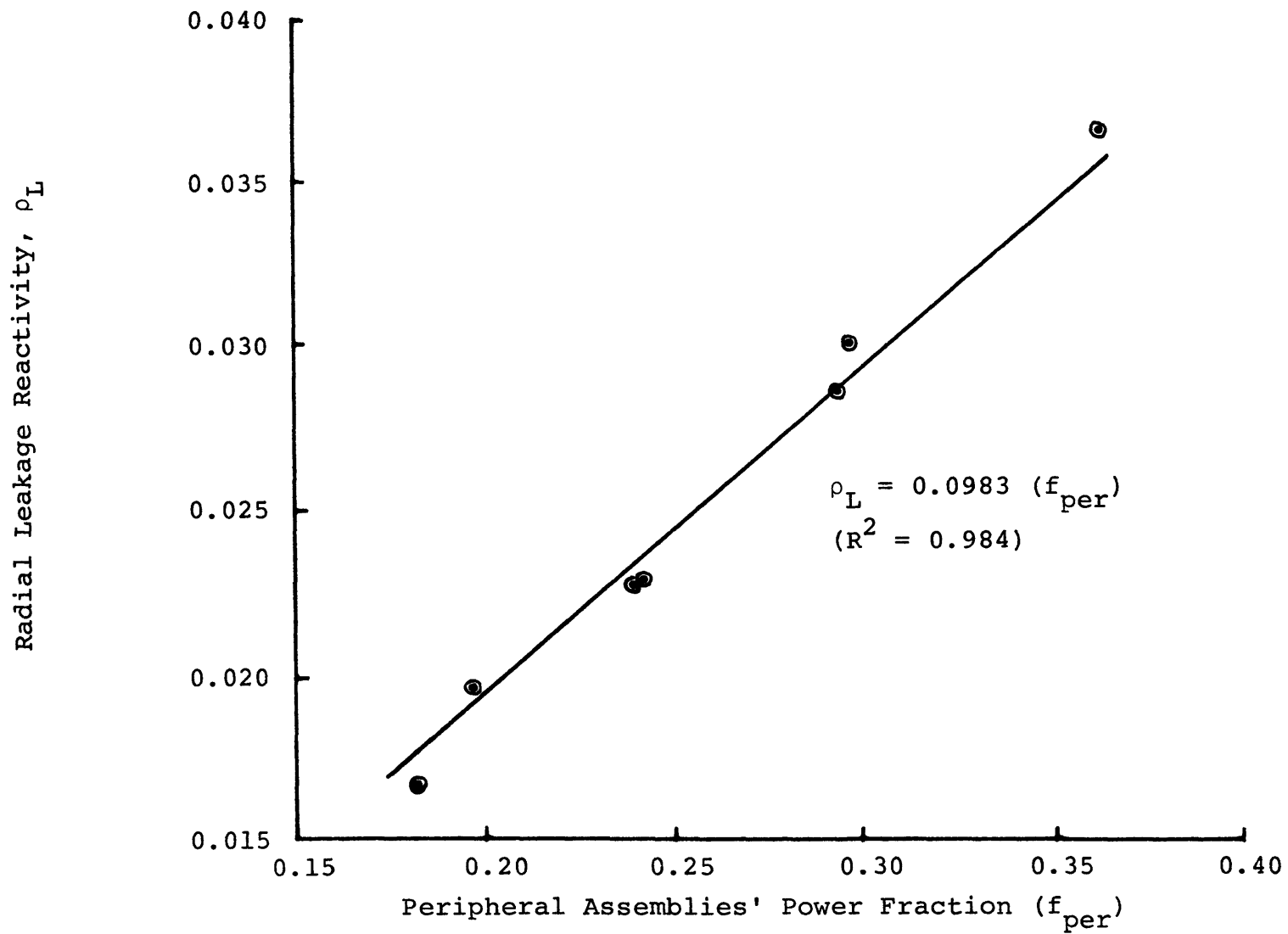
Fig. 3.6 Radial Leakage Reactivity vs. Peripheral Assemblies' Power Fraction

Fresh Fuel
Peripheral

Cycle 2
Peripheral

$$\rho_L = 0.1640 \ (f_{per})$$
$$(R^2 = 0.996)$$

Cycle 3
Peripheral

Cycle 4
Peripheral

Radial Leakage Reactivity, ρ_L

Fraction of Total Core Power in Peripheral Assemblies
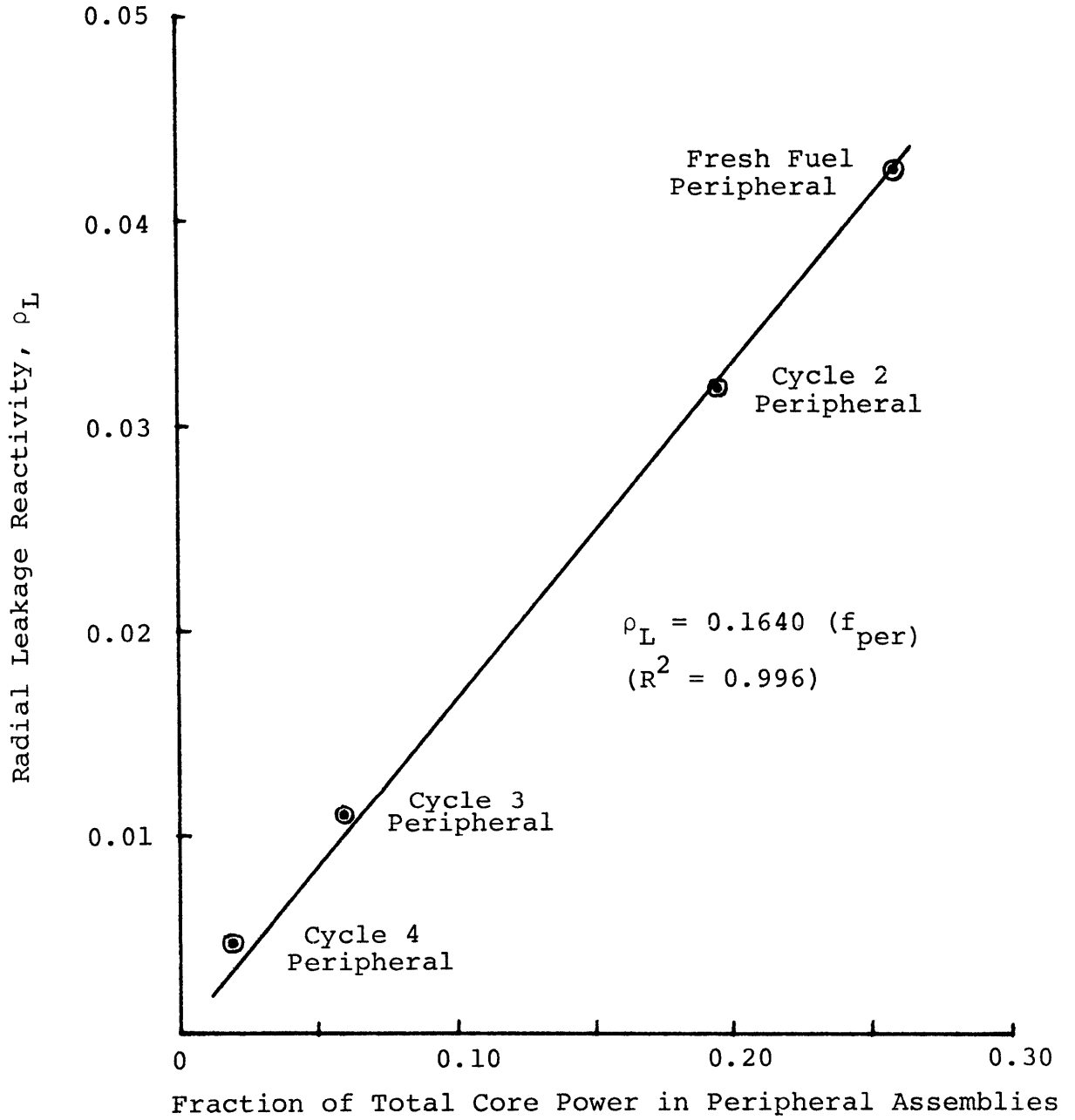
Fig. 3.7 Radial Leakage Reactivity for M.Y. Reactor vs.
Fraction of Core Power Generated in Peripheral
Assemblies

power sharing relation which has a sound theoretical basis will be employed in this research. Empirical power sharing algorithms have been proposed in the past [S-2], for example:

$$f_i \quad \propto \quad \left(\frac{1}{1-\rho_i}\right)^\theta \qquad\qquad (3.35)$$

where f_i and ρ_i are the power fraction and the reactivity of the fuel region i, respectively, and θ is an empirical exponent. Here we will show that relations of this type can be put on a theoretically sound basis.

Using the "group-and-one-half" theory, the power split equation used in this work will be derived. The equation will be verified using results from PDQ-7 calculations of a nine-bundle, zero-current boundary condition problem as well as those from quarter-core analyses.

3.4.1 DERIVATION OF POWER SPLIT EQUATION

The two-group theory requires the solution of the coupled fast and thermal group diffusion equations:

<u>fast group</u> (> 0.6 ev)

$$- D_1\nabla^2\phi_1 \quad + \quad \Sigma_{a1}\phi_1 \quad + \quad \Sigma_{12}\phi_1 \quad - \quad \frac{1}{k}(\nu\Sigma_{f1}\phi_1 + \nu\Sigma_{f2}\phi_2) \quad = \quad 0$$

leakage   absorption   down-   fission source
                      scatter

$$(3.36)$$

thermal group

$$- D_2 \nabla^2 \phi_2 + \Sigma_{a2}\phi_2 - \Sigma_{12}\phi_1 = 0 \qquad (3.37)$$

$$\underset{\text{leakage}}{\qquad} \underset{\text{absorption}}{\qquad} \underset{\substack{\text{in-} \\ \text{scatter}}}{\qquad}$$

where k is the eigenvalue (the neutron multiplication factor) and Σ_{12} is the macroscopic downscatter cross section from group one to group two.

In the "group-and-one-half" model of core neutronics, the thermal neutrons are absorbed at the point of removal from the fast group, or equivalently, the thermal leakage, which is an order of magnitude smaller than the fast leakage, is neglected $(\nabla^2 \phi_2 \simeq 0)$. Equation (3.37) thus becomes

$$\Sigma_{a2}\phi_2 = \Sigma_{12}\phi_1 \qquad (3.38)$$

Equations (3.36) and (3.38) can be manipulated into an equivalent one-group model for the fast group flux; for a critical medium (k=1) we have:

$$\nabla^2 \phi_1 + \frac{1}{M^2} \left(\frac{\rho}{1-\rho}\right) \phi_1 = 0 \qquad (3.39)$$

where M^2 is the migration area

$$= D_1 / (\Sigma_{12} + \Sigma_{a1})$$

and ρ is the local reactivity

$$= (k_\infty - 1)/k_\infty$$

The local thermal power density can be written as

$$q''' = \kappa \Sigma_{f1} \phi_1 + \kappa \Sigma_{f2} \phi_2 \tag{3.40}$$

where κ is the energy released per fission. Substituting ϕ_2 from Eq. (3.38) into Eq. (3.40) we have

$$q''' = \kappa \left[\Sigma_{f1} + \frac{\Sigma_{f2} \Sigma_{12}}{\Sigma_{a2}} \right] \phi_1 \tag{3.41}$$

The two group value of the local eigenvalue k_∞ is given by

$$k_\infty = \frac{\nu \Sigma_{f1}}{\Sigma_{a1} + \Sigma_{12}} + \frac{\Sigma_{12}}{\Sigma_{a1} + \Sigma_{12}} \cdot \frac{\nu \Sigma_{f2}}{\Sigma_{a2}} \tag{3.42}$$

The local thermal power density can therefore be written as

$$q''' = \frac{\kappa}{\nu} (\Sigma_a + \Sigma_{12}) k_\infty \phi_1$$

$$= \left(\frac{\kappa}{\nu}\right) \left(\frac{D_1}{M^2}\right) k_\infty \phi_1 \tag{3.43}$$

Assuming that κ, D_1 and M^2 do not vary with position, substitution of Eq. (3.43) into Eq. (3.39) yields:

$$\nabla^2 \left(\frac{f}{k_\infty}\right) + \frac{1}{M^2} \left[\frac{\rho}{1-\rho} \right] \left[\frac{f}{k_\infty} \right] = 0 \tag{3.44}$$

where f is the normalized local power fraction

$$= Vq'''/Q \ ,$$

V is the nodal volume,

and Q is the total core power.

The Laplacian in Eq. (3.44) can be approximated as the difference between the local value and the average of its surroundings, in which case Eq. (3.44) can be rewritten:

$$\frac{\left(\frac{V_i}{V_s}\right)\left(\frac{\bar{f}}{k_\infty}\right)_s - \left(\frac{f}{k_\infty}\right)_i}{\gamma h^2} + \left(\frac{1}{M}\right)^2 \rho_i f_i = 0 \qquad (3.45)$$

where h is the size of the node -- in our case the width of

an assembly,

γ is a constant,

and subscripts i and s denote the node and its surroundings

(here the sum of 8 nodes), respectively.

Solving Eq. (3.45) for the power fraction in node i gives:

$$f_i = \frac{\left(\frac{V_i}{V_s}\right)\left(\frac{\bar{f}}{k_\infty}\right)_s}{1 - \theta \rho_i} \qquad (3.46)$$

where $\theta = \left(1 + \frac{\gamma h^2}{M^2}\right)$

here treated as a constant, since we are concerned primarily with PWR cores.

Equation (3.46) constitutes the power-sharing algorithm required in the LRM methodology. For a group of assemblies

(usually a fuel reload batch) in a critical core, we will use the form:

$$f_i = \frac{\bar{f}}{1 - \theta \rho_i} \tag{3.47}$$

where $\bar{f}$ is the average power fraction for an aggregation of assemblies of the size in question (for example, $\bar{f} = \frac{1}{n}$ for an n-batch core).

An important constraint which the power split relation must comply to is

$$\sum_{i=1}^{n} f_i = 1 \tag{3.48}$$

or

$$\sum_{i=1}^{n} (f_i - \bar{f}) = \sum_{i=1}^{n} (f_i - \frac{1}{n}) = 0 \tag{3.49}$$

Substituting Eq. (3.47) for f_i, we have

$$\sum_{i=1}^{n} \left[\left(\frac{\frac{1}{n}}{1 - \theta \rho_i} \right) - \frac{1}{n} \right] = \sum_{i=1}^{n} \frac{1}{n} \left[\frac{1 - (1 - \theta \rho_i)}{1 - \theta \rho_i} \right]$$

$$= \sum_{i=1}^{n} \theta \left(\frac{\frac{1}{n}}{1 - \theta \rho_i} \right) \rho_i$$

$$= \theta \sum_{i=1}^{n} f_i \rho_i = 0 \tag{3.50}$$

Since θ is a constant, we will have

$$\sum_{i=1}^{n} f_i \rho_i \ = \ 0 \tag{3.51}$$

This equation can be recognized as the power-weighted prescription for core reactivity averaging, which was independently derived in the previous section (3.3.1) using the definition of reactivity. Hence Eq. (3.47) is a compatible power split formulation.

Finally, suppose we perturb the reactivity locally, say, in region i; the change in the local reactivity ($\Delta\rho_i$) affects the global reactivity according to (Taylor series expansion):

$$\Delta\bar{\rho} \ \simeq \ \sum \left(\frac{\partial\bar{\rho}}{\partial\rho_i} \right) \cdot \Delta\rho_i \tag{3.52}$$

Application of the power split relation (Eq. 3.47) gives:

$$\Delta\bar{\rho} \ \simeq \ \sum \frac{\partial}{\partial\rho_i} \{f_i\rho_i\} \ \Delta\rho_i$$

$$= \ \sum \frac{\partial}{\partial\rho_i} \{ \frac{\frac{1}{n}}{1-\theta\rho_i} \cdot \rho_i \} \ \Delta\rho_i$$

$$= \ \frac{1}{n} \sum \{ \frac{1}{(1-\theta\rho_i)^2} \} \ \Delta\rho_i \tag{3.53}$$

or,

$$\Delta\bar{\rho} \ \simeq \ n \sum f_i^2 \cdot \Delta\rho_i \tag{3.54}$$

Hence the power split relation given by Eq. (3.47) generates the familiar source-squared weighting typical of perturbation

theory methods. This is another argument favoring the use of this form of the power sharing algorithm.

Note that to a first order expansion, the power sharing prescription may be written in many forms:

$$f = \frac{\bar{f}}{1 - \theta\rho} \simeq f(1 + \theta\rho) \qquad (3.47b)$$

$$\simeq \bar{f}(\frac{1}{1-\rho})^{\theta} \equiv \bar{f}k^{\theta} \qquad (3.47c)$$

The last expression is in fact the form deduced by Sefcik [S-2] on purely empirical grounds; the first expression, which is linear in ρ, will prove useful in analytic applications to be discussed later. Also see Appendix E for addditional discussion.

3.4.2 VERIFICATION FOR INTERIOR ASSEMBLIES

The power split relation given by Eq. (3.47) is compatible with several powerful constraints imposed on the linear reactivity model methodology development. However, verification of this power sharing algorithm using results generated from detailed computer analysis is necessary, so as to evaluate the accuracy with which the algorithm describes a specific or generic reactor core environment. Conditions in the interior of the core are considered first, and application of the power split equation to the core peripheral assemblies is featured in the next section.

In the interior of a PWR core (i.e., excluding the peripheral ring of assemblies), the fuel assemblies with higher reactivity

are normally surrounded with low reactivity fuel assemblies
to achieve power flattening. This well shuffled core pattern
can be represented by the configuration and boundary condi-
tions shown in Fig. 3.8. To test the power split relation
given by Eq. (3.46), a series of PDQ-7 calculations were
performed with three successive constant values of k_2 (0.9,
1.0, 1.2) and the values of k_1 were varied over a wide range
of enrichments, burnups, fuel-to-moderator ratios and boron
concentrations. Figure 3.9 shows the plot of $\left[(\frac{V_1}{V_2})(\frac{\overline{f}}{k_\infty})_2\right] / f_1$
versus $\rho_1 = 1 - \frac{1}{k_1}$. Plotted in this manner, the slope of
the curve is just the constant θ. While the linearity of the
relationship is evident, the data scatters significantly
(linear fit $R^2 = 0.831$), in particular the data points
segregate according to the value of k_2. If only $k_2 = 1.0$
data is selected the agreement is considerably improved:
$R^2 = 0.952$. This is not altogether unexpected and can be
explained by the fact that the majority of the data points
do not correspond to a critical configuration -- a condition
imposed on the derivation of the power split equation. Other-
wise the agreement must be considered good in view of the
large variation in assembly properties considered.

A more appropriate set of data for the verification of
the power split equation can be obtained from whole core
analyses. Moreover, a value for the constant θ (See Eq. 3.47)
which characterizes the particular core in question can be
determined. This parameter is required in the application of
the LRM methodology for the purpose of fuel management stra-
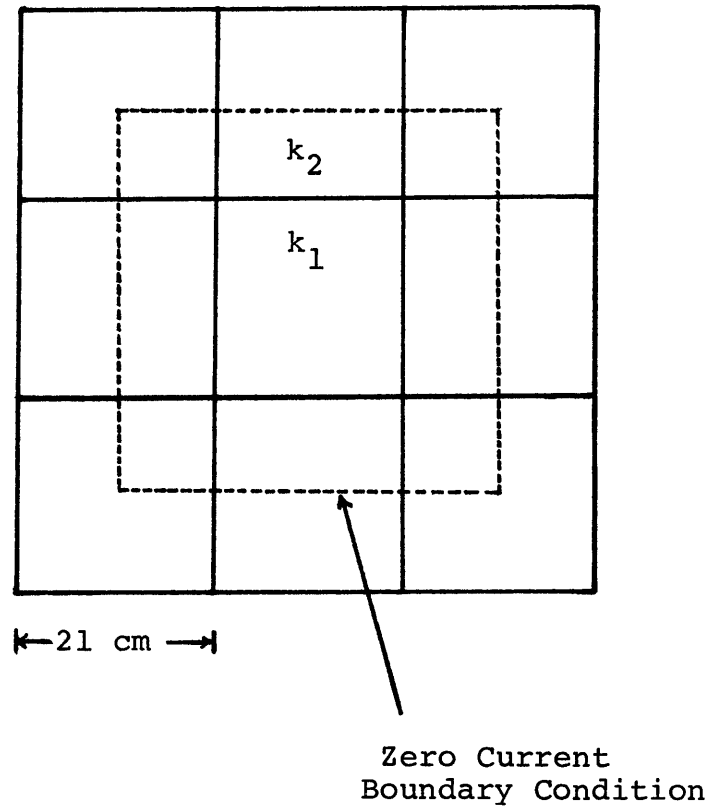
Fig. 3.8 Assembly Configuration for the Verification
of the Power Split Relation (3 x 3 Bundles)
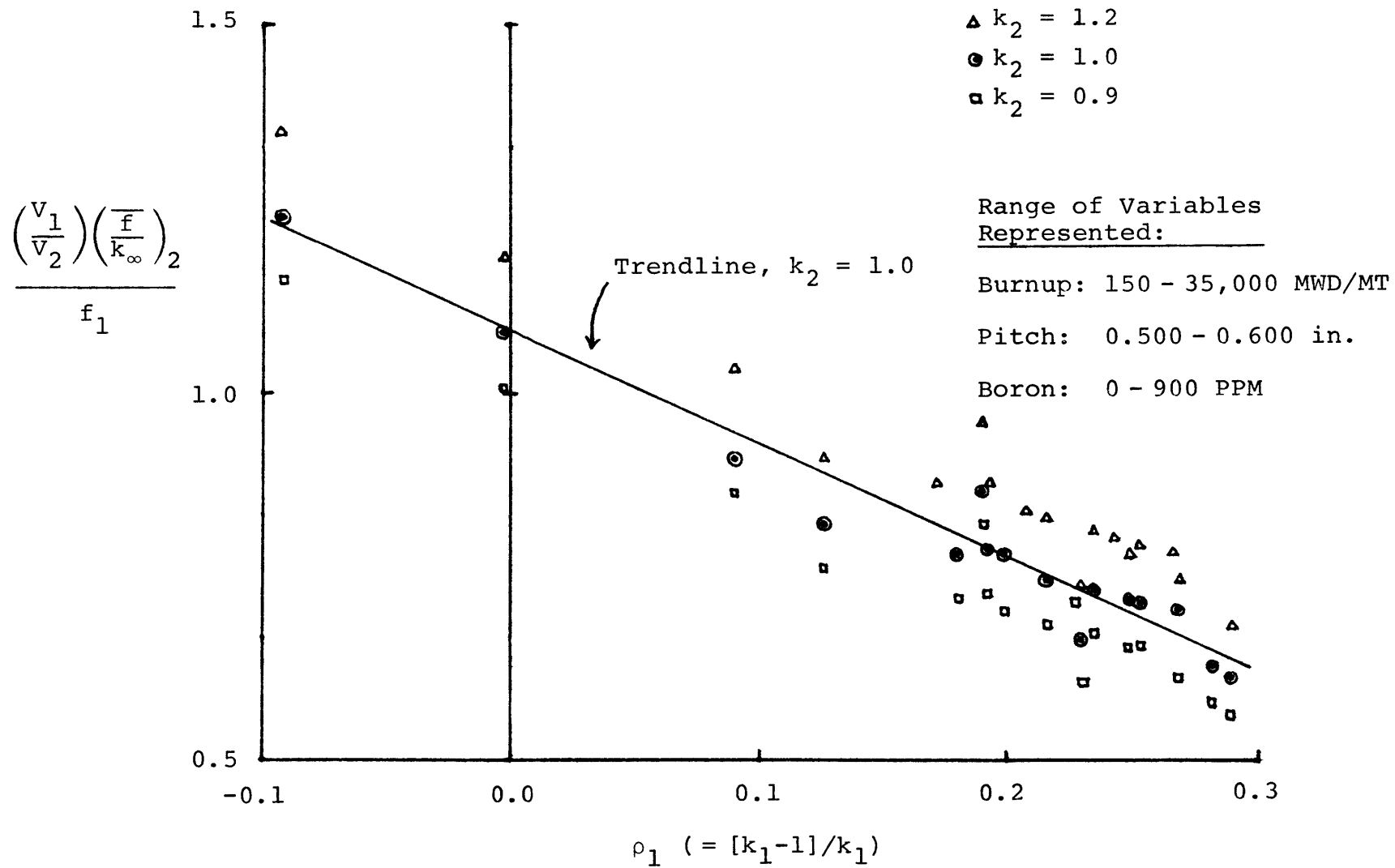
Fig. 3.9 Power Fraction-Reactivity Correlation for a 3 x 3 - Bundle Problem

tegy evaluation.

The two reactor system designs used in this context are the Maine Yankee cycle-four reload design and a representative CE System-80^{TM} core design. The core maps together with the assemly k and its relative power for these two designs are shown in Figs. 3.10 and 3.11. The inverse of the interior assembly powers $(q/\bar{q})^{-1}$ as a function of the assembly reactivity ρ values are plotted in Figs. 3.12 and 3.13 for the Maine Yankee and System-80^{TM} core designs, respectively. The wide scatter among assembly data is evident from the figures. The reason for this observation is similar to that given for the results of the 3 x 3 fuel bundle configuration analyses. However, for the present purpose it is more relevant to plot the data for assemblies grouped into a batch. Moreover, on the batch basis, the criticality constraint assumed in the derivation of the power split equation is more nearly satisfied. Figure 3.14 shows the results for the Maine Yankee cycle 4 reload core design. The best-fit line can be described by the equation

$$\left(\frac{q_{batch}}{q_{average}} \right)^{-1} = \left(\frac{f_{batch}}{\bar{f}} \right)^{-1} = 0.98 - \theta \rho_{batch} \qquad (3.55)$$

The constant θ has a value of 1.42. The coefficient of determination (R^2) for this plot is 0.988. Equation (3.55) can be rewritten as:

$$f_{batch} \simeq \frac{\bar{f}}{1 - \theta \rho_{batch}} \qquad (3.56)$$

The legend box:

$$\frac{k}{q/\bar{q}}$$

Core map (each cell shows k on top and $q/\bar{q}$ on bottom):

							1.194	1.194
							0.689	0.949
				1.194	1.194	1.194	0.909	1.134
				0.698	0.927	1.101	0.952	1.324
			1.194	1.138	0.934	0.928	1.139	0.935
			0.843	1.153	0.891	0.943	1.280	1.062
		1.194	1.138	0.936	1.088	1.003	0.906	1.036
		0.840	1.284	0.987	1.148	0.986	0.937	1.080
	1.194	1.138	0.936	1.075	1.016	0.917	1.103	1.011
	0.696	1.152	0.991	1.200	1.040	0.935	1.179	1.097
	1.194	1.934	1.089	1.016	0.932	1.109	0.912	1.075
	0.920	0.833	1.150	1.045	0.916	1.161	0.896	1.152
	1.195	0.928	1.003	0.917	1.110	1.908	1.082	1.006
	1.087	0.931	0.972	0.929	1.161	0.914	1.090	1.010
1.194	0.909	1.140	0.896	1.103	0.912	1.082	0.910	1.037
0.680	0.936	1.251	0.791	1.158	0.889	1.090	0.832	0.907
1.195	1.139	0.935	1.036	1.011	1.075	1.006	1.036	0.908
0.934	1.300	1.039	1.049	1.078	1.041	1.005	0.905	0.734

Fig. 3.10   Core Map for Maine Yankee Cycle 4 Redesign
[S-2]

Legend box:

$$\frac{k}{q/\bar{q}}$$

	C1	C2	C3	C4	C5	C6	C7	C8
							1.174 / 0.694	1.170 / 0.958
				1.173 / 0.772	1.169 / 0.995	1.168 / 1.123	0.900 / 0.878	1.137 / 1.338
			1.169 / 0.923	1.135 / 1.278	0.975 / 1.038	0.901 / 0.856	1.138 / 1.295	0.900 / 0.966
		1.169 / 0.923	1.135 / 1.306	0.956 / 1.064	1.137 / 1.280	0.919 / 0.816	0.905 / 0.839	1.139 / 1.267
	1.173 / 0.771	1.135 / 1.277	0.956 / 1.063	0.970 / 0.956	0.901 / 0.819	0.926 / 0.817	0.986 / 0.923	0.908 / 0.830
	1.169 / 0.994	0.975 / 1.037	1.137 / 1.279	0.901 / 0.819	0.041 / 1.071	1.055 / 1.133	1.025 / 1.067	1.012 / 1.043
1.174 / 0.694	1.168 / 1.121	0.901 / 0.854	0.919 / 0.815	0.926 / 0.816	1.055 / 1.132	1.040 / 1.120	0.901 / 0.860	1.069 / 1.158
1.170 / 0.956	0.900 / 0.875	1.138 / 1.292	0.905 / 0.837	0.988 / 0.922	1.025 / 1.063	0.901 / 0.852	1.054 / 1.138	1.012 / 1.085
	1.137 / 1.334	0.900 / 0.963	1.139 / 1.264	0.906 / 0.828	1.024 / 1.053	1.040 / 1.095	1.024 / 1.102	0.896 / 0.877

Fig. 3.11 Core Map for Combusion Engineering System-80[TM] Core
[W-1]

$$\frac{1}{(q \, / \, \overline{q})}$$

Assembly Reactivity, ρ
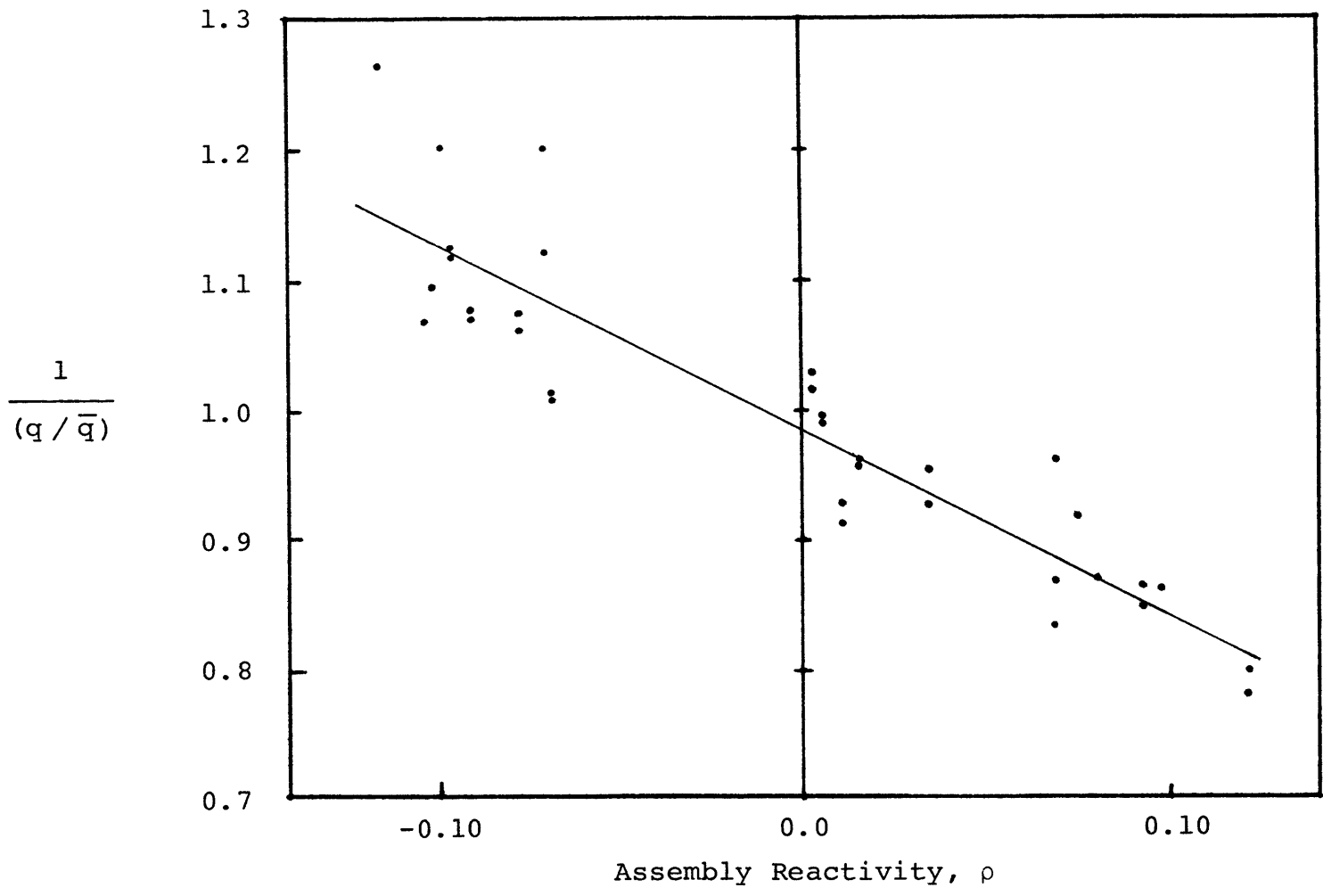
Fig. 3.12   Reciprocal Assembly Power vs. Assembly Reactivity for Interior
Assemblies in the Main Yankee Cycle 4 Reload Design
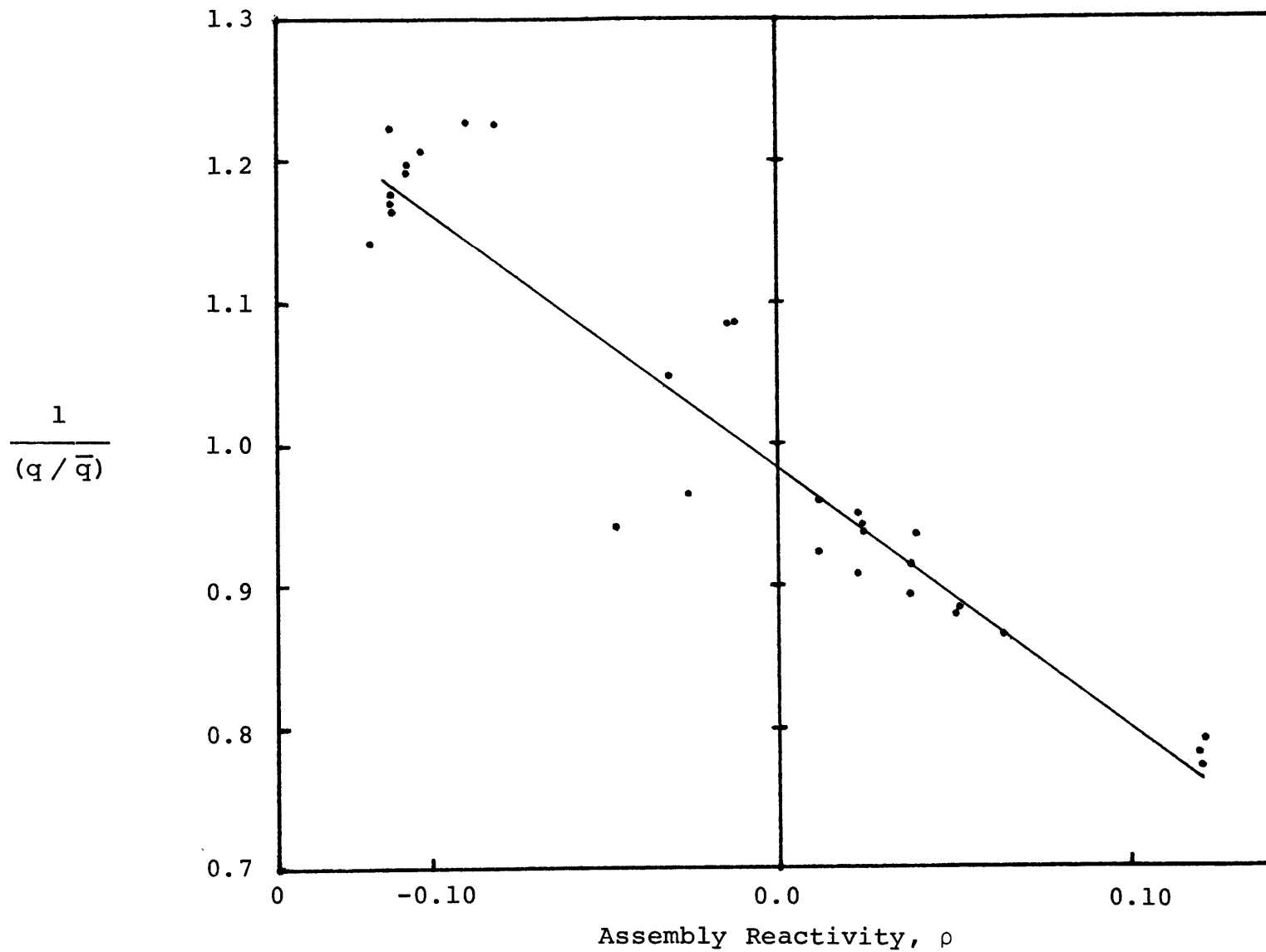
Fig. 3.13 Reciprocal Assembly Power vs. Assembly Reactivity for Interior
Assemblies in a Representative C-E System 80^{TM} Core

$$\frac{1}{\left(\frac{q_{batch}}{q_{average}}\right)}$$

$\theta = 1.42$

$R^2 = 0.988$

1.20

1.10

1.00

0.90

0.80

0.70

-0.15   -0.10   -0.05   0.0   0.05   0.10   0.15

Batch Reactivity, ρ_{batch}
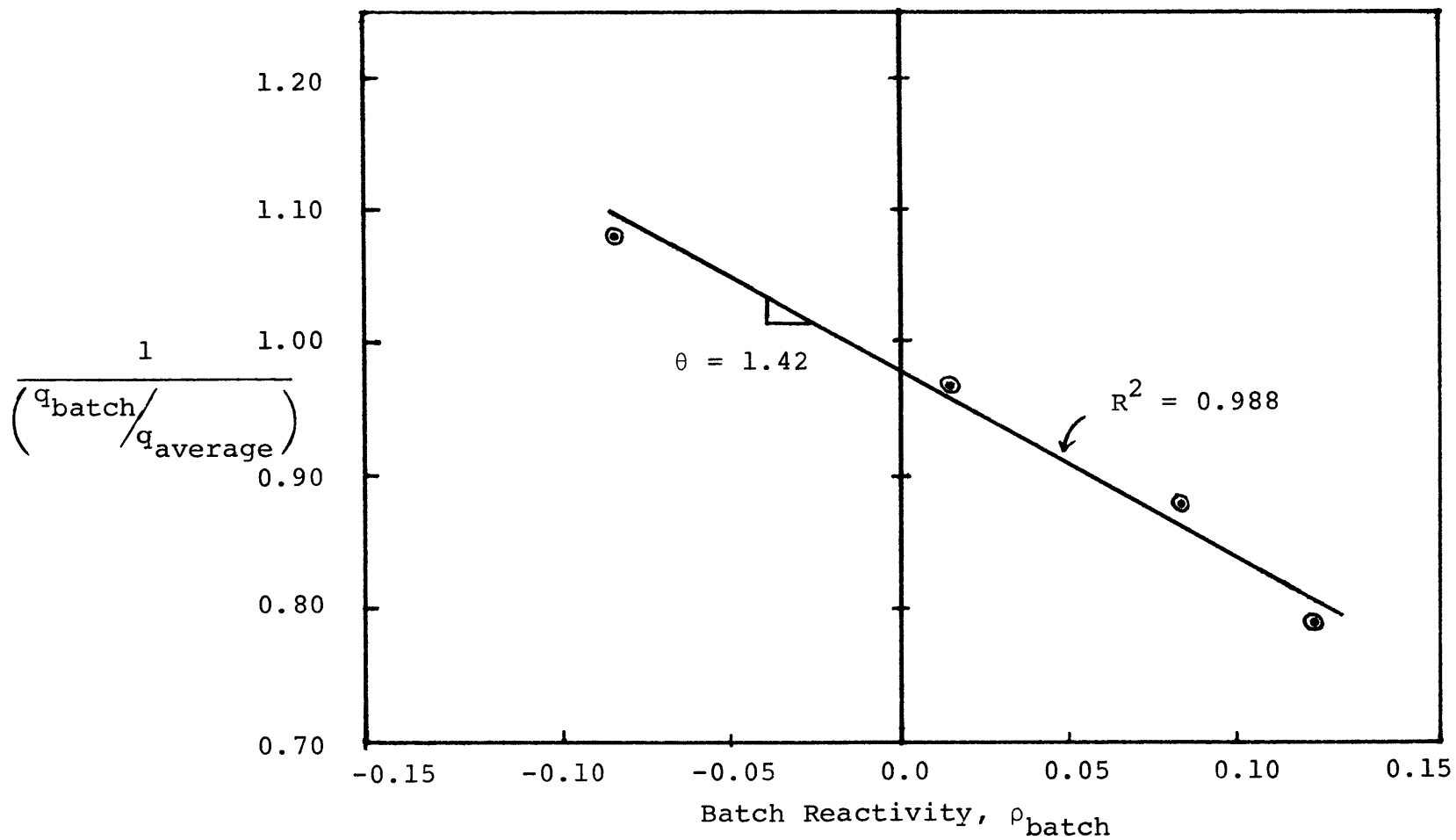
Fig. 3.14   Regression Line of Power vs. Reactivity for Main Yankee Fuel Batches

which corresponds exactly to the power split relation given in Eq. (3.47). A similar analysis for the System-80^{TM} core yielded a θ value of 1.81 with an R^2 value of 0.972. The plot for the batch power versus batch reactivity of this core is shown in Fig. 3.15. Thus, even though individual <u>assembly</u> power cannot be predicted accurately, the <u>batch-wise</u> power splits can be calculated to the level of accuracy required for detailed fuel management analysis.

3.4.3 TREATMENT OF PERIPHERAL ASSEMBLIES

In the derivation of the algorithm for the power sharing relation among assemblies, the implicit assumption in the assemblies' arrangement is that the test assembly is completely surrounded by other fuel assemblies. Such an assembly configuration is representative of the assemblies in the interior of the core. However, assemblies situated at the periphery of the core have one or two of their sides bordered by non-fuel regions of coolant and structure. The power split relation which has been developed so far can be extended to include these peripheral assemblies.

We have shown in the previous section that the leakage reactivity, ρ_L, of the assemblies placed at the core periphery can be correlated to the peripheral power fraction f_{per}:

$$\rho_L = \alpha f_{per} \qquad (3.57)$$

where α is a constant.
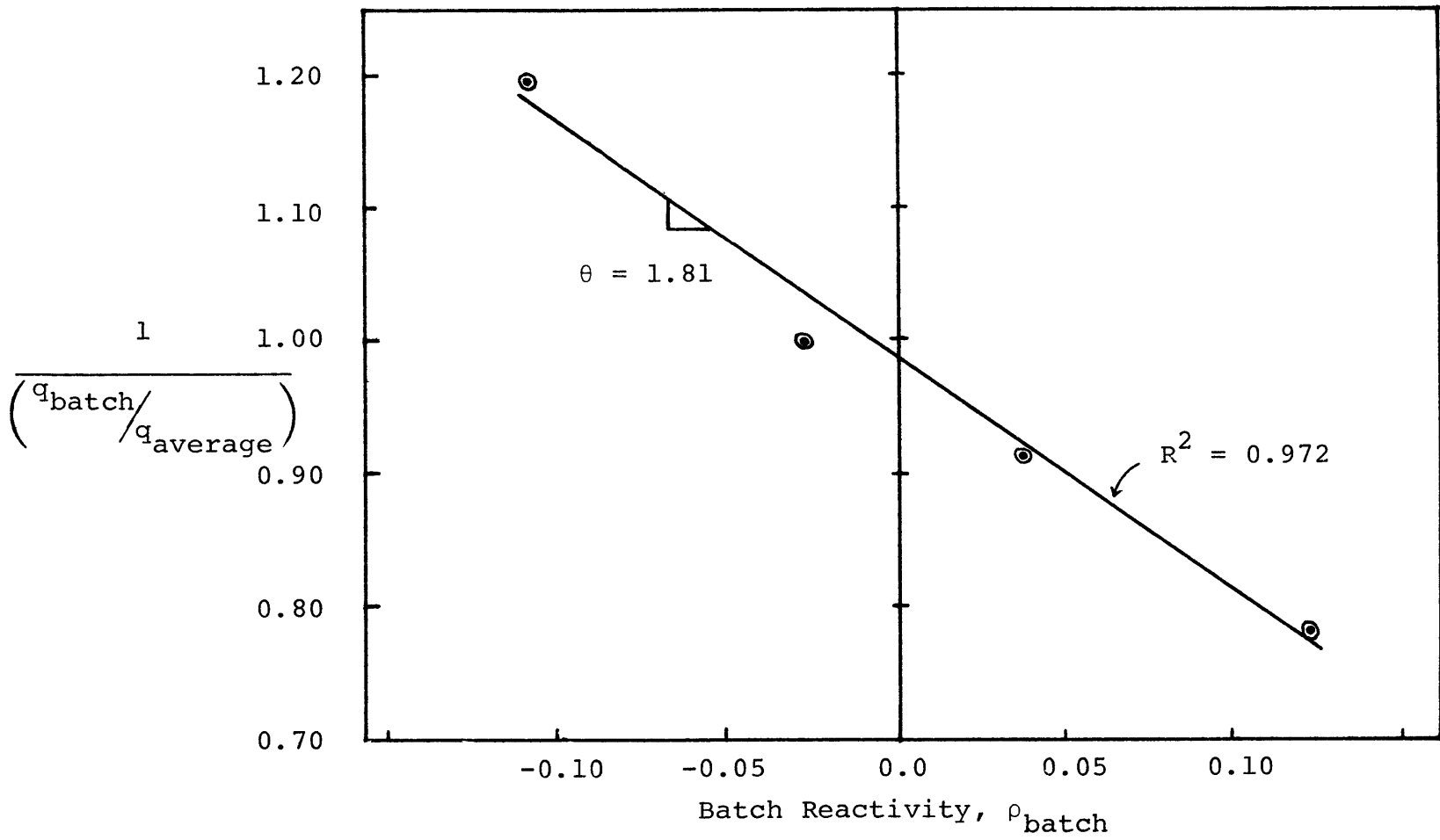
Fig. 3.15 Regression Line of Power vs. Reactivity for C-E System-80^{TM} Fuel Batches

This equation can be rewritten in terms of fuel batches in the peripheral locations:

$$\rho_L = \alpha \sum_{i=1}^{m} f_i \tag{3.58}$$

where $\sum_{i=1}^{m} f_i = f_{per}$ is the power fraction of the core's peripheral batches, m in number. The system reactivity of a steady state core with n fuel batches (m of which are on the core periphery) and leakage reactivity ρ_L has been shown to be

$$\rho_{sys} = \sum_{i=1}^{n} f_i \rho_i - \rho_L \tag{3.59}$$

At the end of cycle, $\rho_{sys} = 0$, and substituting Eq. (3.58) for ρ_L into Eq. (3.59) yields:

$$\sum_{i=1}^{n} f_i \rho_i = \alpha \sum_{i=1}^{m} f_i \tag{3.60}$$

or

$$\underbrace{\sum_{i=1}^{n-m} f_i \rho_i}_{\substack{\text{Interior} \\ \text{Batches}}} + \underbrace{\sum_{i=1}^{m} f_i \rho_i}_{\substack{\text{Peripheral} \\ \text{Batches}}} = \alpha \sum_{i=1}^{m} f_i$$

$$\sum_{i=1}^{n-m} f_i \rho_i + \sum_{i=1}^{m} f_i (\rho_i - \alpha) = 0 \tag{3.61}$$

The power split equation which is compatible with this power-weighted prescription for core reactivity averaging is

$$f_i = \frac{\bar{f}}{1 - \theta(\rho_i - \alpha)} \tag{3.62}$$

where $\alpha = \begin{cases} \alpha & \text{for peripheral batches} \\ 0 & \text{for interior batches} \end{cases}$

One of the key constraints this proposed power split relation must satisfy is the summation of batch power fractions to unity, or equivalently,

$$\sum_{i=1}^{n} f_i - 1 = 0 = \sum_{i=1}^{n} (f_i - \frac{1}{n}) \tag{3.63}$$

This is the same as writing (substituting and reorganizing the f_i from Eq. 3.62):

$$\sum_{i=1}^{n} \left[\frac{\frac{1}{n}}{1 - \theta(\rho_i - \alpha)} - \frac{1}{n} \right] = 0 \tag{3.64}$$

or,

$$\sum_{i=1}^{n-m} \left[\frac{\frac{1}{n}}{1 - \theta\rho_i} - \frac{1}{n} \right] + \sum_{i=1}^{m} \left[\frac{\frac{1}{n}}{1 - \theta(\rho_i - \alpha)} - \frac{1}{n} \right]$$

$$\begin{array}{cc} \text{Interior} & \text{Peripheral} \\ \text{Batches} & \text{Batches} \end{array}$$

$$= \sum_{i=1}^{n-m} \frac{1}{n} \left[\frac{1 - (1 - \theta\rho_i)}{1 - \theta\rho_i} \right] + \sum_{i=1}^{m} \frac{1}{n} \left[\frac{1 - \{1 - \theta(\rho_i - \alpha)\}}{1 - \theta(\rho_i - \alpha)} \right]$$

$$= \theta \sum_{i=1}^{n-m} [\ \frac{\frac{1}{n}}{1-\theta\rho_i} \cdot \rho_i\ ] + \theta \sum_{i=1}^{m} [\ \frac{\frac{1}{n}(\rho_i-\alpha)}{1-\theta(\rho_i-\alpha)}\ ]$$

$$= \theta \sum_{i=1}^{n-m} f_i\rho_i + \theta \sum_{i=1}^{m} f_i(\rho_i-\alpha) = 0 \qquad (3.65)$$

Since θ is a constant, Eq. (3.65) can be rewritten as

$$\sum_{i=1}^{n-m} f_i\rho_i + \sum_{i=1}^{m} f_i(\rho_i-\alpha) = 0 \qquad (3.66)$$

which is the power-weighted prescription for core reactivity averaging given earlier in Eq. (3.61).

3.5 AN ANALYTICAL MODEL FOR DISCHARGE BURNUP

The LRM methodology has now been sufficiently developed to permit the accurate computation of the discharge burnup for various cases of fuel management strategies of contemporary interest. An analytical model will be developed in this section and an automated procedure which numerically calculates the discharge burnup based on the LRM methodology is described in the next chapter. The computer program developed for this purpose can easily handle cases which are too diffi- cult to be modeled in a closed analytical form. In addition, the numerical results obtained are used to check and normalize the analytical ones.

An approximation is required to facilitate the analytical derivation of discharge burnup equations for different power history trajectories. To first order, the power split rela- tion given by Eq. (3.56) becomes

$$f_{batch} = \bar{f}(1 + \theta\rho_{batch}) \qquad (3.67)$$

This linearized version of the power split equation fits core map data equally well, and this is testified to by the plots shown in Figs. 3.16 and 3.17 for the CE System-80^{TM} core design and the Maine Yankee cycle 4 reload design, respectively.

Consider the reactivity versus burnup trace shown in Fig. 3.18. For an n-batch steady-state core, and with the assumption that the average power fractions remain constant over a given cycle,

$$\rho_1 = \rho_o - A \cdot B_c \cdot \bar{f}_1/\bar{f}$$
$$\rho_2 = \rho_o - A \cdot B_c \cdot (\bar{f}_i + \bar{f}_2)/\bar{f}$$
$$\cdot$$
$$\cdot$$
$$\cdot$$
$$\rho_n = \rho_o - A \cdot B_c \cdot (\bar{f}_1 + \bar{f}_2 + \cdots + \bar{f}_n)/\bar{f} \qquad (3.68)$$

where $\bar{f}_i$ is the average power fraction of batch i,

$\bar{f}$ is the core-average power fraction $= \dfrac{1}{n}$

and B_c is the cycle average burnup.

The approach is to weight Eq. (3.68) at the end of cycle using the power split relation given by Eq. (3.67), and then set the system reactivity equal to zero:

$$\rho_{sys} = \sum_{i=1}^{n} f_i \rho_i = 0 \qquad (3.69)$$

Now, from Eq. (3.67), which applies when the core environment
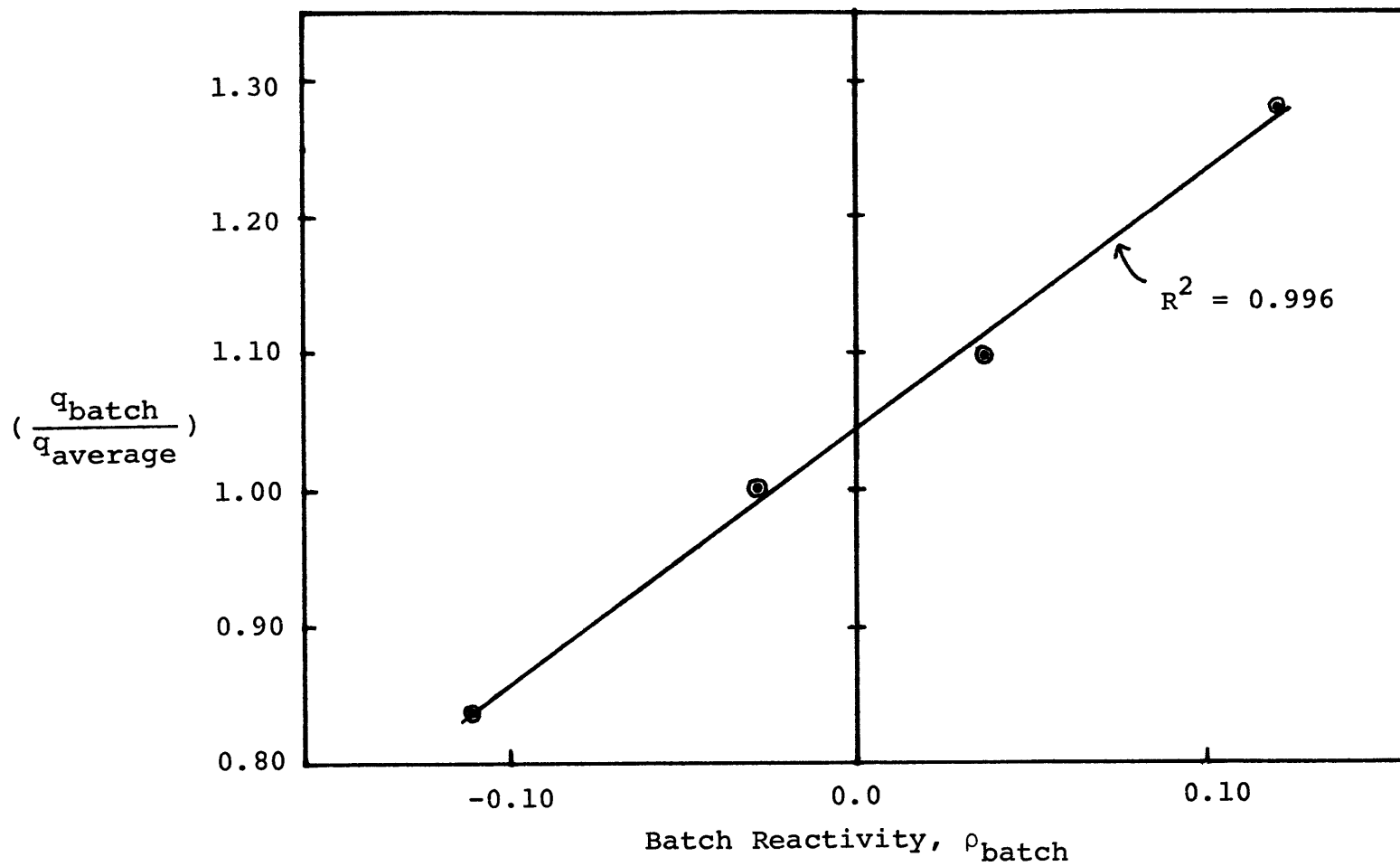
Fig. 3.16 Linearized Power versus Reactivity Correlation for C-E System-80^{TM} Fuel Batches
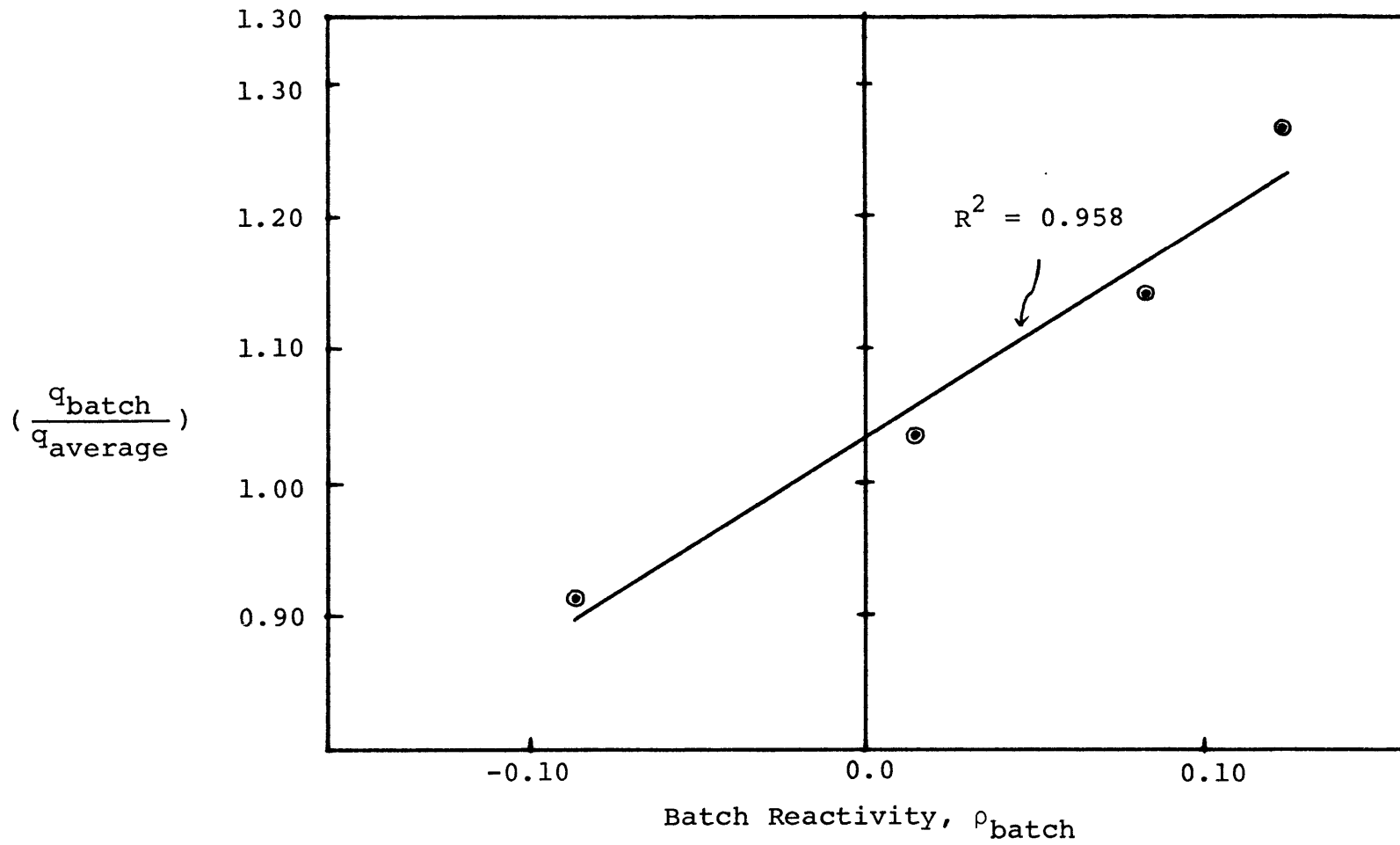
Fig. 3.17   Linearized Power versus Reactivity Correlation for Maine Yankee Fuel Batches

is critical, we can write

$$\bar{f}_i = \bar{f}(1 + \theta\bar{\rho}_i) \qquad (3.70)$$

And, for the jth batch

$$\bar{f}_i + \bar{f}_2 + \cdots \bar{f}_j = j\bar{f}(1 + \theta\bar{\bar{\rho}}_j) \qquad (3.71)$$

where $\bar{\bar{\rho}}_j$ is the average over the in-core history to date, that is,

$$\bar{\bar{\rho}}_j = \frac{\bar{\rho}_1 + \bar{\rho}_2 + \cdots + \bar{\rho}_j}{j}$$

$$= \frac{1}{j} \sum_{i=1}^{j} \bar{\rho}_i \qquad (3.72)$$

But the correct expression for $\bar{\bar{\rho}}_j$ to be used is that in a poisoned core. This implies that the reactivity values must be reduced by (to a good approximation) the cycle average control poison penalty. To determine the poison adjusted reactivity values, we must first get an estimate of the batch reactivity. Using the equal power sharing approximation, the reactivity of batch i at the end of cycle is

$$\rho_i = (1 - \frac{2i}{n+1})\rho_o \qquad (3.73)$$

The cycle average reactivity for batch i, is thus

$$\bar{\rho}_i = \frac{1}{2}(\rho_{i,BOC} + \rho_{i,EOC})$$

$$= \frac{1}{2}[\rho_o(1 - 2\frac{(i-1)}{n+1}) + \rho_o(1 - \frac{2i}{n+1})]$$

$$= (\frac{n+2}{n+1} - \frac{2i}{n+1}) \rho_o \tag{3.74}$$

Substituting this equation into Eq. (3.72), the average reactivity of batch j over its entire in-core history to date, becomes,

$$\bar{\rho}_j = \frac{1}{j} \sum_{i=1}^{j} (\frac{n+2}{n+1} - \frac{2i}{n+1}) \rho_o$$

$$= \frac{1}{j} [(\frac{n+2}{n+1})j - (\frac{2}{n+1}) \frac{j(j+1)}{2}] \rho_o$$

$$= [(\frac{n+2}{n+1}) - (\frac{j+1}{n+1})] \rho_o \tag{3.75}$$

From this expression, we can determine the cycle average excess reactivity which must be suppressed using soluble poison:

$$\bar{\bar{\rho}}_n = [(\frac{n+2}{n+1}) - (\frac{n+1}{n+1})] \rho_o$$

$$= \frac{\rho_o}{(n+1)} \tag{3.76}$$

This is also the cycle average poison which must be subtracted from all the reactivity values. The poison adjusted average reactivity of batch j over its in-core residence to

date, is therefore

$$\vec{\rho}_j = \bar{\bar{\rho}}_j - \bar{\bar{\rho}}_n$$

$$= (\frac{n}{n+1} - \frac{j}{n+1}) \rho_o \tag{3.77}$$

A power-weighted reactivity balance gives (from Eqs. 3.68, 3.69, 3.70, 3.73 and 3.77):

$$\sum_{i=1}^{n} f_i \rho_i = 0 = \rho_o \bar{f} \{ n + \theta \sum_i \rho_i \}$$

$$- A \cdot B_c \cdot \bar{f} \sum_i [1 + \theta (1 - \frac{2i}{n+1})] \cdot i \cdot$$

$$[1 + \theta (\frac{n}{n+1} - \frac{i}{n+1}) \rho_o] \tag{3.78}$$

Expanding and rearranging Eq. (3.78) and noting that when $\theta = 0$ the discharge burnup for the flat power case is

$$B_o = \frac{2n}{n+1} (\frac{\rho_o}{A}) = nB_{co} \tag{3.79}$$

where B_{co} is the cycle average burnup for the equal power sharing case.

We will obtain, after considerable algebra:

$$\frac{B}{B_o} = [1 + (\theta\rho_o)^2 \frac{(n-1)}{3(n+1)^2}]^{-1} \tag{3.80}$$

or

$$B = B_o / (1+\varepsilon) \qquad\qquad (3.81)$$

The factor ε, being a positive number in this case, gives an estimate of the penalty in discharge burnup due to the unequal sharing of power among the fuel batches. As expected, ε will approach zero as n becomes large, for fixed $(\theta\rho_o)$. This simply means that one can approach an equal power sharing condition if the number of reload batches is sufficiently large. However, it must be noted that ε is only a second order effect, and as will be seen, thus is rather small ($< 1\%$).

Using the same approach, equations similar in form to Eq. (3.81) can be derived for the different power history trajectories shown in Fig. 3.19. The $\rho(B)$ trace designated case 4 in Fig. 3.19 is a limiting case which has been identified for assessment vis-à-vis burnable poison control, namely a core controlled entirely by burnable poison in the fresh fuel without the need for soluble poison. In this particular case, we can show that (see Appendix B) the beginning-of-life reactivity of a batch of fuel is equal to its end-of-life reactivity. Or equivalently, the BOC reactivity of the poisoned fresh fuel, $\rho_{1,BOC}$ is equal to the EOC reactivity of the oldest batch of fuel $\rho_{n,EOC}$. The results are summarized in Table 3.3.

Although the effect of leakage or permanent poison shim was not explicitly modeled in the analytical derivation of the discharge burnup, it can be accounted for through its
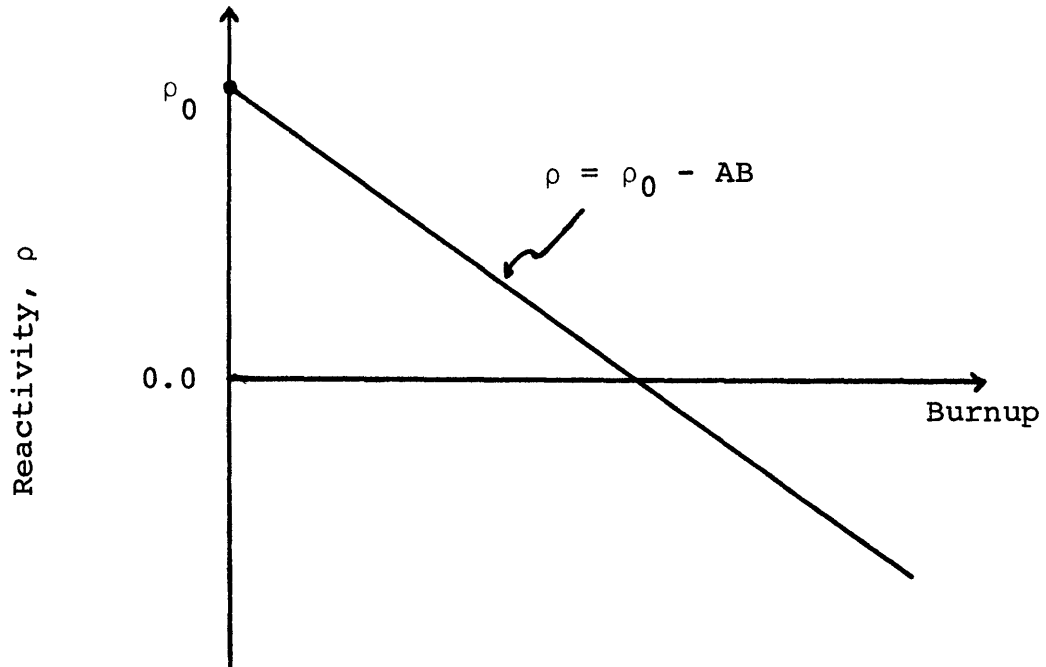
Fig. 3.18 Reactivity versus Burnup Curve for a Fuel
Assembly or Assemblies in a Batch
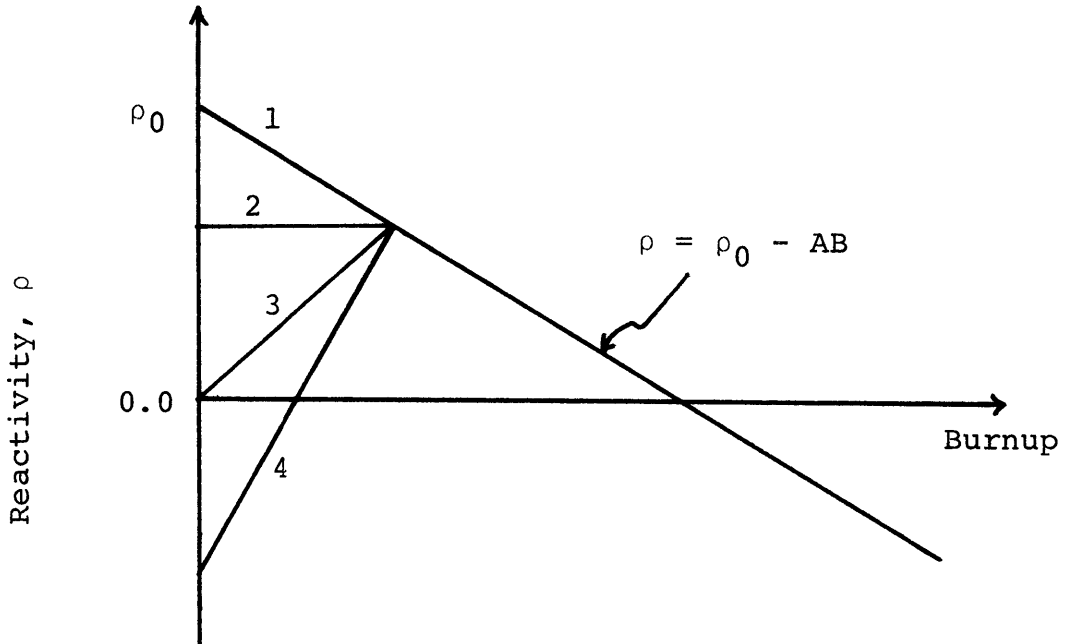
Case 1: No Burnable Poison

Case 2: Constant ρ in the First Cycle

Case 3: Zero ρ at the Beginning of Life

Case 4: All Control via Burnable Poison

Fig. 3.19 Various ρ(B) Traces of Reload Fuel with Burnable Poison

effect on the equal-power-sharing approximation discharge

burnup B_o, that is,

$$B_o' = (\frac{2n}{n+1}) \frac{(\rho_o - \Delta)}{A} \tag{3.82}$$

Where Δ is the reactivity penalty due to neutron leakage

or the presence of chemical shim. Moreover, in cases where

burnable poison is employed in the fresh fuel batch, the asso-

ciated residual poison in this batch of fuel over the remaining

cycles can also be accounted for through Δ. However, the

results given in Table 3.3 assumed the complete burnout of

the burnable poison at the end of cycle.

For the Maine Yankee reactor system, with a 3-batch fuel

management scheme (n=3), typical values of ρ_0, θ and A are

given below:

$$\rho_0 = 0.22351$$

$$A = 9.2721 \times 10^{-6} \text{ MT/MWD}$$

$$\theta \simeq 1.5$$

The discharge burnups corresponding to the various reactivity

versus burnup histories depicted in Fig. 3.19 are given in

Table 3.4. As expected, the penalty in discharge burnup due

to unequal power sharing among fuel batches is only about 0.5%

since it is a second order effect.

A most interesting observation from the results given in

Table 3.4 is that the discharge burnups of those cases emp-

TABLE 3.3   ANALYTICAL RESULTS FOR COMMON REACTIVITY HISTORIES

CASE	PRESCRIPTION FOR ε[*]
1. No burnable poison	$(\theta\rho_o)^2 \dfrac{(n-1)}{3(n+1)^2}$
2. Constant ρ in 1st cycle	$-(\theta\rho_o)\dfrac{(n-1)}{n(n+1)^2} + (\theta\rho_o)^2 \dfrac{(n-1)^2}{3n(n+1)^2}$
3. Zero ρ at BOL	$-(\theta\rho_o)\dfrac{(n-1)}{2n(n+1)} + (\theta\rho_o)^2 \dfrac{(n-1)^2}{6n(n+1)^2}$
4. All control via burnable poison	$-(\theta\rho_o)\dfrac{(n-1)}{(n+1)^2}$

---

[*] Discharge Burnup $B_d = B_o \,/\, (1+\varepsilon)$

and B_o = discharge burnup for hypothetical uniform power history

$$= (\frac{2n}{n+1})\,(\frac{\rho_o}{A})$$

where n = number of staggered reload batches.

TABLE 3.4   REPRESENTATIVE DISCHARGE BURNUPS CORRESPONDING TO
VARIOUS ρ(B) HISTORIES

CASE	ε	B_d(MWD/MT)	% DIFFERENCE[*] FROM THE FLAT POWER CASE, B_o
1. No burnable poison	0.005	35978	-0.5
2. Constant ρ in 1st cycle	-0.011	36560	1.1
3. Zero ρ at BOL	-0.026	37123	2.7
4. All control via burnable poison	-0.042	37743	4.4

[*] $B_d = B_o/(1+\varepsilon)$

and $B_o = (\frac{2n}{n+1})(\frac{\rho_o}{A}) = 36158$ MWD/MT

loying burnable poison are <u>better</u> than that of the flat power case by about 1.0 - 4.4%. Ruling out the case of using burnable poison for all reactivity control as being impracticable, an increase in discharge burnup of about 2.7% over that of the flat power case can be achieved using burnable poison to suppress reactivity in the fresh fuel batch as in case 3 of Fig. 3.19. However, the presence of residual poison may negate the gain in the discharge burnup. We can estimate the residual poison reactivity penalty to break even with respect to discharge burnup compared to the flat power case. From Eq. (3.82), the burnup penalty due to the presence of residual poison can be written as,

$$B_R = (\frac{2n}{n+1}) \frac{\Delta_R}{A} \tag{3.83}$$

where Δ_R is the residual poison reactivity.

Thus, the Δ_R which will give breakeven discharge burnup is given by:

$$B_d - B_o = (\frac{2n}{n+1}) \frac{\Delta_R}{A}$$

or

$$\Delta_R = (\frac{n+1}{2n}) A \cdot (B_d - B_o)$$

$$= (\frac{4}{6}) (9.2721 \times 10^{-6})(37123 - 36158)$$

$$= \quad 0.006$$

$$= \quad 0.6\%, \quad \Delta\rho$$

That is, the amount of residual poison which can be tolerated in case 3 without losing discharge burnup compared to the flat power case is $\sim$ 0.6% $\Delta\rho$. Representative residual $\Delta\rho$ values for gadolinium poison in LWR's are typically quoted as $\sim$ 0.5%, which is lower than breakeven, and thus a small gain in burnup and uranium usage can be credited to the poisoned case.

It must be noted that case 3 has the obvious advantage of an additional reactivity control capability through incorporation of burnable poison. This becomes essential if we go to higher enrichment reload fuel to extend burnup.

Although scoping analyses can be done very quickly using the analytical models for discharge burnup derived in this section, more accurate results can be obtained using numerical methods -- which can also be used to check the analytic approximations. This is done in the next chapter. In addition, the numerical methods can handle cases where leakage of neutrons from the core is required to be explicitly modeled, for example, when comparing the low-leakage and out-in/scatter fuel management strategies. Leakage, it will be recognized, is equivalent to a permanent (i.e., non-burnable) shim introduced into a given batch for one cycle only (instead of for all n-cycles, as in the case of burnable poison residual treated above). This case has proven to be too complicated to handle analytically,

at least in terms of extracting a reasonably simple closed form expression.

3.6 CHAPTER SUMMARY

In this chapter a case has been made for the application of the linear reactivity model for current PWR fuel (U-235/ UO_2) as well as fuel types comprised of other fissile and fertile materials. The LRM methodology, with the incorporation of features such as the power weighting algorithm and the radial leakage correlation, enables one to determine the discharge burnup of various fuel management schemes more realistically and thus more accurately than previously possible with simple models of this genre. An important component in the development of the LRM improved methodology is the derivation of the power split relation among fuel batches using the "group-and-one-half" diffusion theory model. Analytical models for discharge burnup corresponding to fuel management strategies of contemporary interest were obtained using the LRM methodology. These analytical results allow one to perform fast scoping analyses given only a few important core parameters generated by a minimum number of LEOPARD and PDQ-7 calculations. An extension of the LRM methodology using numerical procedures to further improve its accuracy, to validate the approximations which make the above mentioned analytic treatments practicable and to handle cases which are difficult to model analytically is discussed in the next chapter.

CHAPTER 4

DISCHARGE BURNUP CALCULATIONS

4.1 INTRODUCTION

The analytical expressions derived in the previous
chapter permit rapid estimation of discharge burnup for a
fuel batch as a function of power history, and thus facili-
tate quick scoping studies of fuel management strategy. To
establish and improve the accuracy of such analyses it is
necessary that they be checked against and normalized to
more accurate numerical calculations, which is the function
of the present chapter. The general methodology employed in
the analytical and the numerical approaches are basically
similar, except that most of the key approximation of the
former can be relaxed in the latter.

A computer program has been developed for the purpose
of checking the analytical results and performing more ac-
curate and varied analyses. This code, called DISBURN (for
Discharge Burnup), is in many respects an extension as well
as a refinement of the ALARM code previously described in
Ref. [S-2]. The algorithms together with certain key features
of the code are discussed in the next section. Finally,
various fuel management strategies (with and without the
use of burnable poison) will be simulated and analyzed using
the DISBURN code.

4.2 COMPUTER CODE FOR DISCHARGE BURNUP COMPUTATION—DISBURN

The DISBURN code computes the discharge burnup of fuel batches in an n-batch, steady-state reactor core. It is based on the linear reactivity model methodology incorporating features developed in the previous chapter such as the explicit modeling of core leakage in the radial direction and the power weighting of the fuel batch reactivity in determining the system reactivity. The power split equation employed in the code to describe interior as well as peripheral fuel batches was derived from the "group-and-one-half" diffusion theory model.

Although the code, as it is written presently, can only handle linear $\rho(B)$ traces characterizing fuel assemblies in a batch (the input parameters to describe the linear curve being ρ_0—the extrapolated BOL reactivity and A—the slope of the curve), non-linear $\rho(B)$ curves can also be readily evaluated by inserting a simple interpolating routine such as the nth order Lagrangian interpolating routine, into the program; the input in which case will be the ρ versus burnup values (in tabular form) from the assembly spectrum calculation (e.g., LEOPARD or PDQ-7), and interpolation can be performed at each burnup step as required in the computation: this procedure, in fact, is employed in the precursor code, ALARM.

In order to simulate realistic fuel loading patterns, the restriction of having a single type of fuel at the core

periphery is relaxed. Different fractions of the various fuel batches (i.e., subgroups of fuel having different reactivity values) can be placed at the peripheral locations. Table 4.1 gives a summary of the principal features of the code. The algorithm employed in the code is illustrated by the flow chart in Fig. 4.1. A description of the computational procedure is given below:

1. Input data include the extrapolated BOL reactivity ρ_0, the slope of the linear $\rho(B)$ curve, A, the number of batches n, the fractions of a batch in the core interior and on the core periphery, the theta values, Θ, the convergence criterion and the time or burnup step size.

   The options available include soluble poison control (alone or in combination with burnable or fixed poison); burnable poison; and fixed (non-burnable) poison shim or radial leakage (which are mathematically equivalent).

2. The beginning of cycle burnup states of the fuel batches $B_{BOC,i}$ are estimated using the equal power sharing approximation. The BOC point for batch i is given by

$$B_{BOC,i} = \frac{2(i-1)}{(n+1)} \frac{\rho_0}{A} \qquad (4.1)$$

3. The batch reactivity ρ_i, batch power fraction f_i,

TABLE 4.1

PRINCIPAL FEATURES OF THE DISBURN CODE

Item	Comment
1. Linear reactivity vs. burnup curve only.	Can easily be adapted to accommodate non-linear $\rho(B)$ traces.
2. Power-weighted reactivity averaging is used.	$$\rho_{sys} = \sum_{i=1}^{n} f_i \rho_i$$
3. Effect of peripheral leakage is accounted for through a reactivity-power correlation.	$$\rho_L = \alpha f_{per}$$ $$= \alpha \sum_{i=1}^{m} f_i$$ m denotes peripheral batches $$\therefore \rho_{sys} = \sum_{i=1}^{n-m} f_i \rho_i + \sum_{i=1}^{m} f_i (\rho_i - \alpha)$$ interior peripheral batches batches
4. Batches can be apportioned between core interior and periphery.	User specifies fraction of batch i in core interior ($F_{int,i}$) and core periphery ($F_{per,i}$). $$F_{int,i} + F_{per,i} = 1$$
5. Interior batch power is computed using the power split equation.	$$f_{int,i} = \frac{(F_{int,i})\left(\frac{1}{1-\theta\rho_i}\right)}{\sum_{i=1}^{n} f_i}$$
6. Peripheral batch power is computed using a modified power split equation.	$$f_{per,i} = \frac{(F_{per,i})\left[\frac{1}{1-\theta(\rho_i-\alpha)}\right]}{\sum_{i=1}^{n} f_i}$$ where $f_i = f_{int,i} + f_{per,i}$ (i.e., sum in denominator includes all assemblies in batch i).

① Input and Option Selection

② Estimate BOC Burnup States: $B_{BOC,i}$ and $B_{BOC,1} = 0$

Calculate ρ_i and f_i, $i = 1, 2, \ldots, n$

⑥ Update $B_{BOC,i}$

⑤ Increment Burnup $\Delta B = f_i *$ (Burn-up-step)

③ Compute ρ_{sys}

Is $\rho_{sys} = 0$?

YES

Compare EOC burn-ups for batch i, $B_{EOC,i}$ to BOC burnups for batch i+1, $B_{BOC,i+1}$

NOT CONVERGED

NO

④ Add Soluble Poison

Recompute ρ_i, f_i and ρ_{sys}

Is $\rho_{sys} = 0$?

NO

YES

CONVERGED

⑦ Output

STOP

Fig. 4.1 Flowchart for DISBURN COMPUTATIONS

and then the system reactivity ρ_{sys} are computed.
The ρ_{sys} is checked to determine whether the EOC
point has been reached ($\rho_{sys} = 0$).

4. If the end of cycle point has not been reached
   (within a certain convergence criterion on ρ_{sys}—
   a value of ± 0.0001 is presently used in the code),
   the excess system reactivity is suppressed by means
   of soluble poison. This is accomplished by adding
   equal amounts of negative reactivity $[-\Delta\rho_{poison} = \frac{-(\text{Excess system reactivity})}{n}]$ to each fuel batch's
   reactivity value ρ_i. The updated ρ_i and f_i are
   then used to recompute ρ_{sys}. The process is repeated
   until criticality is achieved.

   The adding of equal portions of negative reactivity
   worth to ρ_i (or equivalently, assigning equal solu-
   ble boron worth to all the fuel batches irrespective
   of their different reactivity level) is justified
   by the fact that the dependence of soluble poison
   worth on the reactivity levels of the fuel batches
   is a second order effect. This is evident from the
   linearity of the plot of reactivity vs. coolant
   boron concentration for various burnup points, as
   shown in Fig. 4.2.

5. The next set of burnup points for the fuel batches
   is obtained by adding the burnup increment $\Delta B_i = (f_i/\bar{f}) \cdot (\text{burnup step})$ to the previous batch burnup
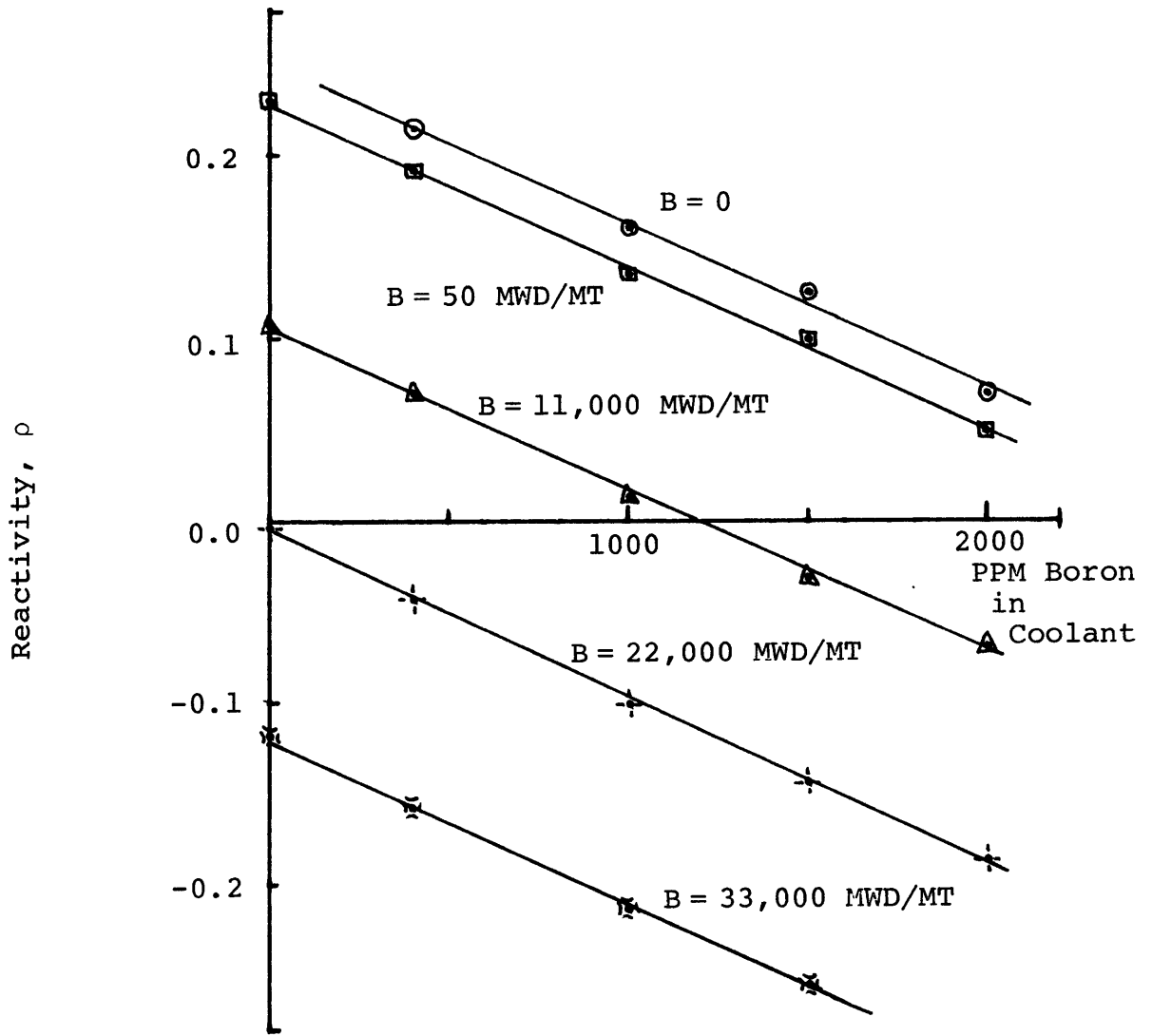
Fig. 4.2 Reactivity Worth of Control Poison—Maine Yankee
PWR Supercell Calculations

point (initially, the BOC points of the fuel
batches). The process (steps 3, 4 and 5) is re-
peated until the end of cycle point is reached
$(\rho_{sys} = 0.0)$.

6. The end of cycle parameter values for batch i
   $(\rho_{EOC,i}$ or $B_{EOC,i})$ are then compared with the
   beginning of cycle values of batch i+1 $(\rho_{BOC,i+1}$
   or $B_{BOC,i+1})$. If convergence (the convergence
   criterion is user prescribed) is not achieved, the
   BOC points of the fuel batches are then updated.
   The outer iteration (comprising steps 3, 4, 5 and 6)
   is repeated until overall convergence is achieved.

7. The burnup and the cycle-average power fraction for
   each batch are printed after each outer iteration.
   The peripheral power fraction and the leakage reac-
   tivity are printed as well.

It should be noted that if the extrapolated BOL reacti-
vity, ρ_0, and the slope of the linear $\rho(B)$ curve, A, input to
the code come from an infinite medium calculation, the
effect of axial leakage can be accounted for by reducing ρ_0.
However, this is not necessary if the data come from a PDQ-7
calculation which has included the effect of axial leakage.
Similarly, the presence of residual burnable poison in the
fuel batch over the remaining cycles can be accounted for
by a reduction in ρ_0. The effective extrapolated BOL reac-
tivity in the two situations discussed above is thus given

by

$$\rho_0' = \rho_0 - \Delta \qquad\qquad (4.2)$$

where Δ represents residual poison reactivity plus
the axial leakage reactivity.
A further description of the code, a listing, and a sample
problem can be found in Appendix C.

To see how well the code predicts the discharge burnup
of fuel batches it was applied to evaluate a five-batch,
extended burnup, 'out-in' fuel management scheme and a com-
parable 'low-leakage' fuel management strategy for the Com-
busion Engineering System-80 reference design [M-1]. The
core has 241 assemblies, 48 of which are located in the
core periphery. From available data [M-1] a leakage corre-
lation was developed: the leakage coefficient α, was found
to be 0.2846. The reactivity versus burnup values for
4.3 w/o and 4.44 w/o U-235 enriched lattices were generated
using the LEOPARD code; from these data the extrapolated BOL
reactivity ρ_0 and the slope of the $\rho(B)$ curve A, were deter-
mined. The 4.3 w/o enrichment was for the 'out-in' case
while the 4.44 w/o value applied to the 'low-leakage' fuel
management scheme. The theta (θ) values for the power split
equation of the interior and peripheral fuel batches of the
core were both set equal to 1.8 (see Fig. 3.15). A residual
poison penalty of 0.5% $\Delta\rho$ was assigned to the low-leakage

case to allow for the use of burnable poison in suppressing
the radial power peaking associated with the fuel management
scheme. Table 4.2 summarizes the relevant parameters for
the two cases evaluated using the DISBURN code. The results
of the calculations are compared in Tables 4.3a and 4.4a
with those obtained using detailed computer analyses, as
published in Ref. [M-1]. A parametric study was also per-
formed: the leakage coefficient, α, was varied from a value
of 0.2650 to the previously obtained value of 0.2846, and
theta values of 1.5 and 2.0 were also analyzed. Tables 4.3
and 4.4 give the results of the calculations for the 'out-
in' and 'low-leakage' fuel management schemes, respectively.

The discharge burnups are more sensitive to the leakage
coefficient, α, than they are to the theta values used in
the calculations. This points to the importance of making
an accurate correlation of the leakage reactivity to the
peripheral power fraction. The cycle burnups in the two
cases analyzed using DISBURN differ by an average of 5.4%
from those obtained using detailed computer calculations,
the discharge burnup values are in even better agreement.
For the 'out-in' fuel management scheme, the discharge
burnup (for the reference case of $\alpha = 0.2846$ and $\theta = 1.8$)
was only about 1% less, while for the 'low-leakage' strategy
the discharge burnup was approximately 2.8% lower. One
possible explanation for the bigger difference in the dis-
charge burnup prediction for the 'low-leakage' scheme is

TABLE 4.2

PARAMETERS USED IN THE EVALUATION OF THE 'OUT-IN'
AND 'LOW-LEAKAGE' FUEL MANAGEMENT SCHEMES
FOR A 5-BATCH, EQUILIBRIUM CORE

Item	Out-in*	Low-leakage**
Fuel Enrichment, ϵ w/o	4.30	4.44
Extrapolated BOL Reactivity, ρ_0	0.2632	0.2660
Slope of $\rho(B)$ Curve, MT/MWD	7.063×10^{-6}	6.885×10^{-6}
Leakage Coefficient	0.2846	0.2846
Theta Value θ for both Interior and Peripheral Batches	1.8	1.8
Residual poison $\Delta\rho$ (%)	—	0.5

*All 48 assemblies of batch 1 (fresh fuel) were treated as
being on the core periphery.

**8 assemblies of batch 1, 36 of batch 2, and 4 of batch 3
were in peripheral locations.

TABLE 4.3a

COMPARISON OF CYCLE EXPOSURES COMPUTED BY
DISBURN AND DETAILED COMPUTER CALCULATIONS
FOR THE 'OUT-IN' FUEL MANAGEMENT SCHEME
[CONSTANT α]

Cycle of Exposure	C-E* (MWD/MT)	DISBURN, α = 0.2846; (MWD/MT)		
		θ = 1.5	θ = 1.8	θ = 2.0
1	9429	8823	8638	8524
2	12160	12213	12775	13157
3	10842	10631	10735	10772
4	9930	9554	9439	9353
5	8309	8740	8523	8375
Total	50665	49961	50110	50181

*Ref. [M-1].

TABLE 4.3b

COMPARISON OF CYCLE EXPOSURES COMPUTED BY
DISBURN AND DETAILED COMPUTER CALCULATIONS
FOR THE 'OUT-IN' FUEL MANAGEMENT SCHEME
[CONSTANT θ]

Cycle of Exposure	C-E* (MWD/MT)	DISBURN, θ = 1.8; (MWD/MT)		
		α = 0.2650	α = 0.2700	α = 0.2846
1	9429	8977	8885	8638
2	12160	12819	12811	12775
3	10842	10777	10766	10735
4	9930	9479	9470	9439
5	8309	8560	8550	8523
Total	50665	50612	50482	50110

*Ref. [M-1].

TABLE 4.4a

COMPARISON OF CYCLE EXPOSURES COMPUTED BY
DISBURN AND DETAILED COMPUTER CALCULATIONS
FOR THE 'LOW-LEAKAGE' FUEL MANAGEMENT SCHEME
[CONSTANT α]

Cycle of Exposure	C-E* (MWD/MT)	DISBURN, α = 0.2846; (MWD/MT)		
		θ = 1.5	θ = 1.8	θ = 2.0
1	13492	13273	14094	14660
2	8648	9163	8974	8845
3	11068	10613	10639	10633
4	10574	9813	9680	9561
5	9878	8983	8757	8599
Total	53660	51845	52144	52298

*Ref. [M-1].

TABLE 4.4b

COMPARISON OF CYCLE EXPOSURES COMPUTED BY
DISBURN AND DETAILED COMPUTER CALCULATIONS
FOR THE 'LOW-LEAKAGE' FUEL MANAGEMENT SCHEME
[CONSTANT θ]

Cycle of Exposure	C-E* (MWD/MT)	DISBURN, θ = 1.8; (MWD/MT)		
		α = 0.2650	α = 0.2700	α = 0.2846
1	13492	14243	14200	14094
2	8648	9176	9129	8974
3	11068	10699	10687	10639
4	10574	9708	9694	9680
5	9879	8789	8786	8757
Total	53660	52615	52496	52144

*Ref. [M-1].

that the suppression of reactivity in the batch 1 (fresh) fuel by means of burnable poison, which will lead (as shown in the next section) to a slight increase in our calculated discharge burnup, is not simulated here. As will be seen later, the observed difference is of the expected magnitude.

In the present work, we are primarily interested in the _relative_ change in the discharge burnup of a modified fuel management scheme compared to a reference case. Figures 4.3 and 4.4 show the relative difference in discharge burn-ups between the out-in and low-leakage fuel management schemes as a function of the power sharing parameter theta and the leakage coefficient α, respectively. It can be seen that the differences between the two fuel management strategies and between the DISBURN and C-E results are quite insensitive to both theta and α. This is an important ob-servation since it confirms that the results are not biased in any important way by the details of the methodology used to establish numerical values for the two dominant free parameters in the model. Considering the complexity of the problem involved, the DISBURN code produces satisfactory agreement with the results of detailed state of the art physics analyses.

4.3   SIMULATION OF DIFFERENT FUEL MANAGEMENT STRATEGIES

The DISBURN code was found to be sufficiently accurate for the type of analyses of interest in the present re-search. Although different fuel management strategies can
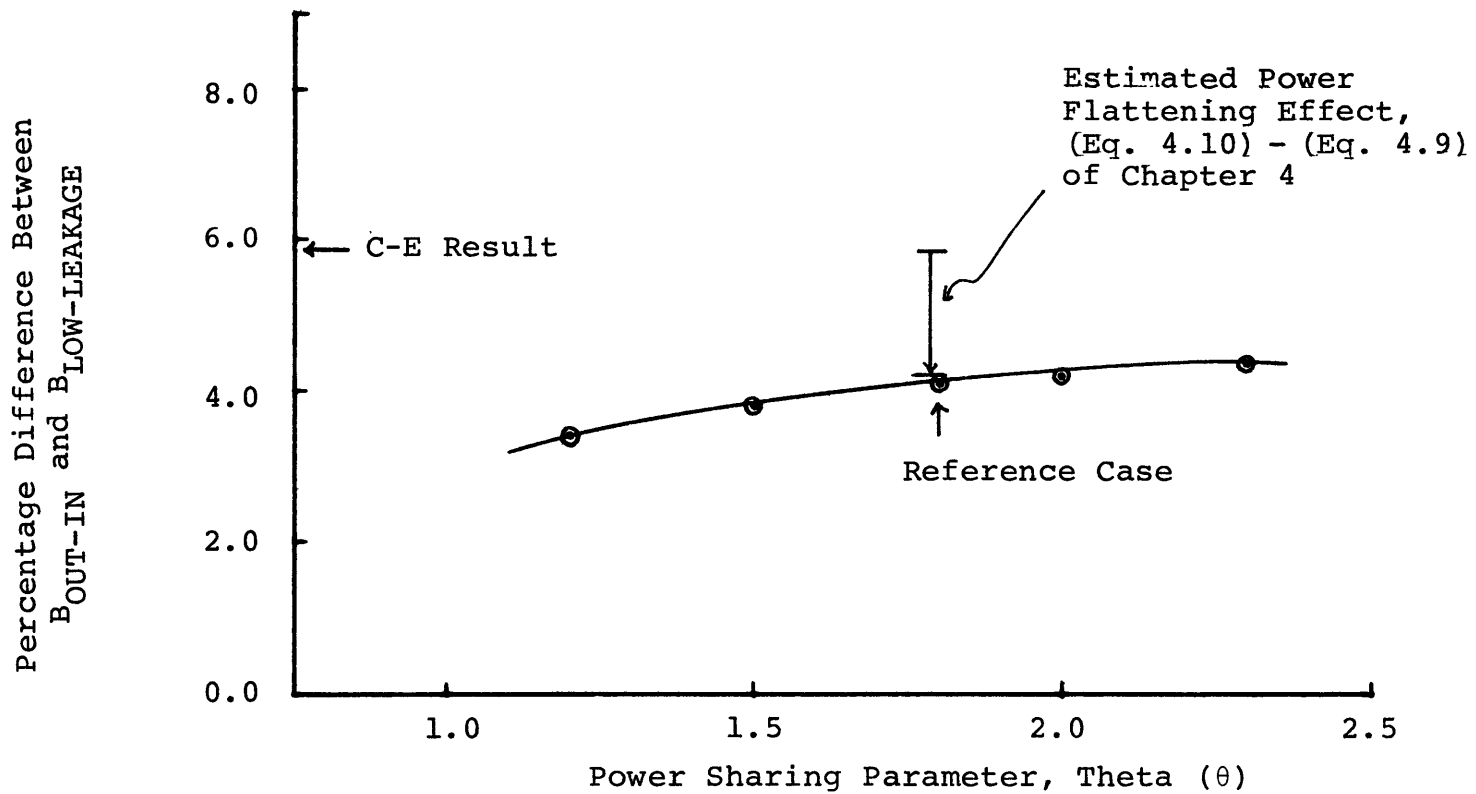
Fig. 4.3 The Percentage Difference between the Discharge Burnup for the
         Out-in and Low-Leakage Fuel Management Schemes, as a Function of
         the Power Sharing Parameter Theta
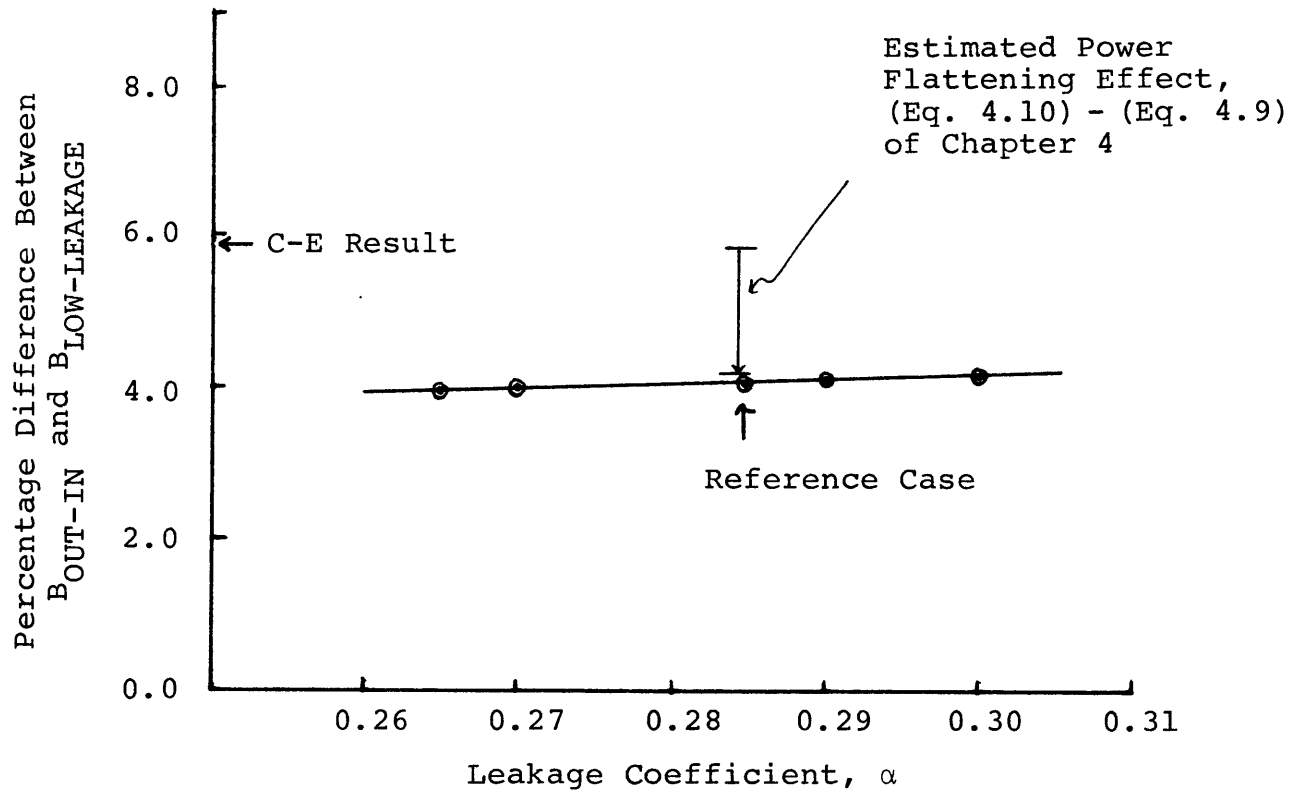
Fig. 4.4 The Percentage Difference between the Discharge
Burnup for the Out-In and Low-Leakage Fuel Management
Schemes as a Function of the Leakage Coefficient

be simulated and analyzed separately, the ultimate objective of these scoping analyses is the determination of the net improvement (or decrease) in uranium utilization arising from the combination of these common strategies.

The first portion of this section deals with the evaluation of the separate fuel management schemes of contemporary interest such as the use of burnable poison to obtain an optimum power history (with respect to maximizing discharge burnup), the use of low-leakage fuel loading patterns, etc.. In the latter part of this section, the discharge burnup (and hence the uranium utilization) of a synthesis of the various methods for improvement of uranium utilization will be computed.

4.3.1 BURNABLE POISON

The primary objectives of employing burnable poison in the fresh fuel assemblies in the low-leakage fuel management and/or extended burnup/cycle-length strategies are to suppress the power density in these assemblies and to keep soluble boron concentrations at the beginning of cycle sufficiently low to obtain an acceptable (slightly negative) moderator temperature coefficient of reactivity. However, it has apparently not been realized in the past that power shaping using burnable poison can lead to a slight increase in the fuel discharge burnup. This was shown to be the case in Chapter 3 using an analytical approach to derive the discharge burnup of a fuel batch whose power history tra-

jectory was shaped by means of burnable poison. (See Table
3.4). This observation is confirmed in this section using
the DISBURN code. Further, an "optimum" (maximum discharge
burnup), burnable-poison-shaped power history profile was
determined, as well as the residual poison reactivity
penalty which can be tolerated to break even with respect
to the discharge burnup, as compared to the same case with-
out burnable poison.

The analyses were done for the Main Yankee reactor
design—a 3-batch, steady-state core with a reload fuel
enrichment of 3 w/o U-235. The parameters associated with
the reactivity versus burnup curve which characterize the
Main Yankee supercell lattice, and the reactor core confi-
guration are:

$$\text{Extrapolated BOL reactivity:} \quad \rho_0 = 0.2235$$
$$\text{Slope:} \quad A = 0.9272 \times 10^{-5}, \text{ MT/MWD}$$
$$\text{Theta value:} \quad \theta = 1.5$$

For the moment, the effect of core leakage and the presence
of any residual poison were neglected. It was further
assumed that the burnable poison was depleted completely
just before the end-of-cycle point. Two cases of interest,
as shown in Fig. 4.5, were considered: in the first, the
reactivity in the first cycle was tailored to increase
linearly from a beginning-of-life value, ρ_{BOL}, until it

Constant Reactivity in 1st Cycle:

$\rho = \rho_0 - AB$

Linear Reactivity Ramp in 1st Cycle:

$\rho = \rho_0 - AB$

$B_{EOC,1}$ = EOC Point for Cycle 1

ρ_{BOL} = BOL Reactivity Value
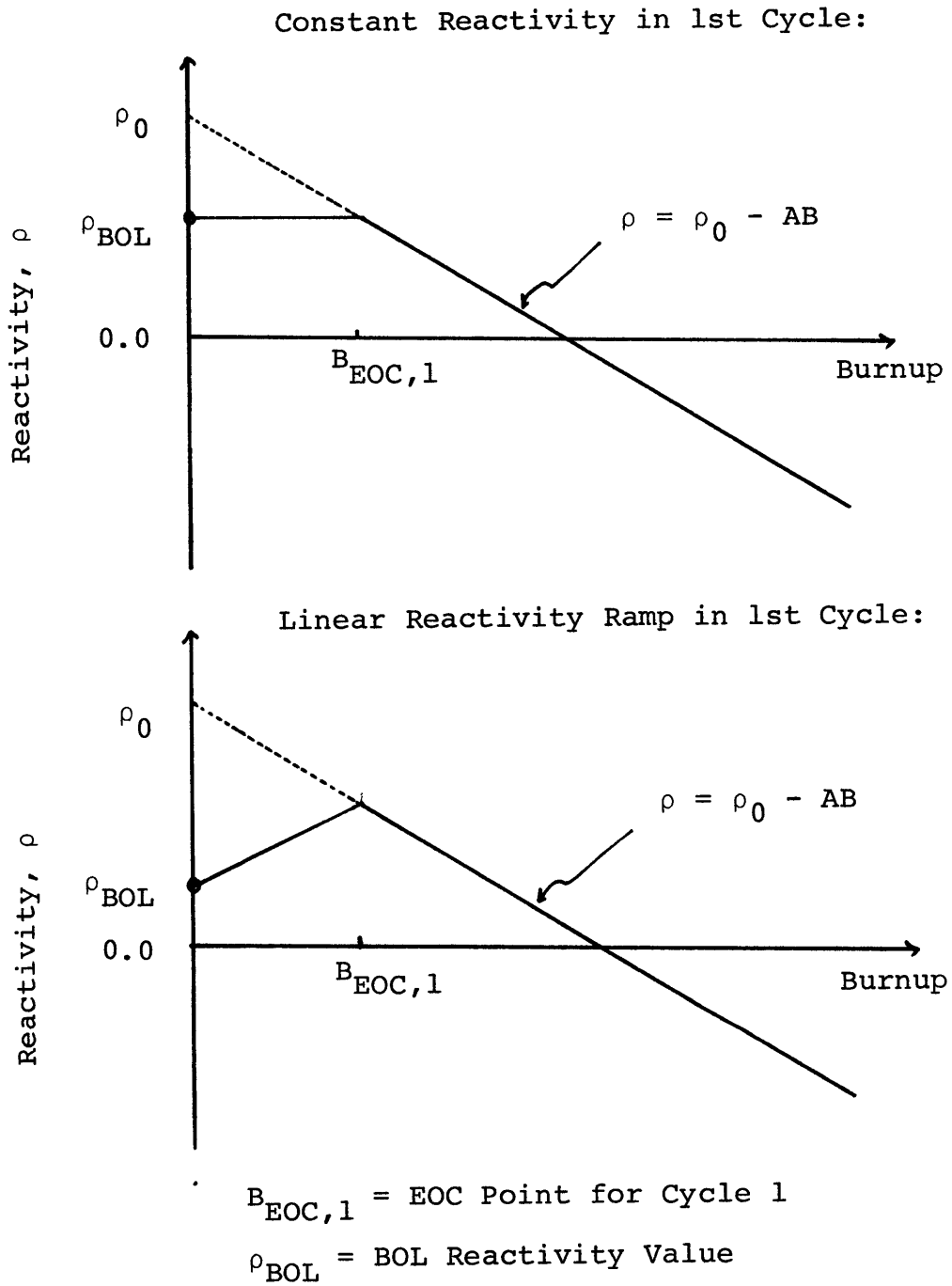
Fig. 4.5 Reactivity versus Burnup History Profiles

reaches the burnable poison burnout point, which is also the
end of cycle point. In the latter case, ρ_{BOL} was varied
in order to determine the "optimum" (maximum discharge
burn-up) reactivity versus burnup history profile. The
results are shown in Table 4.5. By shaping the power pro-
file history using burnable poison, the discharge burnup was
increased by about 2.0% for the case of constant reactivity
in the first cycle to approximately 3.5% for the case of a
zero beginning-of-life reactivity value. Although the dis-
charge burnup can be further increased by decreasing the BOL
reactivity ρ_{BOL}, to a slightly negative value, this option
was not investigated in detail for several reasons. In the
first place, achieving a negative BOL reactivity value will
require a higher concentration of burnable poison and hence
higher residual poison, which may negate any additional gain
in the discharge burnup compared to those cases with zero
or positive BOL reactivity values. The second reason is
that we may have to require the burnable poison to deplete
at a much faster rate than that readily achievable in real
applications. A third practical deterrent is the large re-
lative power swing of the poisoned batch over its first
cycle. Finally, when strong negative BOL ρ values are used,
DISBURN runs show that the system may encounter premature
zero reactivity states part way through a cycle. Thus, the
case with a zero BOL reactivity value (case 2(d) in Table
4.5) was taken to be the one having an "optimum" reactivity

TABLE 4.5

INCREASE IN DISCHARGE BURNUP FOR DIFFERENT REACTIVITY VS. BURNUP HISTORY PROFILES

Cases	BOL Reactivity, ρ_{BOL}	EOC Point, $B_{EOC,1}$ MWD/MT	Discharge Burnup, MWD/MT	Increase in Discharge Burnup* Over Case With No Burnable Poison (%)
1. Constant Reactivity in 1st cycle	0.0982	13545	36530	1.95
2. Variable Reactivity in 1st cycle				
2(a)	0.06	13397	36753	2.57
2(b)	0.04	13308	36868	2.89
2(c)	0.02	13228	36973	3.19
2(d)	0.00	13146	37082	3.49
2(e)	-0.02	13085	37168	3.73

*Discharge burnup for the case lacking burnable poison is 35831 MWD/MT; residual poison penalty is not assessed.

versus burnup history profile, and will be referred to as such in the analyses performed in the remaining portion of this section.

The use of burnable poison in the fresh fuel assemblies will always leave a small but finite amount of residual poison reactivity in the subsequent cycles. When gadolinium oxide (Gd_2O_3) is admixed with uranium oxide fuel, the residual reactivity is caused by a quasi-steady-state transmutation of the low cross section even-A gadolinium isotopes into the high cross section odd-A gadolinium isotopes. For boron shim, however, the residual poison reactivity is due to the incomplete depletion of the boron-10 at the end of the first and subsequent cycles: here the residual reactivity will diminish with burnup. The amount of the residual poison reactivity depends upon several factors: among them are (1) the type of burnable poison material used, (2) the burnable poison loading in the fresh fuel assemblies, and (3) the design of the fuel rods containing burnable poison (burnable poison admixed with UO_2), the design of the separate shim rods (lumped burnable poison), and the design of the fuel assemblies which contain burnable poison (i.e., the number of fuel rods with burnable poison, the number of shim rods and the locations in the assembly in which these rods are placed). It has been estimated [M-1, H-3] that for an equilibrium cycle the residual reactivity amounts to about 0.3% - 0.5% $\Delta\rho$ on a core average basis for contemporary

burnable poison materials and designs.

Calculations were performed to determine the residual poison reactivity penalty to break even with respect to the discharge burnup compared to a core without burnable poison. The first set of analyses was done for the case in which the reactivity level in the first cycle remained constant, and the second series of calculations was performed for the "optimum" case. The results are shown in Tables 4.6 and 4.7, respectively. For constant reactivity in cycle 1, the breakeven value of the residual reactivity penalty is about 0.4% $\Delta\rho$, whereas for the optimum ρ(B) profile, the breakeven value is approximately 0.7% $\Delta\rho$. Since the residual reactivity penalty cited for reactivity versus burnup history profiles similar to the former case (i.e., constant reactivity in cycle 1) is in the range of 0.2 - 0.3% $\Delta\rho$ [H-3], there is a net gain in the discharge burnup from suppressing the reactivity of the fresh fuel using burnable poison. The same can be said of the optimum ρ(B) profile case.

The residual poison penalty (particularly when gadolinium is used) should, to first order, be proportional to the amount of poison reactivity initially present: $(\rho_0 - \rho_{BOL})$ in Fig. 4.3. This observation is supported in a recent study by Combustion Engineering [H-3] on the use of gadolinium in PWR extended-burnup cycles, in which it is shown that the residual reactivity holddown was approximately proportional to the weight percent gadolinium oxide loading

TABLE 4.6

DISCHARGE BURNUP FOR THE CASE
OF CONSTANT CYCLE 1 REACTIVITY
AT DIFFERENT RESIDUAL POISON LEVELS

Residual Poison Reactivity ($\%$ $\Delta\rho$)	Discharge Burnup MWD/MT	Increase in Discharge Burnup* Over Core Without Burnable Poison ($\%$)
0.0	36530	1.95
0.1	36371	1.51
0.2	36211	1.06
0.3	36038	0.58
0.4	35872	0.11
0.5	35711	-0.33

*Discharge burnup for a core lacking burnable poison is 35831 MWD/MT.

TABLE 4.7

DISCHARGE BURNUP FOR THE "OPTIMUM"
REACTIVITY-BURNUP HISTORY PROFILE
AT DIFFERENT RESIDUAL POISON LEVELS

Residual Poison Reactivity ($\% \Delta\rho$)	Discharge Burnup MWD/MT	Increase in Discharge Burnup* Over Core Without Burnable Poison ($\%$)
0.0	37082	3.49
0.1	36919	3.04
0.3	36575	2.08
0.5	36215	1.07
0.7	35875	0.12
0.9	35514	-0.88

*Discharge burnup for a core lacking burnable poison is 35831 MWD/MT.

in the fuel. If this is so, then the more highly poisoned
cases, while they improve the power history profile (which
improve uranium utilization) also suffer a larger compen-
sating penalty due to residual poison. Assuming a 0.3% $\Delta\rho$
penalty for the constant-reactivity case, and scaling this
penalty proportional to $(\rho_0 - \rho_{BOL})$, we find that the net
increase in discharge burnup for cases 2(a) - 2(d) is reduced
to the point where all burnable poison cases are essentially
equivalent. This is shown in Table 4.8. Thus, the "optimum"
reactivity versus burnup history profile cited earlier in
this section is, in reality, only marginally preferable when
the effect of the anticipated residual poison penalty is
taken into account. In view of this, a fuel designer can
select the poison loading to meet other criteria such as
BOC or EOC peak power or power swing over a cycle in or
between assemblies.

4.3.2 LOW-LEAKAGE FUEL MANAGEMENT

The DISBURN code has been employed to analyze the effect
of low-leakage fuel management on the discharge burnup of
the Maine Yankee reactor. The initial analyses were done
without the use of burnable poison to shape or suppress the
reactivity of the fresh fuel when placed in the core inte-
rior as required by this scheme. Later in this section, the
additional effect of reactivity suppression in the fresh
fuel assemblies located in the core interior by means of
burnable poison, on the discharge burnup (and hence, uranium

TABLE 4.8

THE EFFECT OF THE LARGER RESIDUAL POISON REACTIVITY ASSOCIATED WITH A HIGHER BURNABLE POISON LOADING

Case	BOL Reactivity, ρ_{BOL}	Initial Poison* Reactivity, $\rho_0 - \rho_{BOL}$	Residual Poison Reactivity, (% $\Delta\rho$)	Discharge Burnup, (MWD/MT)	Increase in Discharge Burnup** Over Case With No Poison (%)
1. Constant Reactivity in 1st cycle	0.0982	0.1253	0.30	36038	0.58
2. Variable Reactivity in 1st cycle					
2(a)	0.060	0.1635	0.39	36070	0.67
2(b)	0.040	0.1835	0.44	36101	0.75
2(c)	0.020	0.2035	0.49	36108	0.77
2(d)	0.000	0.2235	0.54	36140	0.86

*ρ_0 = 0.2235.

**Discharge Burnup for the case lacking burnable poison is 35831 MWD/MT.

utilization) is discussed.

Three cases were examined. The first case (the reference case) consisted of a reload having 48 of the 72 assemblies of 3.0 w/o U-235 fuel placed on the core periphery (i.e., in a normal out-in/scatter refueling mode, as there are only 48 peripheral locations). In the second and third cases, the same number of assemblies of once- or twice-burned fuel, respectively, were loaded on the core periphery—the former case is designated the 'in-out-in' fuel management scheme while the latter is an 'in-in-out' (or in/scatter-out) scheme; both are commonly referred to as low-leakage schemes. The leakage correlation for the Maine Yankee reactor developed in Chapter 3 was used; the leakage coefficient in this case was $\alpha = 0.1640$. Table 4.9 summarizes the results of this initial analysis. An increase in the discharge burnup of about 3.0% was achieved in going from the current, out-in scheme to the low-leakage strategy. This was also the percentage improvement found for the uranium utilization.

The placing of fresh fuel assemblies in the core interior necessitates the use of burnable poison to maintain the power density below acceptable limits and to keep soluble boron concentrations at the BOC sufficiently low to obtain a slightly negative moderator temperature coefficient of reactivity. However, it was shown in the previous section that the resultant shaping of the reactivity vs.

TABLE 4.9

COMPARISON OF LOW-LEAKAGE FUEL MANAGEMENT
WITH CURRENT, OUT-IN FUEL MANAGEMENT

Case	Discharge Burnup (MWD/MT)	Increase in Discharge Burnup over the Out-In Fuel Management Case (%)
1. Current Out-In	30505	0.0
2. In-Out-In Scheme*, i.e., once-burned fuel on core periphery	30990	1.59
3. In-In-Out Scheme* low-leakage with twice-burned fuel on core periphery	31419	3.00

*Without the incorporation of burnable poison.

burnup history profile due to the incorporation of burnable poison can lead to a slight improvement in the discharge burnup. Analyses were done to determine the net increase in discharge burnup (hence, improvement in uranium utilization) due to the incorporation of burnable poison in the fresh fuel batch for the in-in-out low-leakage fuel management scheme. Two cases were considered: in the first, the reactivity of the fresh fuel was held constant by burnable poison in the first cycle, and in the second case, the reactivity in cycle 1 was tailored by means of burnable poison to increase linearly from a value of $\rho_{BOL} = 0.02$ (case 2(c) in Table 4.5). The reasons for selecting $\rho_{BOL} = 0.02$ as opposed to $\rho_{BOL} = 0.0$ are: there was no significant difference in the net increase in their discharge burnups when their respective residual poison reactivity penalties were taken into account, and in the case with $\rho_{BOL} = 0.0$, we might encounter premature zero reactivity states part way through a cycle, since the leakage of neutrons from the core (which has the effect of lowering the overall system reactivity) was considered in these analyses. The residual poison reactivity penalties associated with the two poisoned $\rho(B)$ profiles adopted in the analyses were taken from Table 4.8. The results are shown in Table 4.10. The additional gain in the discharge burnup of the low-leakage scheme over the out-in scheme due to the employment of the burnable poison in the fresh reload fuel was less than 1%.

TABLE 4.10

THE EFFECT OF USING BURNABLE POISON
IN THE IN-IN-OUT LOW-LEAKAGE
FUEL MANAGEMENT SCHEME

Case	Discharge Burnup, (MWD/MT)	Increase In Discharge Burnup Over the Current Out-In Scheme (%)
Current, Out-In scheme	30505	0.0
Low-Leakage scheme	31419	3.00
Low-Leakage with constant-reactivity in Cycle 1 (no residual poison penalty)	31979	4.83
Low-Leakage with constant-reactivity in Cycle 1 (Residual $\Delta\rho$ = 0.3%)	31479	3.19
Low-Leakage with BOL reactivity value ρ_{BOL} = 0.02 (no residual poison penalty)	32467	6.43
Low-Leakage with BOL reactivity value ρ_{BOL} = 0.02 (Residual $\Delta\rho$ = 0.49%)	31610	3.62

However, the benefit of using burnable poison in the low-leakage fuel management strategy, in addition to benefiting the moderator temperature coefficient of reactivity and the suppression of power peaking, is in the reduction of the radial (global) power peaking factor compared to the case without burnable poison, as shown in Table 4.11. Penalties associated with this factor will be discussed in a subsequent section of this chapter.

4.3.3 EXTENDED CYCLE LENGTH/BURNUP

In recent years, a large number of utilities have seriously considered extending cycle length (18 intead of 12 months) while keeping the number of feed assemblies the same. The primary incentive for this switch is that one refueling outage is eliminated every three years, which allows a higher plant capacity factor, and therefore significant savings in replacement power costs. This strategy can also improve uranium utilization through its inherent reliance upon extended burnup. The steady-state cycle average burnup can be related to the calendar time between startups by:

$$ B_c \text{ (MWD/MT)} = \frac{365 \ Q_{TH} \ (t-t_R) \ L'}{(A_T) \ (M)} \tag{4.3} $$

where
Q_{TH} = Reactor thermal power rating (MWth)

t = Time between startups (years)

t_R = Downtime for refueling (years)

$t-t_R$ = Time the reactor is producing power (years)

TABLE 4.11

THE EFFECT OF BURNABLE POISON
ON THE GLOBAL, BATCH-AVERAGE
RADIAL POWER PEAKING FACTOR

Item	Relative Radial Power Peaking Factor
1. Current Out-In/Scatter scheme	1.00 (reference value)
2. Low-Leakage In-In-Out scheme without burnable poison	1.15
3. Low-Leakage scheme with constant-reactivity in Cycle 1 (Residual $\Delta\rho$ = 0.3%)	1.09
4. Low-Leakage scheme with BOL reactivity value ρ_{BOL} = 0.02 (Residual $\Delta\rho$ = 0.49%)	1.05

L' = Availablility-based capacity factor

A_T = Total number of assemblies in core

M = Heavy metal loading per assembly (Metric

Tons Uranium)

In our previous analyses of the Main Yankee PWR the discharge burnup, under steady-state conditions, for the 3-batch, out-in fuel management scheme, was 30505 MWD/MT (see Table 4.9). If the corresponding time interval between startups is equal to 12 months, then the discharge burnup that must be achieved to extend the cycle length to about 18 months according to Eq. 4.3 is around 46000 MWD/MT. Several analyses were performed to determine the effect of extended cycle length on the busbar and system costs of the plant, and to evaluate the improvement on the uranium utilization of the reactor. For the present purposes, the uranium utilization is defined in terms of MegaWatt-Days per Metric Ton of natural uranium feed (MWD/MTF):

$$U = \frac{B_{dis}}{(F/P)} \quad (MWD/MTF) \tag{4.4}$$

where B_{dis} is the discharge burnup, and the feed-to-product ratio is given by

$$\frac{F}{P} = \frac{(x_P - x_T)}{(x_F - x_T)} \tag{4.5}$$

with x_P = enrichment of the product (reactor reload

fuel), w/o

x_F = enrichment of the natural uranium feed

(= 0.711 w/o)

x_T = enrichment of the tails stream (typically

0.2 w/o)

Equation 4.4 can thus be rewritten as:

$$U \ (MWD/MTF) \ = \ \frac{0.511 \ B_{dis}}{(x_p \ - \ 0.2)} \qquad (4.6)$$

The analyses were again done for the Maine Yankee reactor design, with a reload fuel enrichment of 4.34 w/o U-235. The parameters describing the ρ(B) curve which characterizes the Main Yankee supercell lattice are:

ρ_0 = 0.2661

A = 0.7154 x 10^{-5}, MT/MWD

The theta value and the leakage coefficient employed in the analyses remain the same as before (θ = 1.5 and α = 0.1640). The results are given in Table 4.12. The use of extended cycle, out-in fuel management results in a 6.3% reduction in uranium requirements. If the extended cycle design is operated in a low-leakage configuration, a saving of 8.8% in uranium usage is obtained.

The analyses were repeated with the incorporation of burnable poison in the low-leakage fuel management scheme.

TABLE 4.12

COMPARISON OF EXTENDED CYCLE AND LOW-LEAKAGE EXTENDED CYCLE
FUEL MANAGEMENT WITH CURRENT, THREE-BATCH, OUT-IN/SCATTER FUEL MANAGEMENT

Case	Reload Enrichment, x_P (w/o U-235)	Discharge Burnup (MWD/MT)	U (MWD/MTF)	Uranium Requirement (MTF/MWD)
Current Out-In/Scatter	3.0	30505	5567	1.796×10^{-4}
Extended Cycle, Out-In/Scatter	4.34	48176	5946	1.682×10^{-4}
Extended Cycle, In/Scatter-Out (Low-Leakage)	4.34	49473	6106	1.638×10^{-4}

The appropriate residual poison reactivity penalties were also accounted for in the analyses. Table 4.13 summarizes the results. An improvement in uranium utilization of about 11% is realized in the extended cycle low-leakage fuel management with burnable poison being used to suppress the reactivity of the fresh fuel located in the core interior. Additional economic benefits of the extended cycle low-leakage fuel management scheme are derived from the higher plant capacity factor which significantly affects the system cost of the power plant. Further discussion of the economic benefits of the use of burnable poison in this particular scheme is postponed until later in this chapter.

4.4 COMPARISON OF ANALYTICAL WITH NUMERICAL RESULTS

In Chapter 3, analytical expressions for the discharge burnup of a batch of fuel for various reactivity versus burnup history profiles were derived. In this section, the analytical results are checked against those generated using the DISBURN code. Analytical results which depart significantly from the numerical ones, are normalized to force better agreement.

The discharge burnup equations which were derived analytically were expressed in the form:

$$B_{dis} = B_0 / (1+\epsilon) \qquad (4.7)$$

where B_0 is the discharge burnup for the hypothetical

TABLE 4.13

THE EFFECT OF BURNABLE POISON ON THE
URANIUM UTILIZATION OF LOW-LEAKAGE
EXTENDED CYCLE FUEL MANAGEMENT

Case	Discharge Burnup (MWD/MT)	Improvement in Uranium Utilization (%)
Current Out-In/Scatter	30505	0.0 (reference case)
Burnable Poison Cases:		
Extended Cycle, Low-Leakage with Constant Reactivity in Cycle 1	50632	12.3
Extended Cycle, Low-Leakage with Constant Reactivity in Cycle 1 (Residual $\Delta\rho$ = 0.3%)	49991	10.8
Extended Cycle, Low-Leakage with ρ_{BOL} = 0.04	51366	13.9
Extended Cycle, Low-Leakage with ρ_{BOL} = 0.04 (Residual $\Delta\rho$ = 0.54%)	50111	11.1

flat power case:

$$= (\frac{2n}{n+1})\frac{\rho_0}{A}$$

in which n is the number of batches

ρ_0 is the extrapolated BOL reactivity

A is the slope of the linear $\rho(B)$ curve

and ε is the factor which corrects for the departure

of discharge burnup from the flat power case.

The 'ε factors' for the various power history trajectories are available in a closed analytical form (see Table 3.3). These anlytical expressions for the 'ε factor' were compared with the numerically evaluated results, rather than the discharge burnup itself. The transformation between the 'ε factor' and the corresponding discharge burnup is straightforward (Eq. 4.7).

4.4.1 REACTIVITY CONTROL WITH SOLUBLE POISON ONLY

The expression for the 'ε factor' in this case is given by

$$\varepsilon = (\theta\rho_0)^2 \frac{(n-1)}{3(n+1)^2} \tag{4.8}$$

Figures 4.6 and 4.7 show the analytical and the numerical results for ε. Although the quantitative agreement is apparently poor, it must be noted that the values of ε in this particular case are rather small—a second order effect on B_0. Also, the trends in the variation of ε with both
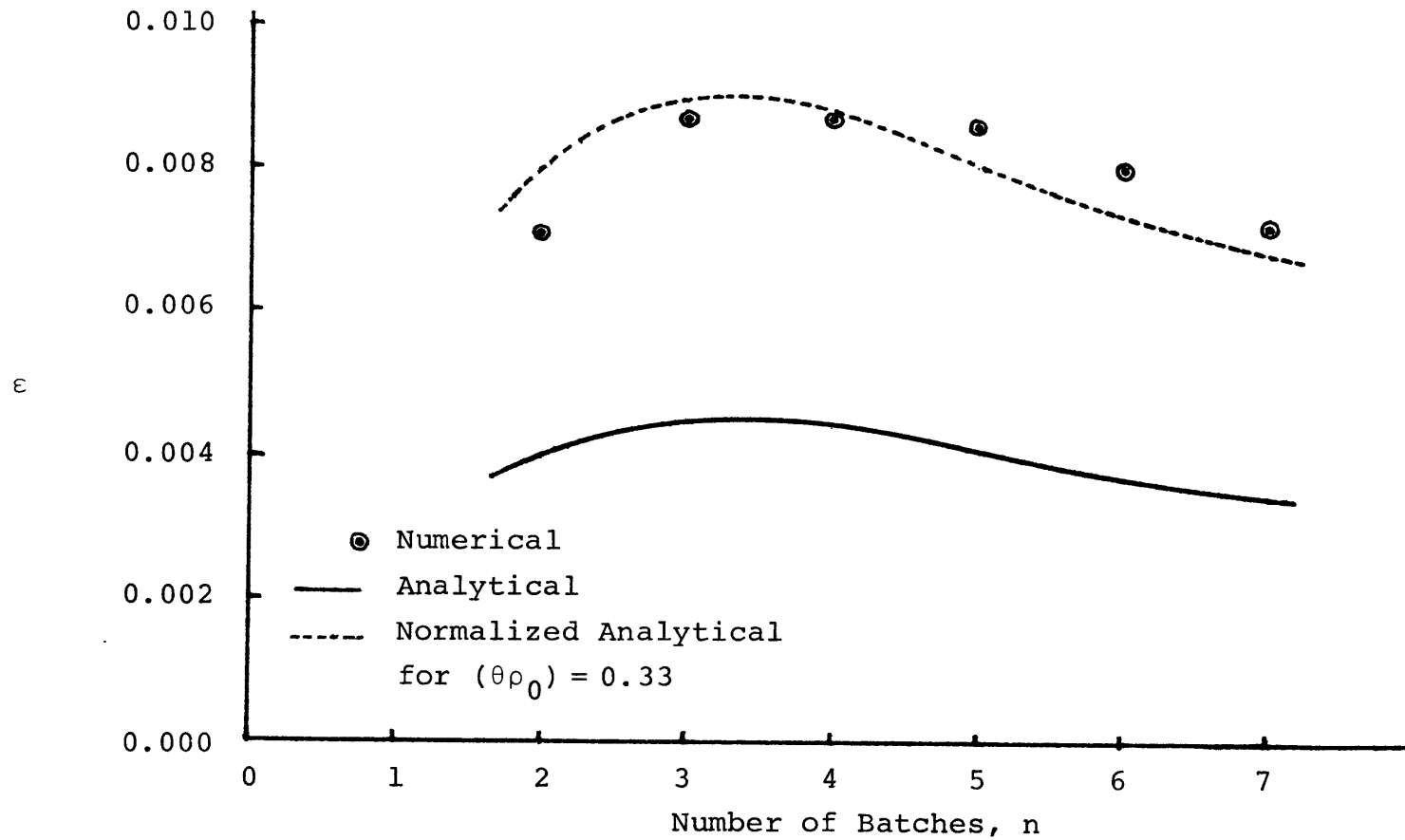
Fig. 4.6 ε as a Function of the Number of Batches for the Case of Reactivity Control by Means of Soluble Poison only
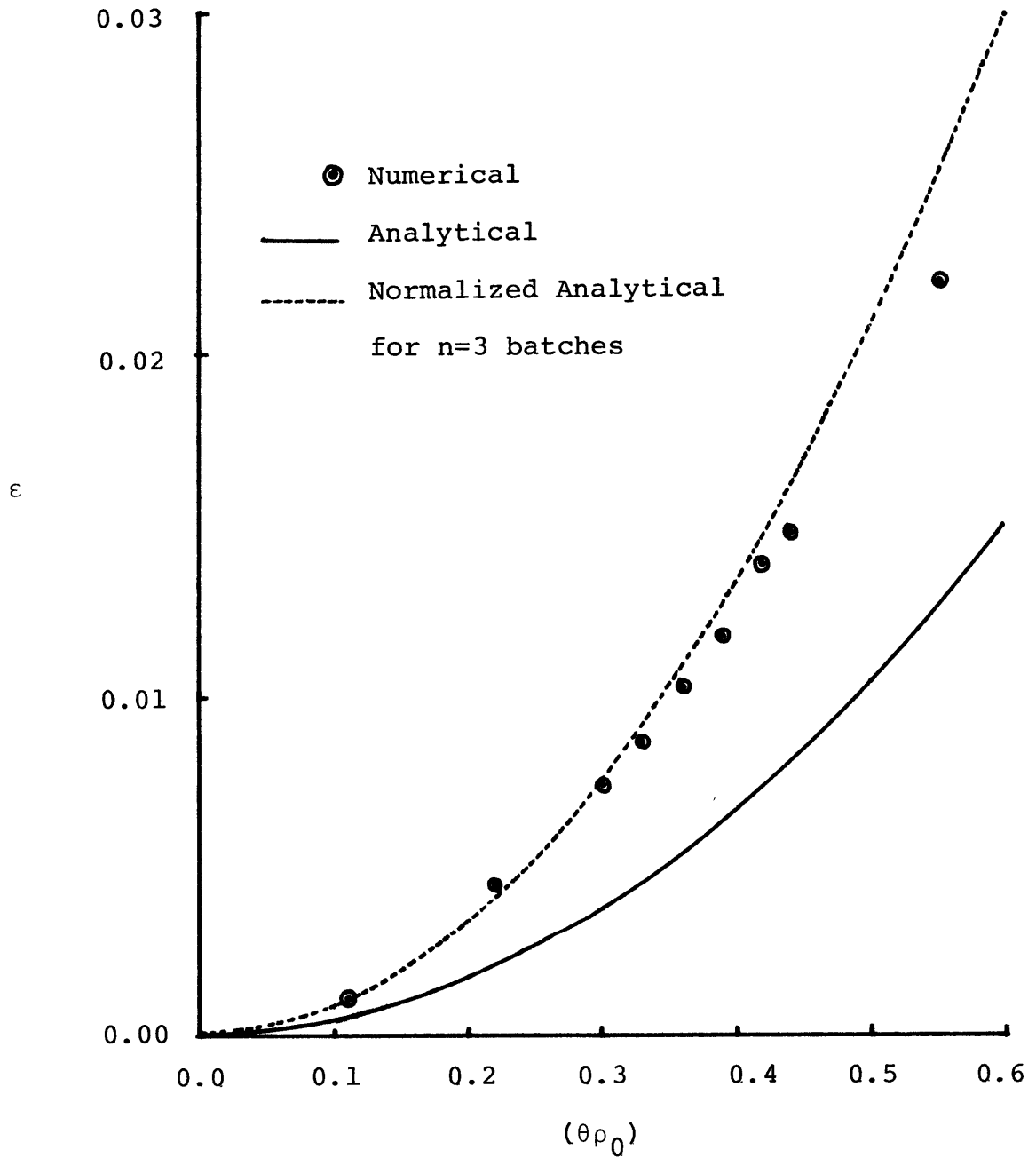
Fig. 4.7 ε as a Function of $(\theta\rho_0)$ for the Case of Reactivity Control by Means of Soluble Poison only

the number of batches n, and $(\theta\rho_0)$ are correctly predicted by the analytical expression of Eq. 4.6. The analytical results were normalized to the accurate numerical ones through the multiplication of Eq. 4.8 by a constant factor of two. The normalized ε factor is thus given by

$$\varepsilon' = \frac{2(\theta\rho_0)^2(n-1)}{3(n+1)^2} \qquad (4.9)$$

The normalized results are also plotted in Figs. 4.6 and 4.7; the agreement is quite good.

4.4.2 REACTIVITY CONTROL USING BURNABLE POISON

Two cases of interest were considered in Chapter 3 with regard to the suppression of reactivity in the fresh fuel by means of burnable poison. In the first case, burnable poison was employed to hold the reactivity at a constant value in the first cycle. The expression for the ε factor for this situation is

$$\varepsilon = -(\theta\rho_0)\frac{(n-1)}{n(n+1)^2} + (\theta\rho_0)^2\frac{(n-1)}{3n(n+1)^2} \qquad (4.10)$$

Figures 4.8 and 4.9 show good agreement between the results obtained numerically and those from the analytical expression of Eq. 4.10, both in magnitude and in the trend.

In the second case, the reactivity of the fuel batch was tailored by means of burnable poison, to increase linearly from a zero value. The ε factor in this case was
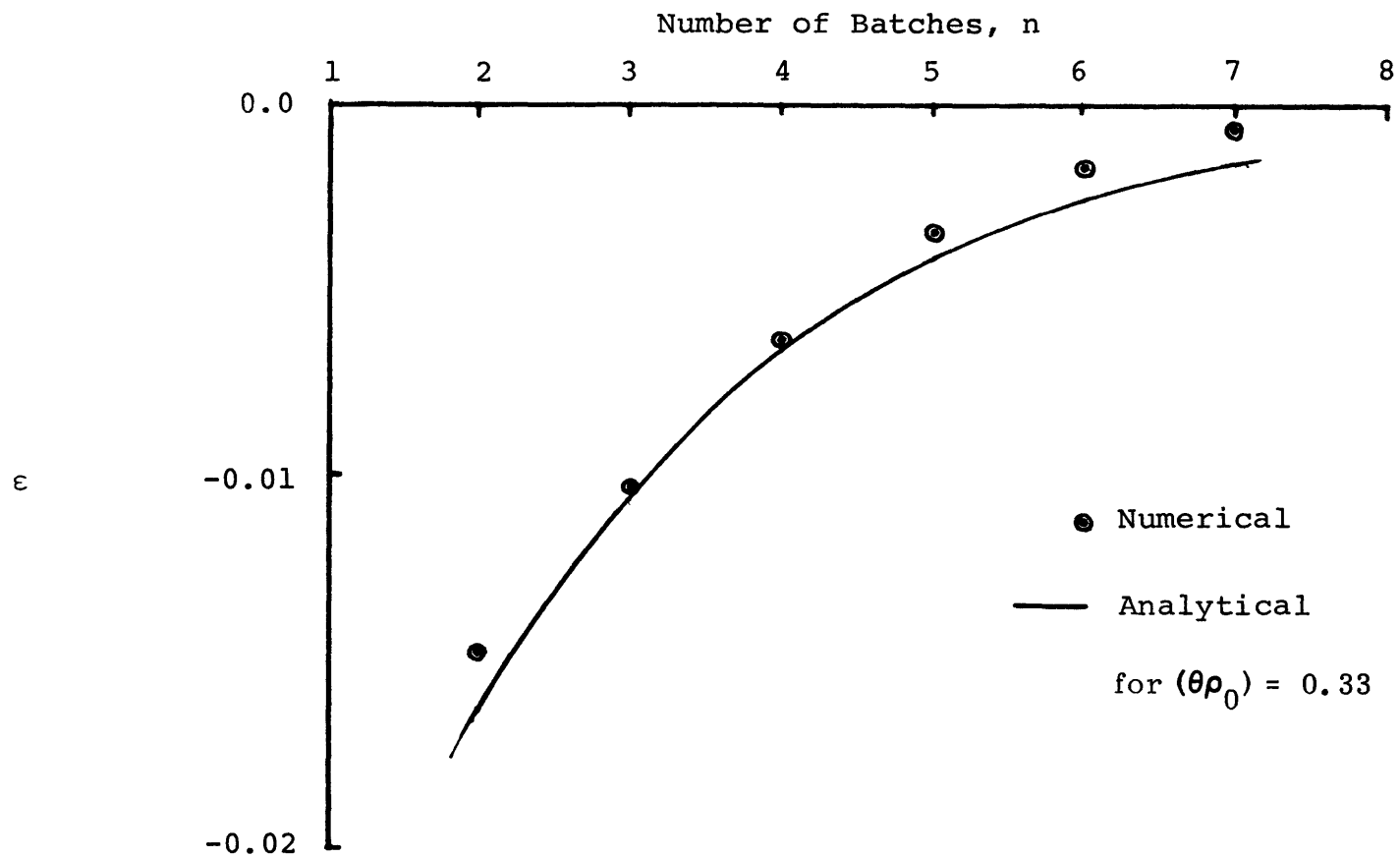
Fig. 4.8 ε as a Function of the Number of Batches, for the case of
Constant Reactivity in the First Cycle
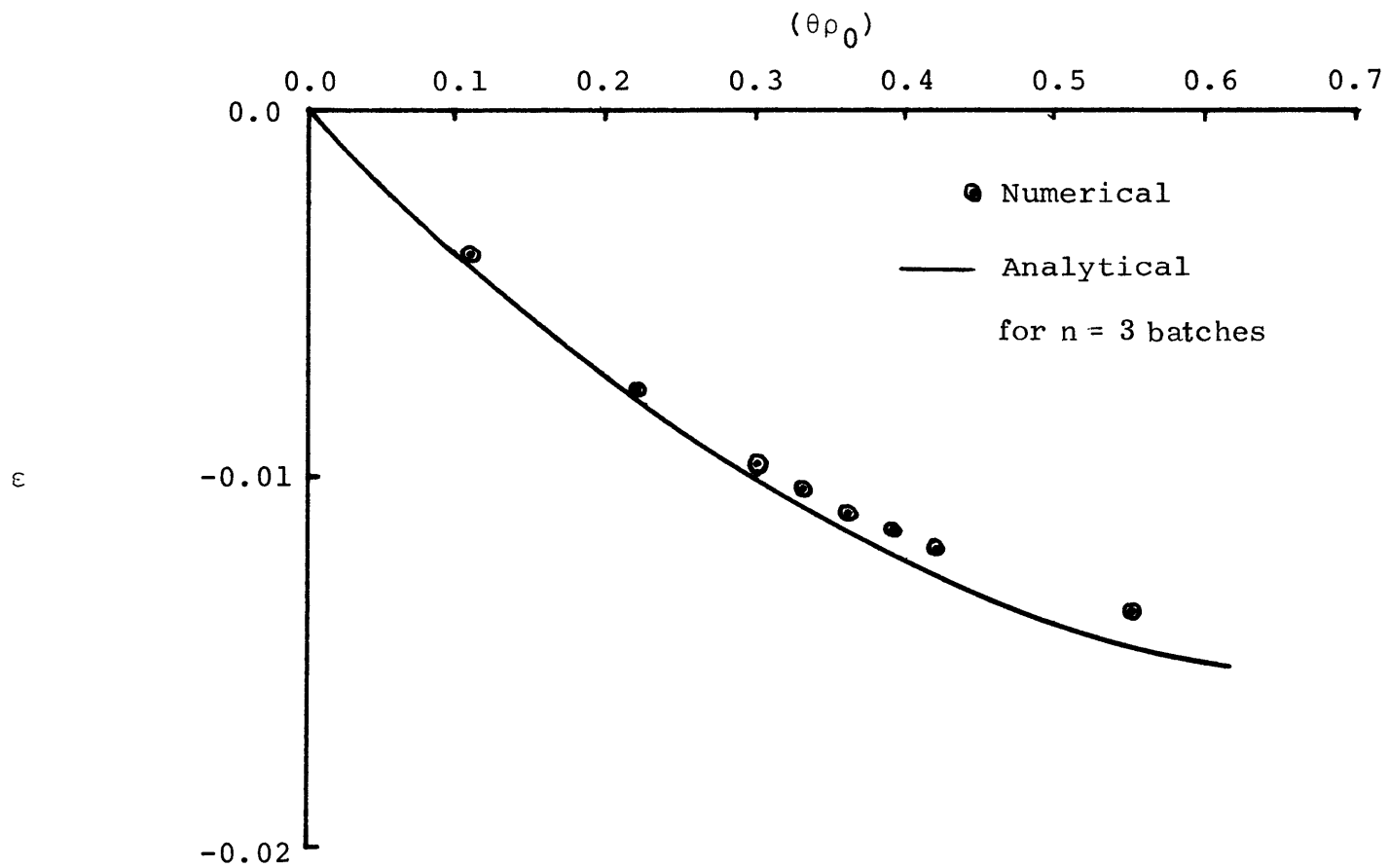
Fig. 4.9 ε as a Function of $(\theta\rho_0)$ for the Case of Constant Reactivity
in the First Cycle

given by

$$\varepsilon = -\frac{(\theta\rho_0)(n-1)}{2n(n+1)} + \frac{(\theta\rho_0)^2(n-1)^2}{6n(n+1)^2} \qquad (4.11)$$

Again, the agreement between the analytical and the numerical results was good, as shown in Figs. 4.10 and 4.11. Hence, no empirical normalization is required in these instances.

4.4.3 REACTIVITY CONTROL USING FIXED POISON SHIMS OR LEAKAGE

The insertion of fixed poison shim in a batch of fuel over a given cycle is mathematically equivalent to subjecting the same batch of fuel to a fixed leakage (for example, by placing the fuel batch on the core periphery) since in both cases, the net effect is to impose a fixed reactivity penalty. The situation is depicted in the reactivity versus burnup trace of Fig. 4.12.

It was pointed out in the previous chapter that there was considerable difficulty for this particular reactivity history in deriving an analytical expression for the discharge burnup (and thus, the ε factor) in a closed form. Therefore, numerical computations were performed to determine the functional dependency of the ε factor on parameters such as the number of batches n, the batch or cycle in which the shim is present, j, the reactivity associated with the shim or leakage, etc.. Figures 4.13 to 4.16 show some of
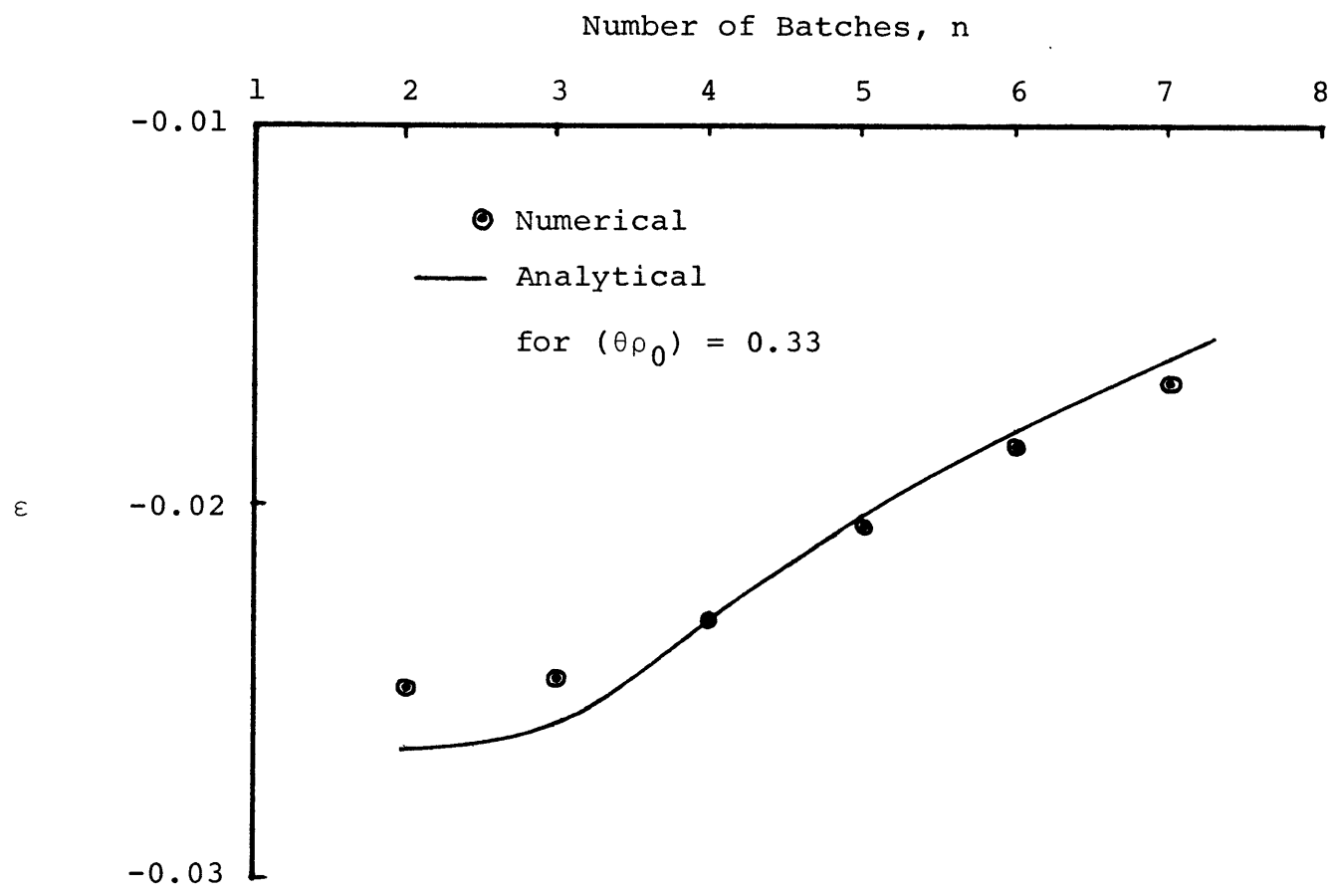
Fig. 4.10 ε as a Function of the Number of Batches for the Case of Reactivity Value at BOL equal to zero ($\rho_{BOL} = 0.0$)

Fig. 4.11 ε as a Function of $(\theta \rho_0)$ for the Case of Reactivity Value at
BOL Equal to Zero $(\rho_{BOL} = 0.0)$
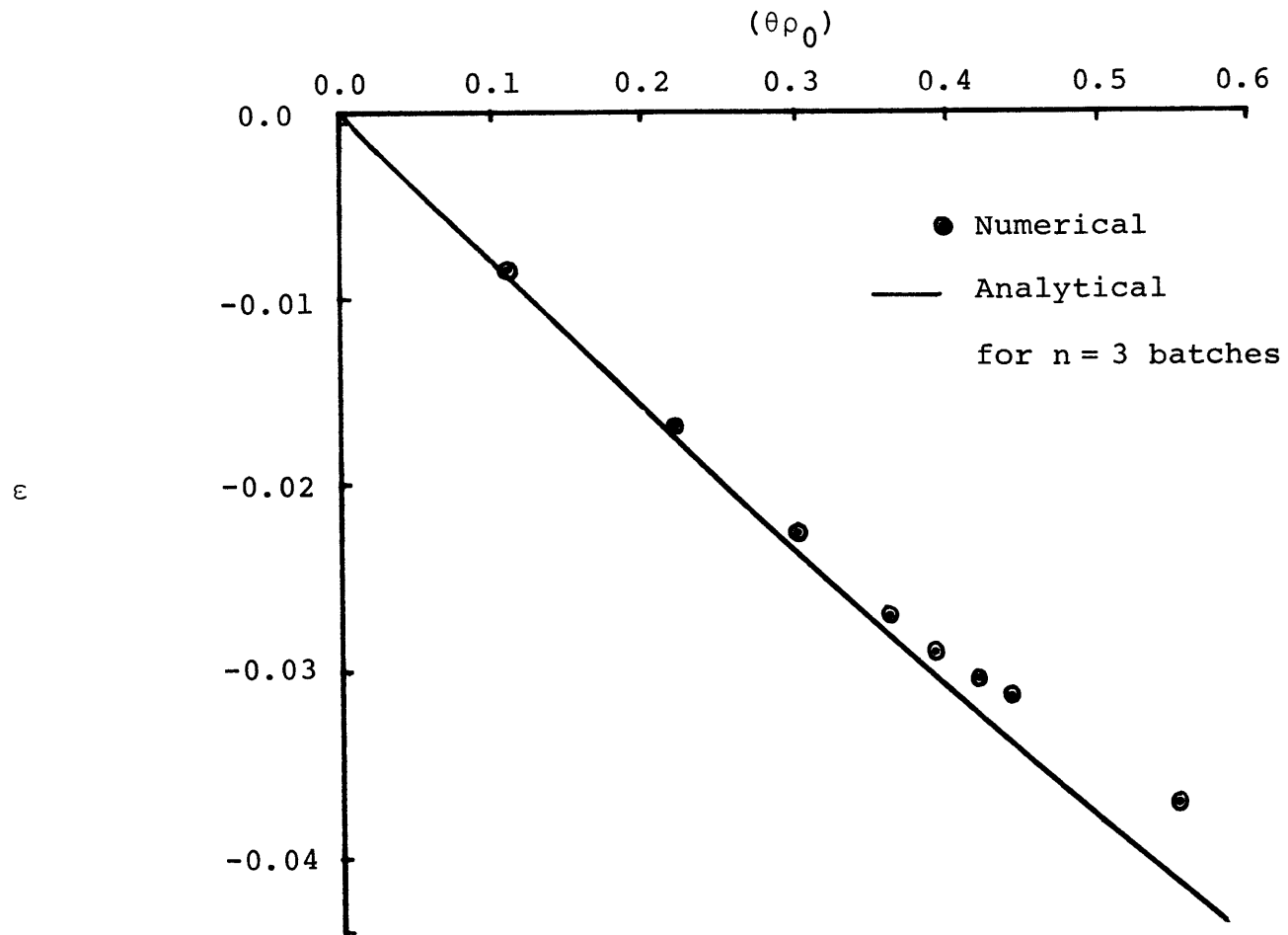
$\Delta\rho$ = Fixed Poison Shim Reactivity
or Leakage Reactivity
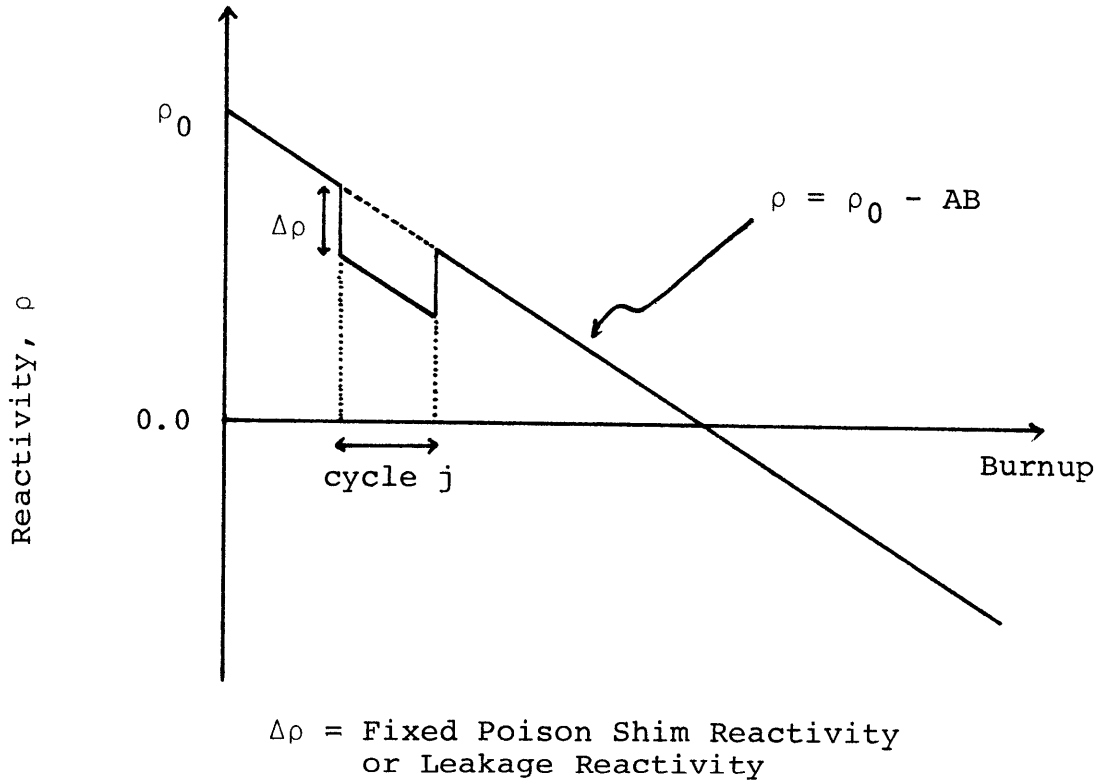
Fig. 4.12 Reactivity versus Burnup Trace for the Case of
the Presence of Fixed Poison Shim or Leakage
in cycle j
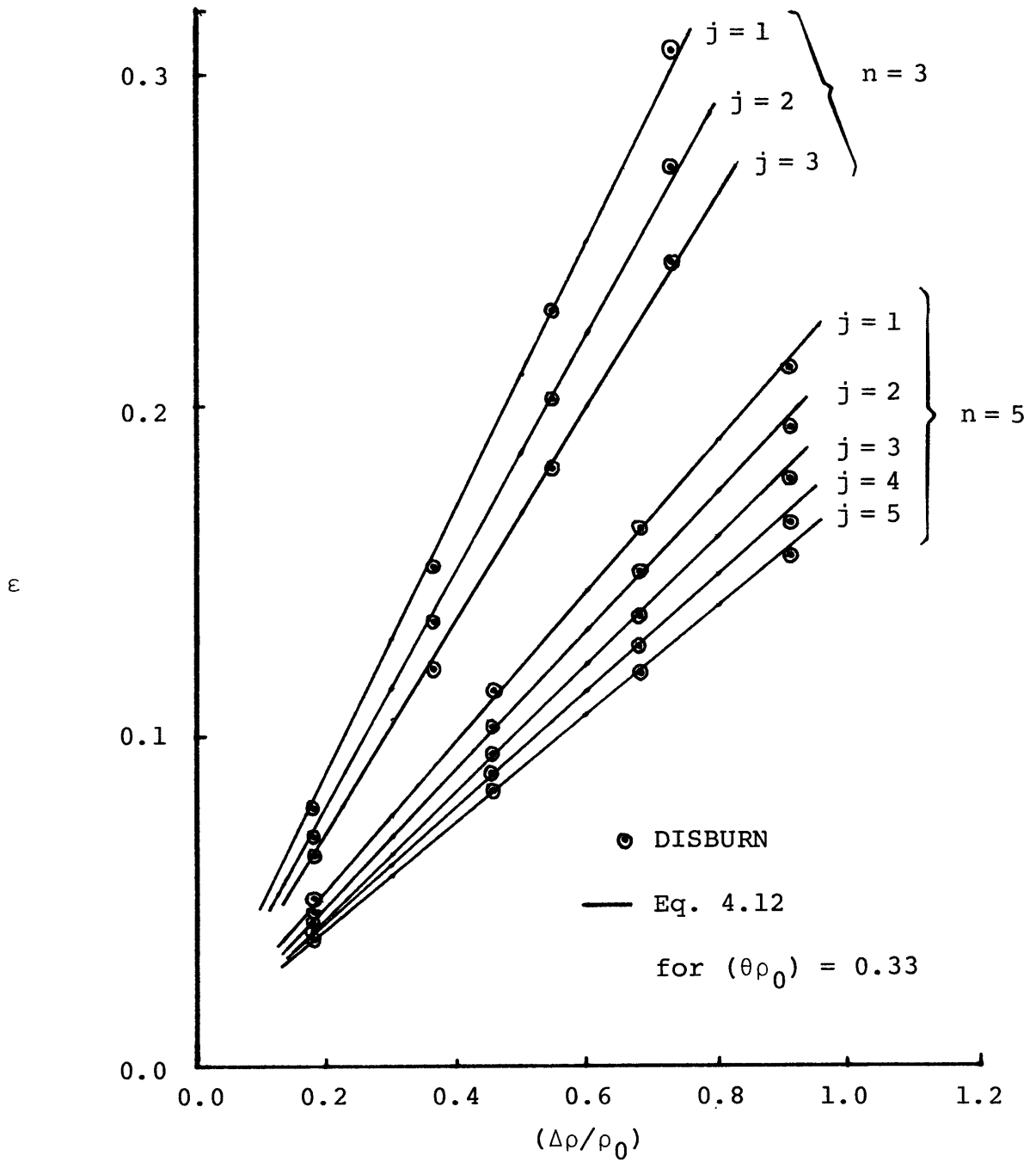
Fig. 4.13 ε as a Function of $(\Delta\rho/\rho_0)$ for the Case of Reactivity Control using Fixed Poison Shim or Leakage in Cycle j
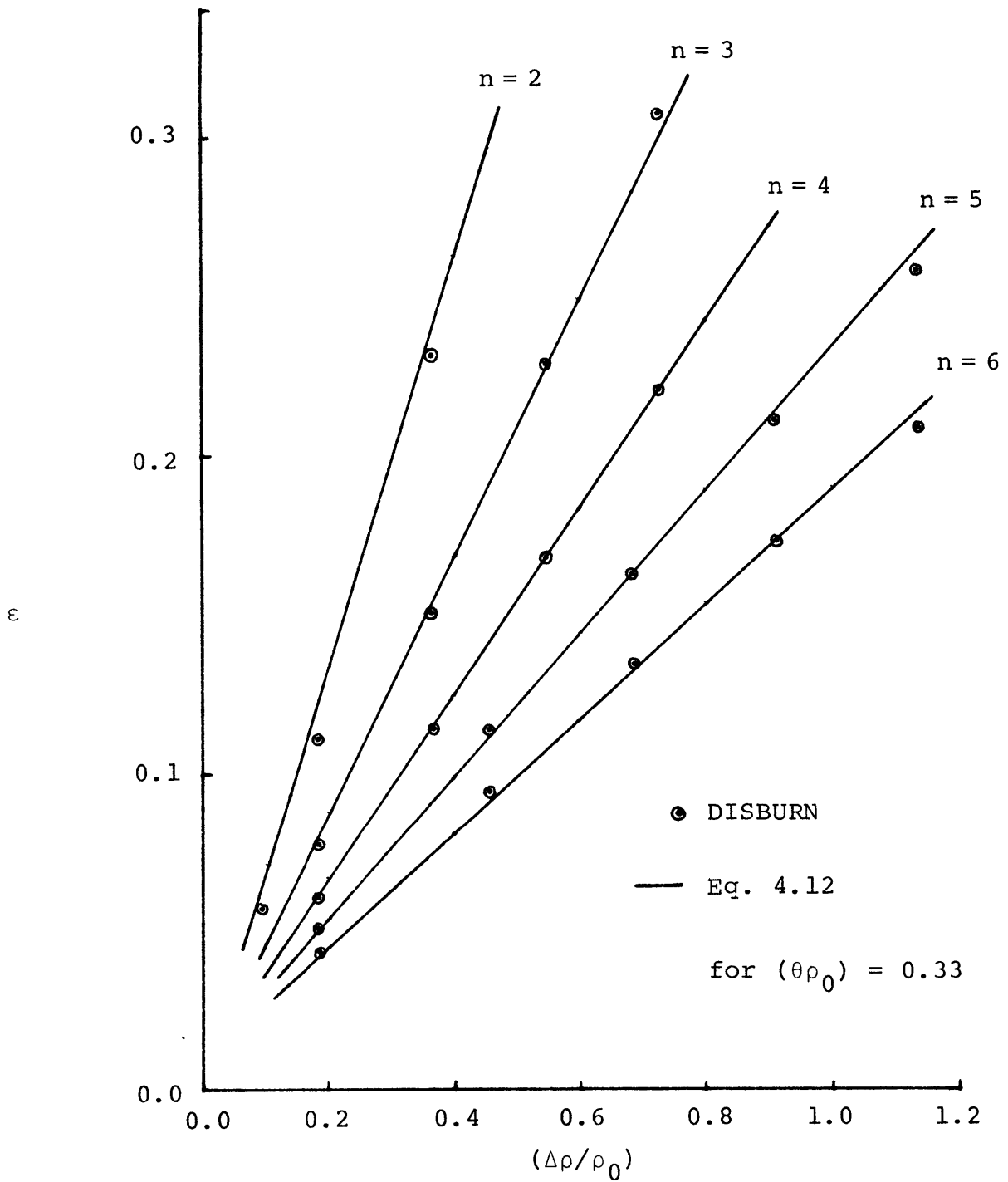
Fig. 4.14 ε as a Function of $(\Delta\rho/\rho_0)$ for the Case of Reactivity Control using Fixed Poison Shim or Leakage in Cycle 1 for Various Numbers of Batches
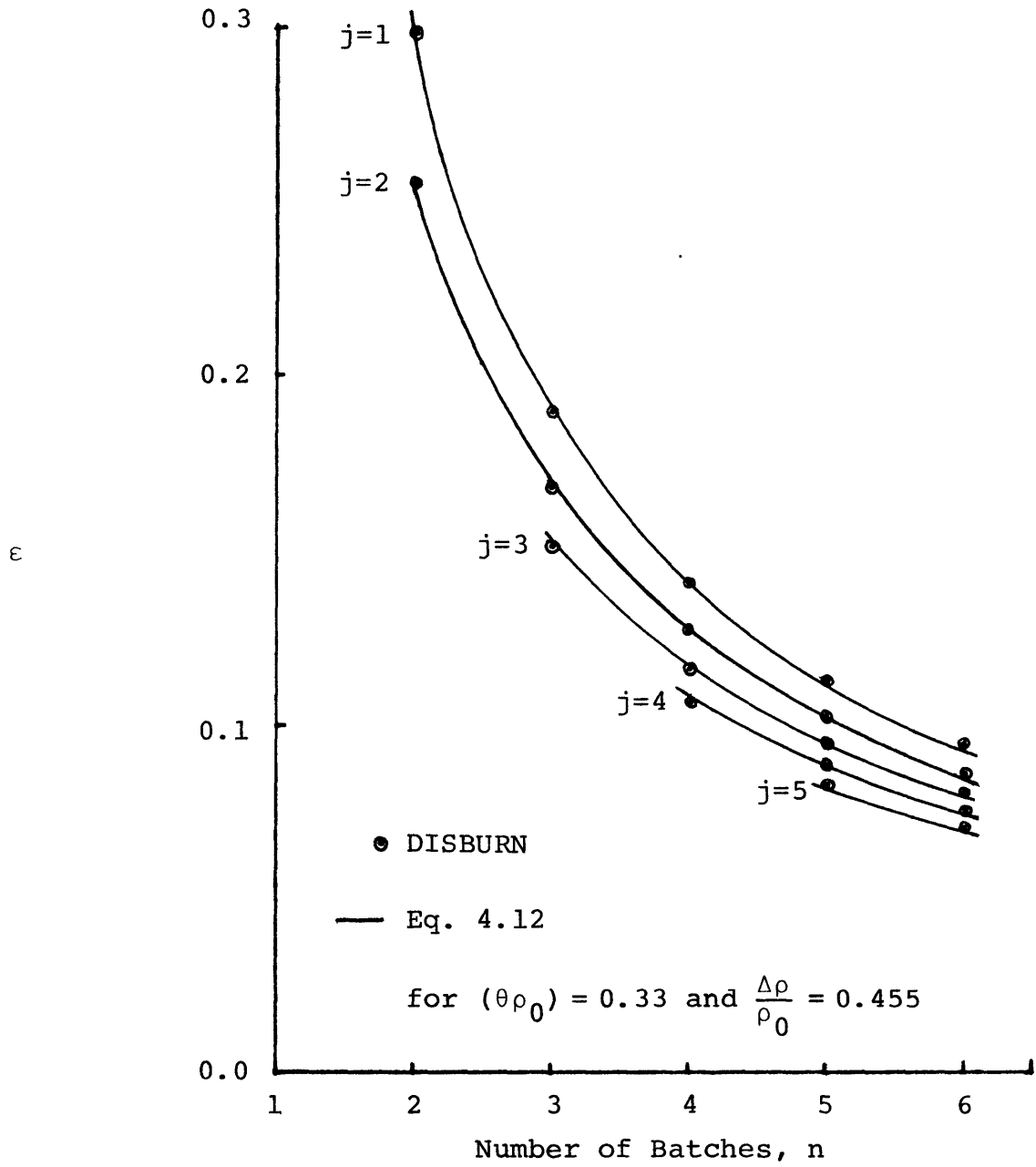
Fig. 4.15 ε as a Function of the Number of Batches for the Case of Reactivity Control by Using Fixed Poison Shim or Leakage in Cycle j
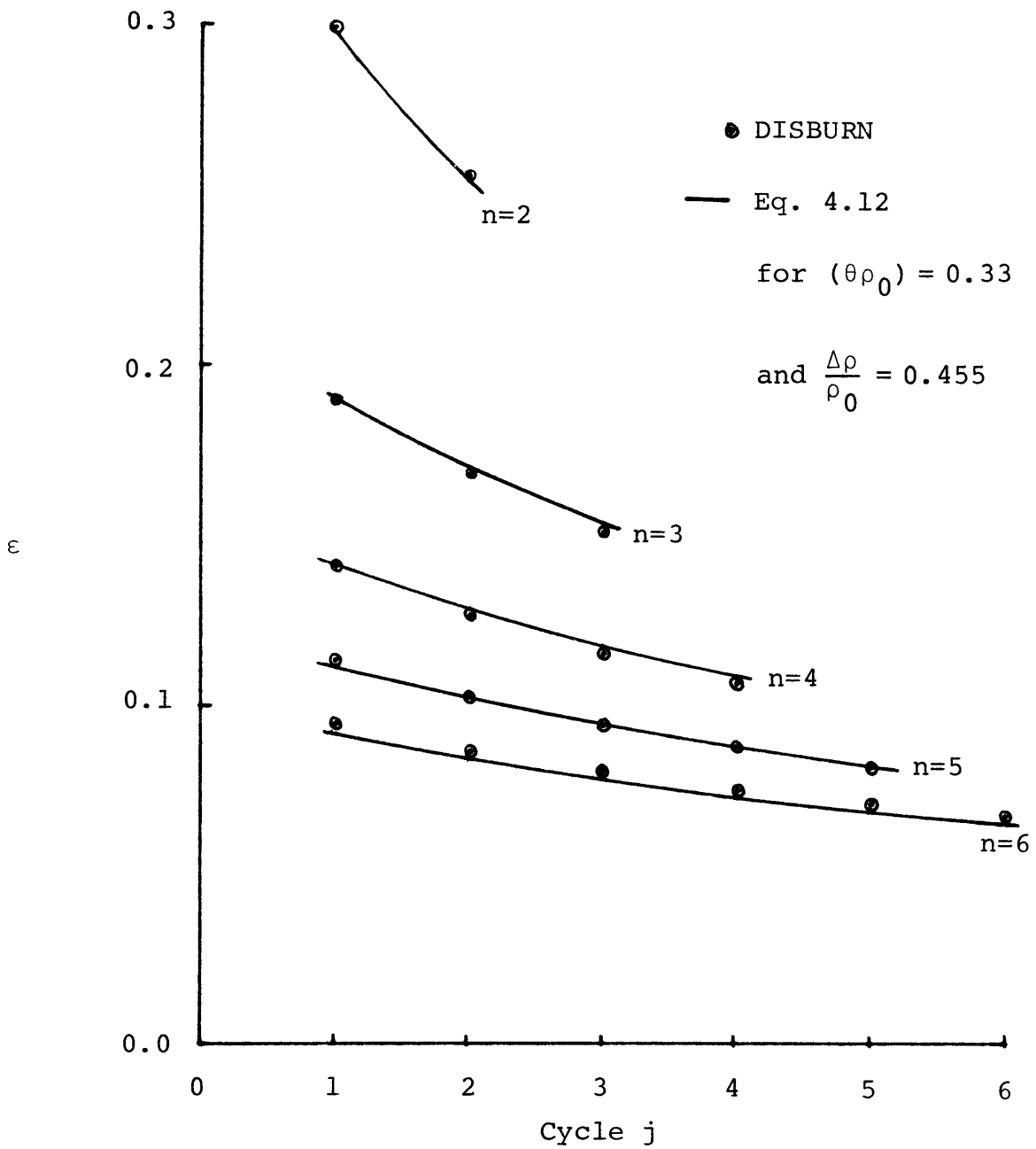
Fig. 4.16 ε as a Function of Cycle j for the Case of Reactivity Control Using Fixed Poison Shim or Leakage for Various Numbers of Batches

the results of these calculations. An empirical correlation
for the ε factor was extracted from these results, and is
given by

$$\varepsilon = \frac{(15.6-n)(6.8+n)R(\theta\rho_0)}{[(38n-25)+(2n+7)j]} + \frac{2(\theta\rho)^2(n-1)}{3(n+1)^2} \qquad (4.12)$$

where $R = (\Delta\rho / \rho_0)$, the ratio of the shim or leakage
          reactivity penalty to the initial extrapolated
          reactivity,

and $j = 1, 2, \ldots, n$.

When no fixed poison shim or leakage is present (i.e., $\Delta\rho = $
0.0), Eq. 4.12 reduces to the case of reactivity control by
soluble poison only (i.e., a linear $\rho(B)$ assembly history—
without burnable poison or leakage reactivity penalties)—
the second term on the right hand side of Eq. 4.12 is the
normalized ε factor of the soluble poison case.

We are now in a position to determine the ε factor and
the corresponding discharge burnup for any situation in-
volving fixed poison shim or leakage of neutrons from the
core, using Eq. 4.12, given just the values of the para-
meters required in the equation.

4.4.4 SUPERPOSITION OF ANALYTICAL RESULTS

Although the analytical and empirical expressions for
the ε factor obtained thus far permit us to calculate the
the discharge burnups of a fuel batch with various reacti-

vity versus burnup trajectories; corresponding to individual elements of a fuel management scheme, their utility is still limited in that practical situations involve the combination of the different fuel management strategies—i.e., a reactor core may be operated using a low-leakage loading pattern with burnable poison being employed to suppress the reactivity of the fresh fuel over its first cycle. This and other combinations of fuel management strategies can be readily handled by the DISBURN code, as was demonstrated in the previous sections of this chapter. However, superposition of analytical results for the various individual schemes would, if verified as being sufficiently accurate, allow us to compute the discharge burnup resulting from a synthesis of a wide variety of fuel management tactics. This proposition was examined by considering the discharge burnup of the reference flat power case, B_0. For an individual fuel management scheme, designated subscript ℓ, the penalty or gain in the discharge burnup is given by

$$\Delta B_\ell = B_0 - B_{dis,\ell} \qquad (4.13)$$

where $B_{dis,\ell}$ is the discharge burnup for the particular scheme.

Substituting Eq. 4.7 (i.e., in terms of the ε factor) for $B_{dis,\ell}$ into Eq. 4.13, we have

$$\Delta B_\ell = B_0 - \frac{B_0}{(1+\varepsilon_\ell)} = B_0 \left(\frac{\varepsilon_\ell}{1+\varepsilon_\ell}\right) \qquad (4.14)$$

Note that the ε factor is a negative number if there is a gain in the discharge burnup.

If we have a combination of m fuel management schemes, the net discharge burnup penalty or gain is

$$\Delta B^m_{net} = \sum_{\ell=1}^{m} \Delta B_\ell$$

$$= B_0 \sum_{\ell=1}^{m} \left(\frac{\varepsilon_\ell}{1+\varepsilon_\ell}\right) \qquad (4.15)$$

The corresponding discharge burnup for the synthesis of m of these schemes is (from Eq. 4.13) therefore,

$$B^m_{dis} = B_0 - \Delta B^m_{net} \qquad (4.16)$$

Substituting ΔB^m_{net} from Eq. 4.15 into Eq. 4.16 yields

$$B^m_{dis} = B_0 - B_0 \sum_{\ell=1}^{m} \left(\frac{\varepsilon_\ell}{1+\varepsilon_\ell}\right)$$

$$= B_0 \left[1 - \sum_{\ell=1}^{m} \left(\frac{\varepsilon_\ell}{1+\varepsilon_\ell}\right) \right] \qquad (4.17)$$

The discharge burnups for a number of combinations of individual fuel management strategies were calculated using the prescription given by Eq. 4.17. These results were compared

to those obtained using the DISBURN code. Tables 4.14 and
4.15 show the differences between the two sets of results.
For these cases B_0 = 36184 MWD/MT; hence the total correc-
tion factors (bracketed term in Eq. 4.17) were in the range
of 4.2 to 13.5%. It can be seen that the discharge burnups
calculated using Eq. 4.17 are typically biased—running
consistently about 1% less than those computed using the
DISBURN code. Hence the relative accuracy case-to-case is
very nearly perfect—a highly desirable situation because
of the projected use of these relations for strategic com-
parisons. Considering the simplicity of the prescription
developed from the superposition of the analytical expres-
sions for the ε factors and the complexity of the problems
involved, its agreement with the more accurate numerical
method is rather satisfactory.

The use of superposition should permit evaluation of
essentially all combinations of contemporary interest;
should schemes be envisioned which cannot be handled in
this manner, the DISBURN code can be used.

TABLE 4.14

COMPARISON OF DISCHARGE BURNUPS CALCULATED
USING SUPERPOSITION WITH DISBURN RESULTS
(BURNABLE POISON USED TO HOLD REACTIVITY IN
CYCLE 1 TO A CONSTANT VALUE: LOW-LEAKAGE SCHEME)

Case	Discharge Burnup from Super-position of Analytical Results (MWD/MT)	Discharge Burnup from the DISBURN Code (MWD/MT)	Difference (%)
1. Fixed Poison Shim or leakage in Cycle 2			
1(a) Shim Poison $\Delta\rho = 4\%$	34099	34447	1.0
1(b) Shim Poison $\Delta\rho = 10\%$	31315	31551	0.7
2. Fixed Poison Shim or leakage in Cycle 3			
2(a) Shim Poison $\Delta\rho = 3.5\%$	34537	34874	1.0
2(b) Shim Poison $\Delta\rho = 8.0\%$	32560	32869	0.9

TABLE 4.15

COMPARISON OF DISCHARGE BURNUPS CALCULATED
USING SUPERPOSITION WITH DISBURN RESULTS
(BURNABLE POISON USED TO TAILOR THE REACTIVITY IN
CYCLE 1 TO INCREASE LINEARLY FROM
AN INITIAL VALUE OF ZERO)

Case	Discharge Burnup from Super- position of Analytical Results (MWD/MT)	Discharge Burnup from the DISBURN Code (MWD/MT)	Difference (%)
1. Fixed Poison Shim or leakage in Cycle 2			
1(a) Shim Poison $\Delta\rho$ = 4.0%	34672	35025	1.0
1(b) Shim Poison $\Delta\rho$ = 6.0%	33690	34011	0.9
2. Fixed Poison Shim or leakage in Cycle 3			
2(a) Shim Poison $\Delta\rho$ = 5.0%	34425	34759	1.0
2(b) Shim Poison $\Delta\rho$ = 8.0%	33133	33416	0.8

4.5 SOME ELEMENTARY ECONOMIC CONSIDERATIONS

It was pointed out earlier in this chapter that, in addition to benefiting the moderator temperature coefficient of reactivity, the use of burnable poison in the low-leakage fuel management scheme reduces the global radial power peaking factor. Since a nuclear plant must be operated subject to certain thermal constraints, this reduction in the global radial power peaking by means of burnable poison is beneficial with respect to the plant thermodynamic efficiency, its capacity factor and thus the overall economics of the facility.

An approach has been developed to characterize the effects of the thermal limits on the various cost components (e.g., the busbar cost and the system cost) and subsequently, to measure the impact of the global radial power flattening benefits due to the use of burnable poison. In what follows, the economic penalty of system derating will be computed. It is clear that the plant designers/operators would not actually tolerate such penalties, but would take steps to mitigate them. Hence the results developed here should be interpreted as "breakeven avoidance cost": the amount which could be spent on mitigation.

The fuel cycle cost, e_f, the busbar cost, e_b, and the system cost, e_s, are related as follows:

$$e_f = \frac{C}{\eta B} \qquad (4.18)$$

$$e_b = \frac{A}{L} + e_f \qquad\qquad (4.19)$$

$$e_s = e_b L + (1-L)e_r \qquad\qquad (4.20)$$

where C and A are parameters proportional to fuel and capital costs, respectively, and

η = plant thermodynamic efficiency

B = discharge burnup

L = plant capacity factor

e_r = cost of replacement electricity

For small changes from a reference design, assuming for present purposes that A and C remain unchanged, the following relations hold, to first order:

$$\Delta e_f \approx \frac{\partial e_f}{\partial \eta} \cdot \Delta\eta + \frac{\partial e_f}{\partial B} \cdot \Delta B \qquad\qquad (4.21)$$

$$\Delta e_b \approx \frac{\partial e_b}{\partial L} \cdot \Delta L + \frac{\partial e_b}{\partial e_f} \Delta e_f \qquad\qquad (4.22)$$

$$\Delta e_s \approx \frac{\partial e_s}{\partial e_b} \Delta e_b + \frac{\partial e_s}{\partial L} \cdot \Delta L \qquad\qquad (4.23)$$

The partial derivatives can be calculated given appropriate constraints. The two constraints that have been considered are:

CONSTRAINT (1): Coolant exit enthalpy (temperature)

is limiting. Thus, increased as-
sembly power requires a reduction
in exit enthalpy (i.e., a decrease
in the mean core exit temperature)
with a corresponding decrease in
plant efficiency.

CONSTRAINT (2): Local temperature or power peaking
are limiting. This requires power
level derating at constant thermal
dynamic efficiency.

For constraint (1) we have the following relationship between
the plant capacity factor, L, and the efficiency, η:

$$\frac{L}{\eta} = \frac{L_0}{\eta_0} \qquad (4.24)$$

where the subscript "0" refers to the reference case. For
constraint (2), since the efficiency is unchanged, the effect
on the capacity factor is directly through the thermal power
production:

$$\frac{\Delta L}{L} = \left(\frac{\Delta Q}{Q}\right)_{thermal} = -\frac{\Delta F}{F} \qquad (4.25)$$

where Q is the thermal power and F the radial power peaking
factor. Equations 4.24 and 4.25 have been used in conjunction
with Eqs. 4.18 through 4.23 to evaluate the relative changes
in fuel cycle, busbar, and system costs under the two limiting

constraints. The final expressions are as follows:

CONSTRAINT (1): Exit enthalpy is limiting.

$$\left(\frac{\Delta e_f}{e_f}\right)_1 = -\frac{\Delta\eta}{\eta} - \frac{\Delta B}{B} \tag{4.26}$$

$$\left(\frac{\Delta e_b}{e_b}\right)_1 = -\frac{\Delta\eta}{\eta} - \left(\frac{e_f}{e_b}\right)\frac{\Delta B}{B} \tag{4.27}$$

$$\left(\frac{\Delta e_s}{e_s}\right)_1 = -\frac{e_r L}{e_s}\frac{\Delta\eta}{\eta} - \frac{e_f L}{e_s}\frac{\Delta B}{B} \tag{4.28}$$

CONSTRAINT (2): Local temperature or power peaking
are limiting.

$$\left(\frac{\Delta e_f}{e_f}\right)_2 = -\frac{\Delta B}{B} \tag{4.29}$$

$$\left(\frac{\Delta e_b}{e_b}\right)_2 = +\left(1 - \frac{e_f}{e_b}\right)\frac{\Delta F}{F} - \frac{e_f}{e_b}\frac{\Delta B}{B} \tag{4.30}$$

$$\left(\frac{\Delta e_s}{e_s}\right)_2 = +\frac{L(e_r - e_f)}{e_s}\frac{\Delta F}{F} - \frac{e_f}{e_s}\cdot\frac{\Delta B}{B} \tag{4.31}$$

The change in radial power factors and discharge burnups
between a reference case and a modified design can be evalu-
ated using the DISBURN code, and the change in efficiency from
an expression such as

$$\eta \simeq 1 - \frac{T_c}{T}(1 + u) \tag{4.32}$$

where T_c = mean condenser temperature (assumed constant)

T = mixed mean core exit temperature

u = unavailability (assumed constant)

Again letting the subscript "0" represent the reference (current 3-batch, out-in fuel management) case and subscript "1" the new fuel management scheme, the change in thermodynamic efficiency from the reference case can be obtained from Eq. 4.32:

$$\frac{\Delta \eta}{\eta_0} = \frac{\eta_1 - \eta_0}{\eta_0}$$

$$= -\frac{(1 - \eta_0)}{\eta_0} \frac{(T_0 - T_1)}{T_1}$$

$$= -\frac{(1 - \eta_0)}{\eta_0} \frac{(\Delta T)}{T_1} \tag{4.33}$$

where T_0, T_1 = the mixed mean core exit temperatures of the reference and the new scheme, respectively

ΔT = core exit temperature degradation due to radial power peaking in the new scheme.

Assuming that the inlet core temperatures of both cases have the same constant value, we can write:

$$F_0 (T_0 - T_{in}) = F_1 (T_1 - T_{in}) \tag{4.34}$$

where F_0, F_1 = the radial peak/average power ratio of the

reference and the new fuel management

scheme, respectively

T_{in} = the inlet core temperature of both designs.

Substituting T_1 from Eq. 4.34 into Eq. 4.33, the change in

thermodynamic efficiency from the reference case can be ex-

pressed in terms of $\Delta F = F_1 - F_0$, and the parameters associated

with the reference case, to give:

$$\frac{\Delta \eta}{\eta_0} = - \frac{(1 - \eta_0)}{\eta_0} \left[\frac{\Delta F (T_0 - T_{in})}{\Delta F T_{in} + F_0 T_0} \right] \qquad (4.35)$$

The preceding analysis has been applied to evaluate the

improvements in the fuel cycle cost, the busbar cost, and the

system cost over the reference out-in fuel management scheme

due to the implementation of the low-leakage fuel management

strategy—in particular, we want to determine the effects of

employing burnable poison (to suppress the reactivity of

fresh fuel) in the low-leakage scheme, on the fuel cycle, the

busbar, and the system cost of the plant. The low-leakage

fuel management scheme has been analyzed in an earlier section

of this chapter, and Table 4.16 summarizes the results of the

analyses. The relevant parameters for the reference base case

(current, 3-batch out-in scheme) employed in the cost evalua-

tions are shown in Table 4.17, and Table 4.18 gives the

results of the evaluations. Under constraint (1), the posi-

tive impact on the fuel cycle, busbar, and system cost due to

TABLE 4.16

BURNUP AND POWER PEAKING CHARACTERISTICS OF
LOW-LEAKAGE (IN-IN-OUT) FUEL MANAGEMENT

Case	Increase in Discharge Burnup over the Reference Out-In Scheme (%)	Relative Radial Power Peaking* Factor (BATCH AVERAGE)
Case with No Burnable Poison	3.00	1.15
Burnable Poison Cases:		
Constant Reactivity in Cycle 1 (Residual $\Delta\rho$ = 0.3%)	3.19	1.09
BOL Reactivity Value ρ_{BOL} = 0.02) (Residual $\Delta\rho$ = 0.49%)	3.62	1.05

*Reference Relative Radial Power Peaking Factor is 1.00.

TABLE 4.17

RELEVANT PARAMETERS FOR THE REFERENCE
3-BATCH, OUT-IN FUEL MANAGEMENT
CASE USED IN COST CALCULATIONS

Item	Value
Fuel cycle cost, e_f	6.4 mills/kwhr
Busbar cost, e_b	40.0 mills/kwhr
Replacement energy cost, e_r	60.0 mills/kwhr
System cost, e_s	46.0 mills/kwhr
Capacity factor, L_0	0.7
Thermodynamic efficiency, η_0	0.33
Relative radial power peaking factor, F_0	1.00
Inlet core temperature, T_{in}	290°C
Mixed mean core exit temperature, T_0	319°C
Discharge Burnup	30,000 MWD/MT

TABLE 4.18

POTENTIAL CHANGES IN THE FUEL CYCLE, BUSBAR,
AND SYSTEM COSTS DUE TO THE IMPLEMENTATION
OF LOW-LEAKAGE (IN-IN-OUT) FUEL MANAGEMENT

	$\left(\dfrac{\Delta e_f}{e_f}\right)^*$ %	$\left(\dfrac{\Delta e_b}{e_b}\right)^*$ %	$\left(\dfrac{\Delta e_s}{e_s}\right)^*$ %
<u>CONSTRAINT (1)</u>: EXIT ENTHALPY IS LIMITING.			
Case with No Burnable Poison	-1.7	0.8	0.9
Burnable Poison Cases:			
Constant Reactivity in Cycle 1 (Residual $\Delta\rho$ = 0.3%)	-2.4	0.3	0.4
BOL Reactivity Value ρ_{BOL} = 0.02 (Residual $\Delta\rho$ = 0.49%)	-3.1	-0.1	0.1
<u>CONSTRAINT (2)</u>: LOCAL POWER PEAKING OR TEMPERATURE IS LIMITING.			
Case with No Burnable Poison	-3.0	-0.4	-0.3
Burnable Poison Cases:			
Constant Reactivity in Cycle 1 (Residual $\Delta\rho$ = 0.3%)	-3.2	-0.4	-0.4
BOL Reactivity Value ρ_{BOL} = 0.02 (Residual $\Delta\rho$ = 0.49%)	-3.6	-0.5	-0.5

*All increments are relative to use of the same fuel without
burnable poison in a conventional out-in/scatter fuel manage-
ment scheme. A negative value represents a savings.

the reduction of the global radial power peaking factor by
means of burnable poison in the low-leakage scheme can be
observed. Whereas under constraint (2), which requires ther-
mal power reduction at constant thermodynamic efficiency,
because power peaking is limiting, the impact of the burnable
poison is less significant, but still beneficial.

Thus the use of burnable poison can be assessed in terms
of avoidance costs. For purposes of comparison, note that:

- 1% in fuel cycle cost corresponds to roughly 10 $/kg
  HM in fuel fabrication costs, and
- 1% in busbar cost corresponds to roughly 2×10^6 $/yr
  in the cost of electricity.

On this basis one could afford to implement the use of burn-
able poison if it increased fuel assembly costs by as much as
5 to 10%. These estimates are only approximate, of course,
and much more specific analyses should be done on a case-by-
case basis.

4.6 CHAPTER SUMMARY

In this chapter, the DISBURN code was evaluated as a
tool for computing the fuel discharge burnup for a given fuel
management scheme. It was shown to predict the relative
changes in the discharge burnup due to modifications in a re-
ference design quite accurately, and not biased to any signi-
ficant degree by the details of the method used to obtain the
two most important free parameters of the model, i.e., the
leakage coefficient, α, and the power sharing parameter, θ.

Analyses performed using the DISBURN code have indicated that proper shaping of the reactivity versus burnup trace of a fuel batch by means of burnable poison can improve the discharge burnup by as much as 3.5%; this value is reduced to roughly 1% when the anticipated residual poison reactivity penalty is also considered. When burnable poison is employed in conjunction with a low-leakage fuel management strategy and cycle length extension, the global radial power peaking factor of the core is significantly reduced. The avoidance costs of plant derating or efficiency degradation appear sufficient to cover the added expenses of poison use.

The overall improvement in the uranium utilization for the standard cycle length low-leakage fuel management scheme with the incorporation of burnable poison, and accounting for the anticipated residual poison reactivity penalty, was about 3.6%, while the corresponding uranium utilization increase for an extended cycle length low-leakage fuel management scheme was approximately 11.1% over the reference case.

Finally, the discharge burnups resulting from synthesis of a variety of fuel management strategies, calculated using superposition of analytical expressions for the ε factors for the various individual schemes, were found to be in good agreement with values obtained using the DISBURN code. Hence, quick scoping analyses can be performed using the analytical expressions for the ε factors developed in the present work.

CHAPTER 5

SUMMARY, CONCLUSIONS, AND RECOMMENDATIONS

5.1 INTRODUCTION

In recent years, considerable interest in the achievement of higher fuel burnup in light water reactors has been generated by a number of factors: a need for resource conservation due to the delay in the commercialization of nuclear fuel reprocessing and the development of breeder reactors, a desire by utilities to extend the cycle length of reactor operation in order to increase plant capacity factor and to improve the overall economics of their systems.

Recent M.I.T. work, including that reported here, has been concerned with the self-consistent evaluation of ways to facilitate the realization of high burnup and improved neutron economy. An important part of the present effort is the development and improvement of a simple model which has a sound theoretical basis and is capable of evaluating the effects of small changes in core design and fuel management schemes on a consistent basis. Another major focus of the present work has been on the development of an optimum strategy for the use of a generalized burnable poison to alleviate the power peaking which typically characterizes higher burnup assembly designs and core arrangements, and in the process further improve the discharge burnup of a fuel batch through the shaping of its power history profile.

The work described in this report was undertaken as part of the D.O.E.'s LWR Technology Program for Improved Uranium Utilization.

5.2 THE LINEAR REACTIVITY MODEL

The linear reactivity model (LRM) is based on the observation that the reactivity, ρ, of a PWR fuel lattice varies linearly with burnup within the current range of interest with respect to fuel lattice parameters. As a point of interest, we also found that the LRM methodology is applicable to other fuel types (combinations of other fissile and fertile isotopes such as U-233, Pu-239, Pu-241 and Th-232), since quite linear $\rho(B)$ traces are also observed for these lattices (with the exception of Pu/Th-232 lattice: see Figs. 5.1 and 5.2).

To analyze fuel management strategies of contemporary interest, two important features which reflect the actual behavior of PWR cores were incorporated into the methodology. The first was the appropriate algorithm for the combination of the reactivity of fuel batches in a core—a power-reactivity weighting scheme; the system reactivity is thus given by

$$\rho_{sys} = \sum_{i=1}^{n} f_i \rho_i \qquad (5.1)$$

The discharge burnup of the fuel batch can be obtained by performing a reactivity balance for an n-batch, steady-state core:
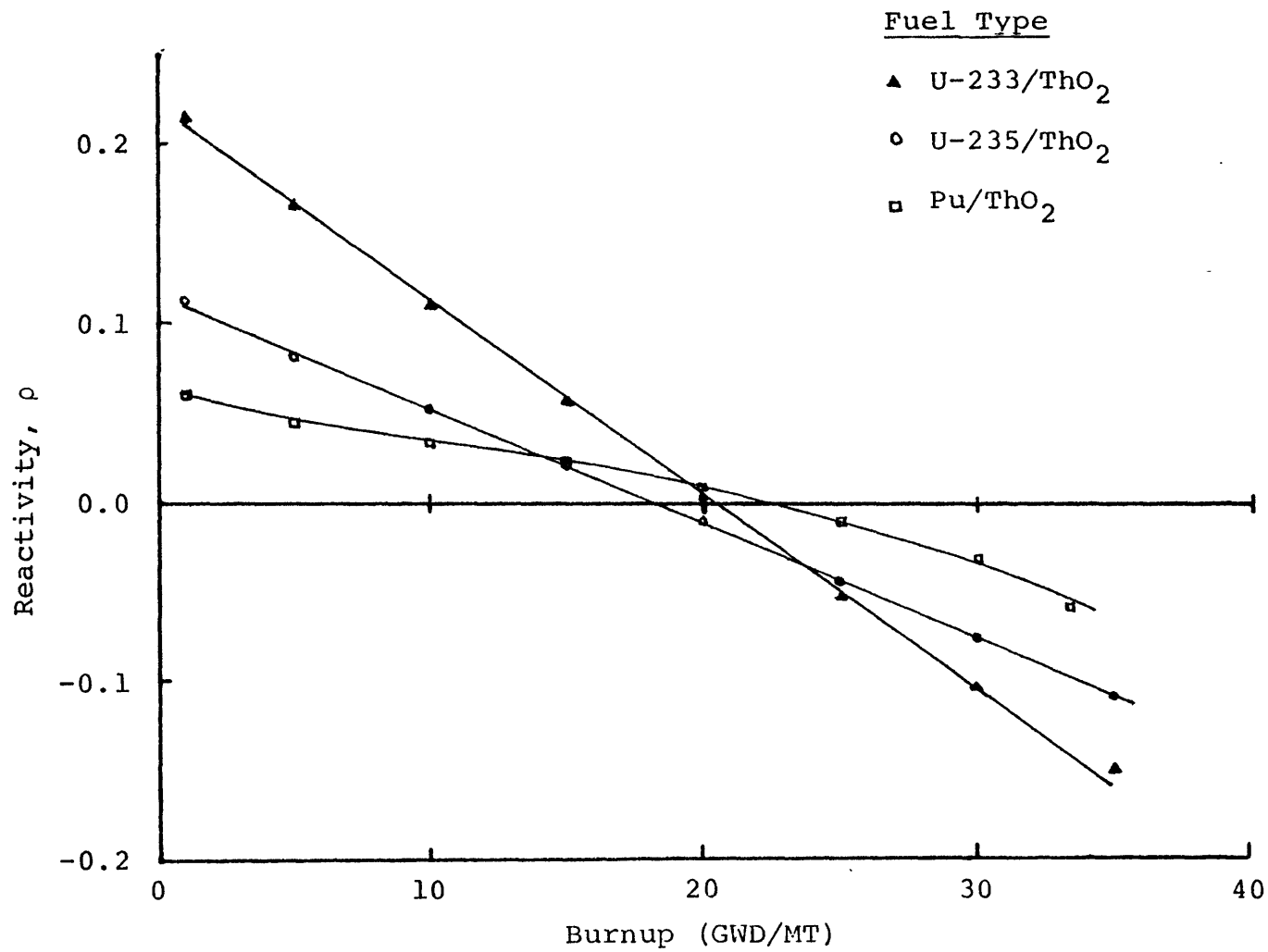
Fig. 5.1   Reactivity versus Burnup for Various Fissile
           Materials in ThO_2
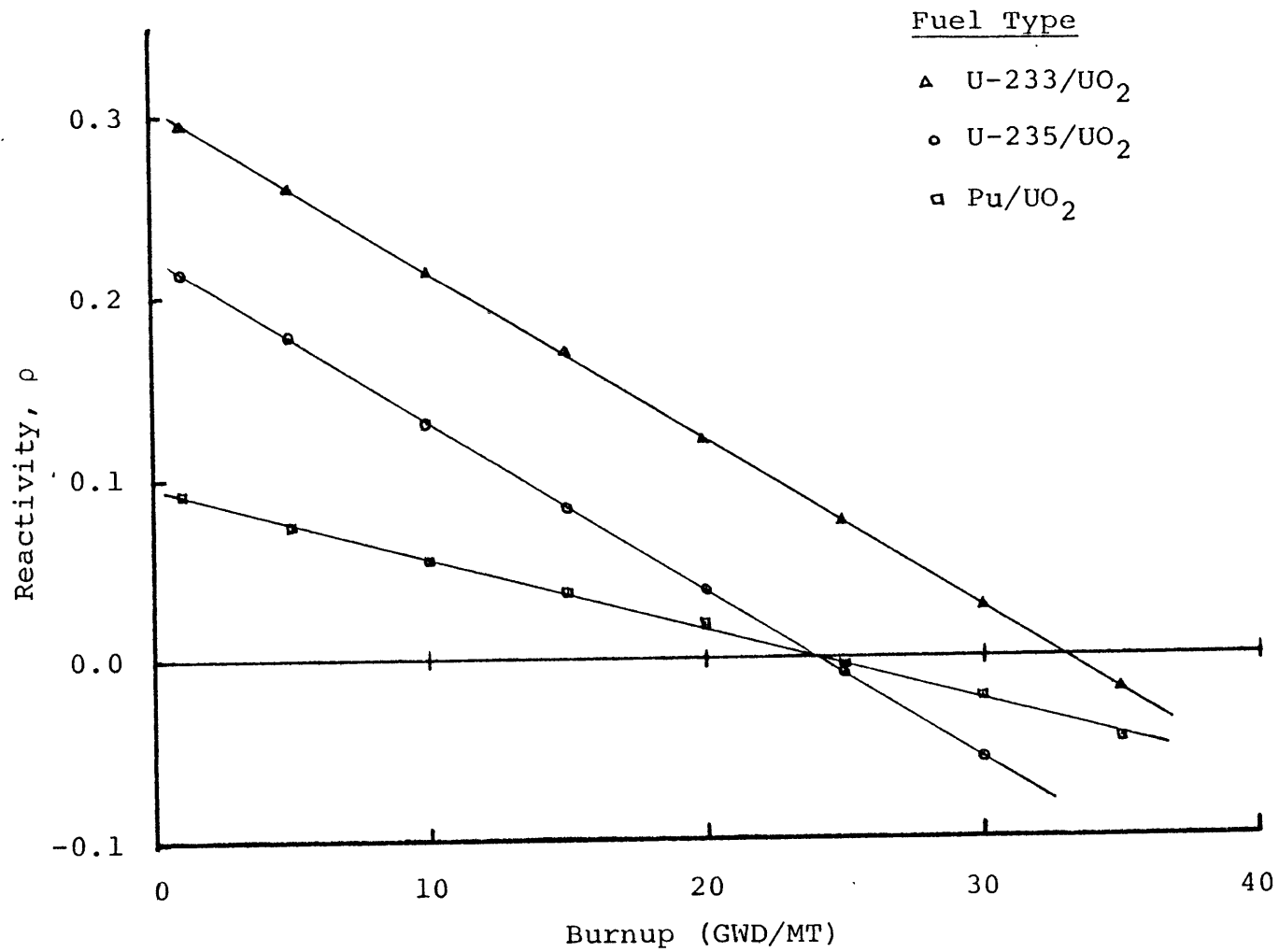
Fig. 5.2 Reactivity versus Burnup for Various Fissile Materials in UO_2

$$\rho_1 = \rho_0 - AB_{dis}\overline{f}_1$$

$$\rho_2 = \rho_0 - AB_{dis}(\overline{f}_1 + \overline{f}_2)$$

.
.
.

$$\rho_n = \rho_0 - AB_{dis}(\overline{f}_1 + \overline{f}_2 + \ldots + \overline{f}_n) \tag{5.2}$$

where ρ_0 is the extrapolated beginning-of-life reactivity

A is the slope of the linear $\rho(B)$ curve, MT/MWD

B_{dis} is the discharge burnup, MWD/MT

and assuming that the batch i cycle burnup is proportional to its average power level $\overline{f}_i$. At end-of-cycle (reactivity-limited condition), and with thermal power fraction f_i at EOC, one will have

$$B_{dis} = \frac{\rho_0}{A\left[\displaystyle\sum_{i=1}^{n}\sum_{j=1}^{i} f_i\overline{f}_j\right]} \tag{5.3}$$

The second feature introduced into the methodology accounts for neutron leakage from a core. The effect of leakage on the system's reactivity is given by

$$\rho_{sys} = \sum_{i=1}^{n} f_i\rho_i - \rho_L \tag{5.4}$$

where the reactivity associated with leakage is defined as:

$$\rho_L = \frac{A_{ex-core}}{\sum\limits_{i=1}^{n} \nu F_i} \qquad (5.5)$$

with $A_{ex-core}$ = neutron absorption rate in the ex-core region

$\sum\limits_{i=1}^{n} \nu F_i$ = total neutron production rate in the core

The corresponding discharge burnup is thus,

$$B_{dis} = \frac{\rho_0 - \rho_L}{A\left[\sum\limits_{i=1}^{n} \sum\limits_{j=1}^{i} f_i \bar{f}_j\right]} \qquad (5.6)$$

The leakage effect was found to be most prominent within the last few migration lengths of the core periphery, and it was found that the radial leakage reactivity can be correlated with the peripheral assemblies' power:

$$\rho_L = \alpha f_{per} \qquad (5.7)$$

where f_{per} is the peripheral power fraction

and α is the leakage coefficient, a constant.

The remaining ingredient necessary for the implementation of the LRM methodology is a power sharing relationship for the fuel batches in a PWR core. This relation was derived using the "group-and-one-half" theory (which neglects thermal leakage):

Fast Group (>0.6 eV)

$$-D_1 \nabla^2 \phi_1 + \Sigma_{a1} \phi_1 + \Sigma_{12} \phi_1 - \frac{1}{k}(\nu \Sigma_{f1} \phi_1 + \nu \Sigma_{f2} \phi_2) = 0$$

leakage   absorp-   down-   fission source   (5.8)
          tion   scatter

Thermal Group

$$\Sigma_{a2} \phi_2 - \Sigma_{12} \phi_1 = 0 \qquad\qquad (5.9)$$

absorp-   in-
tion   scatter

With the additional assumptions that the energy released per fission (κ), the migration area (M^2), and the fast diffusion coefficient (D_1) do not vary with position within the core, one obtains

$$f_i = \frac{(\frac{V_i}{V_s})(\frac{\overline{f}}{k_\infty})_s}{1 - \theta \rho_i} \qquad\qquad (5.10)$$

where $\theta = 1 + \dfrac{\gamma h^2}{M^2}$

h = size of the node (width of an assembly)

V_i/V_s = volume of the node/that of all the surrounding nodes

γ = constant

and subscripts 'i' and 's' denote the node and its surroundings, respectively.

For a fuel batch, in a critical core, we can use the form:

$$f_i \cong \frac{\bar{f}}{1 - \theta \rho_i} \tag{5.11}$$

where $\bar{f}$ is the average power fraction (equal to $\frac{1}{n}$ for an n-batch core). This power split relation was verified using data from whole core analyses. Figure 5.3 shows the plot for assemblies grouped into a batch in the Main Yankee Cycle 4 reload core design.

The power split relation was extended to include the peripheral batches/assemblies of a core through the leakage reactivity:

$$\rho_L = \alpha f_{per}$$

$$= \alpha \sum_{i=1}^{m} f_i \tag{5.12}$$

where $f_{per} = \sum_{i=1}^{m} f_i$ is the power fraction of the core's peripheral batches, m in number. At the EOC ($\rho_{sys} = 0.0$), we have

$$\underbrace{\sum_{i=1}^{n-m} f_i \rho_i}_{\substack{\text{Interior} \\ \text{batches}}} + \underbrace{\sum_{i=1}^{m} f_i (\rho_i - \alpha)}_{\substack{\text{Peripheral} \\ \text{batches}}} = 0 \tag{5.13}$$

The generalized power split equation which is compatible with Eq. 5.13 is,

$$\dfrac{1}{\left(q_{batch}\Big/q_{average}\right)}$$

$\theta = 1.42$

$R^2 = 0.988$

Batch Reactivity, ρ_{batch}
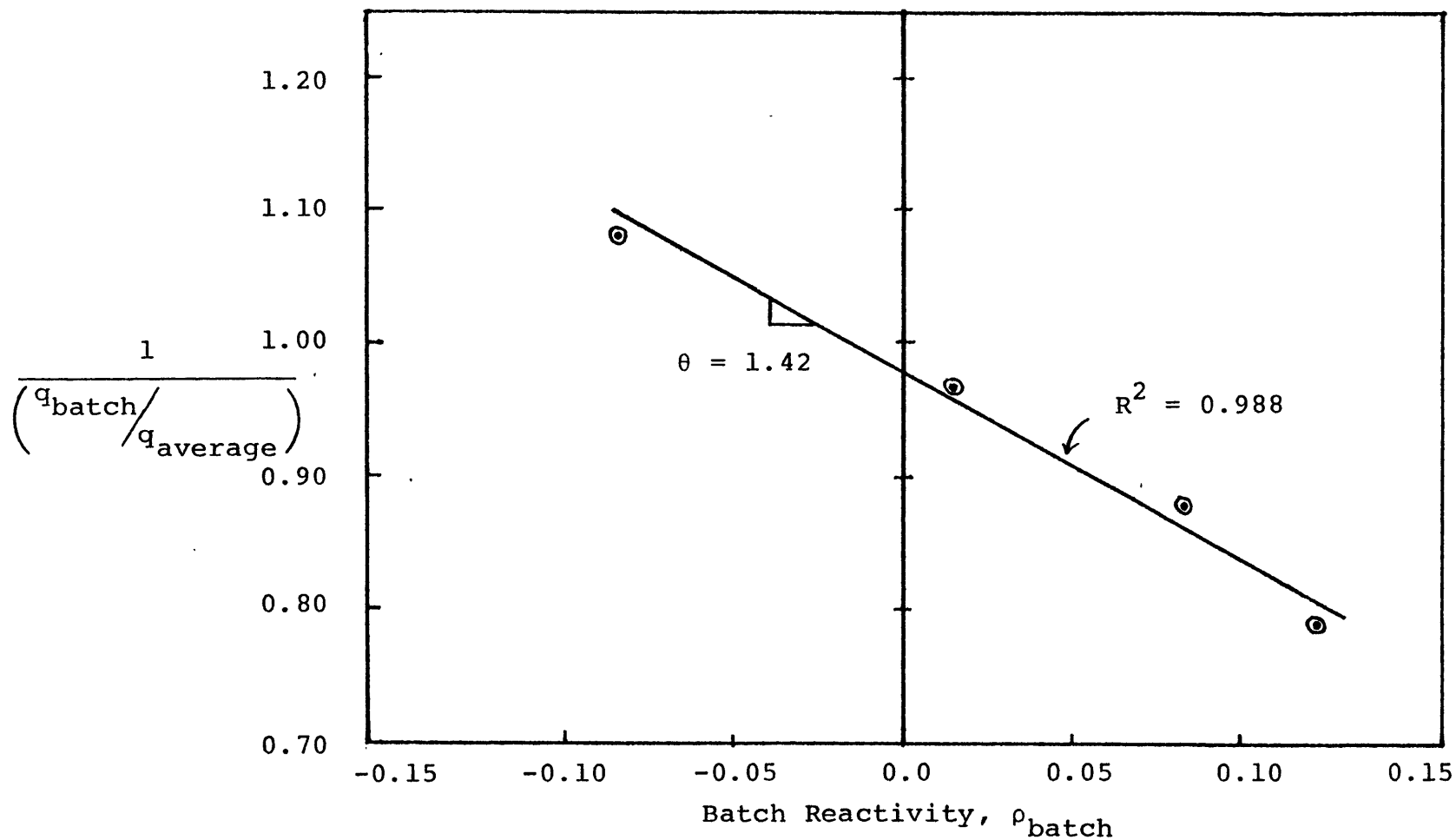
Fig. 5.3   Regression Line of Power vs. Reactivity for Main Yankee Fuel Batches

$$f_i = \frac{\overline{f}}{1 - \theta(\rho_i - \alpha)} \tag{5.14}$$

where $\quad \alpha = \begin{cases} \alpha \text{ for peripheral batches} \\ 0 \text{ for interior batches} \end{cases}$

One of the important constraints which the generalized power split equation satisfies is the summation of batch power fraction to unity,

$$\sum_{i=1}^{n} f_i = 1 \tag{5.15}$$

5.3 THE DISBURN CODE

The LRM methodology has been sufficiently developed to permit the accurate computation of the discharge burnup for various cases of fuel management strategies of contemporary interest. An automated procedure has been developed, and a computer code called DISBURN (for Discharge Burnup) programmed to facilitate its application. Table 5.1 gives a summary of the main features of the code, and the algorithms employed in DISBURN are illustrated by the flow chart in Fig. 5.4.

The code was applied to evaluate a five-batch, extended burnup, 'out-in' fuel management scheme and a comparable 'low-leakage' fuel management strategy for the C-E System-80 reference design [M-1]. The two key parameters essential for the analyses (the power split parameter, θ, and the leakage coef-

TABLE 5.1

PRINCIPAL FEATURES OF THE DISBURN CODE

Item	Comment
1. Linear reactivity vs. burnup curve only.	Can easily be adapted to accommodate non-linear $\rho(B)$ traces.
2. Power-weighted reactivity averaging is used.	$\rho_{sys} = \sum_{i=1}^{n} f_i \rho_i$
3. Effect of peripheral leakage is accounted for through a reactivity-power correlation.	$\rho_L = \alpha f_{per}$ $= \alpha \sum_{i=1}^{m} f_i$ m denotes peripheral batches $\therefore \rho_{sys} = \underbrace{\sum_{i=1}^{n-m} f_i \rho_i}_{\substack{\text{interior} \\ \text{batches}}} + \underbrace{\sum_{i=1}^{m} f_i (\rho_i - \alpha)}_{\substack{\text{peripheral} \\ \text{batches}}}$
4. Batches can be apportioned between core interior and periphery.	User specifies fraction of batch i in core interior $(F_{int,i})$ and core periphery $(F_{per,i})$. $F_{int,i} + F_{per,i} = 1$
5. Interior batch power is computed using the power split equation.	$f_{int,i} = \dfrac{(F_{int,i})\left(\frac{1}{1-\theta\rho_i}\right)}{\sum\limits_{i=1}^{n} f_i}$
6. Peripheral batch power is computed using a modified power split equation.	$f_{per,i} = \dfrac{(F_{per,i})\left[\frac{1}{1-\theta(\rho_i - \alpha)}\right]}{\sum\limits_{i=1}^{n} f_i}$ where $f_i = f_{int,i} + f_{per,i}$ (i.e., sum in denominator includes all assemblies in batch i).

Fig. 5.4   Flowchart for DISBURN Computations

ficient, α) were derived from data published in Ref. [M-1].
The analyses revealed that the difference between the two
fuel management strategies and between the DISBURN and C-E
results are quite insensitive to both theta and α, and the
overall agreement between the two sets of results is good,
considering the complexity of the problem involved.

5.4 ANALYSES OF DIFFERENT FUEL MANAGEMENT STRATEGIES

The DISBURN code was employed to evaluate separate fuel
management schemes of contemporary interest such as the use
of burnable poison to shape the power history profile, the
use of low-leakage fuel loading patterns, etc. The analyses
were also extended to include combinations of these schemes.

5.4.1 BURNABLE POISON

It is shown in the present work that the use of burnable
poison in the fresh reload fuel batch in a low-leakage fuel
loading can lead to a slight increase in the fuel discharge
burnup (in addition to benefiting the moderator temperature
coefficient of reactivity and suppressing the power density in
the fuel) through the shaping of the cycle-by-cycle power
history profile of the fuel batch. Two cases of interest were
considered: in the first, the as-poisoned reactivity value in
the first cycle was taken to be constant, and in the second,
the reactivity in the first cycle was tailored to increase
linearly from a BOL value ρ_{BOL} = 0.0, until it reaches the EOC
point, where it burns out completely. Neglecting, for the

moment, the leakage effect and the presence of any residual poison, an increase of about 2% and 3.5% in the discharge burnup can be realized for the constant Cycle 1 reactivity case and the ρ_{BOL} = 0.0 case, respectively. However, when the anticipated residual poison reactivity penalties were taken into account, the net increase in the discharge burnup for both cases was only about 1%.

5.4.2 LOW-LEAKAGE FUEL MANAGEMENT

It was found that low-leakage fuel management (an In-In-Out scheme) for a representative core (3-batch fuel management) improves steady state discharge burnup (hence uranium utlization) by about 3%. When burnable poison was incorporated in the fresh reload fuel batch in this fuel management scheme, and when the anticipated residual poison reactivity penalty is accounted for, the discharge burnup was increased by a further 0.6%. However, the major benefit in the employment of burnable poison in the fresh fuel batch in the low-leakage fuel management scheme, was the significant reduction (∿10%) of the global radial (batch average) power peaking factor. This factor would have otherwise affected the overall plant economics negatively.

5.4.3 EXTENDED CYCLE LENGTH/BURNUP

The use of extended cycle, out-in/scatter fuel management results in a 6.8% improvement in uranium utilization over the out-in/scatter fuel management scheme common in current prac-

tice. When the extended cycle design is instead operated in a low-leakage configuration, an increase of 9.7% in uranium utilization was obtained. When burnable poison was incorporated in the low-leakage fuel management scheme, and with the appropriate residual poison reactivity penalty taken into account, a uranium utilization improvement of about 11% was realized. However, it must again be noted that a more important consequence of the use of burnable poison in this situation is the supression of the global radial power peaking factor by as much as 10%.

5.5 ANALYTICAL MODELS FOR DISCHARGE BURNUP

Analytical models were developed to calculate the fuel discharge burnup for several common fuel management tactics based upon the LRM methodology. To facilitate the derivation of the discharge burnup equations for different power history profiles, a linearized version of the power split equation (which fits core map data equally well) was employed:

$$f_{batch} = \bar{f}(1 + \theta\rho_{batch})$$ (5.16)

After considerable algebra, the discharge burnups for the different power history trajectories were cast in the form:

$$B = B_0 / (1 + \varepsilon)$$ (5.17)

where B_0 is the discharge burnup for the hypothetical flat

power case:

$$B_0 = (\frac{2n}{n+1}) \frac{\rho_0}{A}$$

in which   n   is the number of batches

ρ_0 is the extrapolated BOL reactivity

A is the slope of the linear $\rho(B)$ curve

and ε is the factor which corrects for the departure

of discharge burnup from the flat power case.

In the particular case of when a fixed poison shim was in-cluded in a batch of fuel over a given cycle (mathematically equivalent to subjecting the same batch of fuel to a fixed leakage penalty—e.g., by placing the fuel batch on the core periphery), it was difficult to obtain an expression for the discharge burnup in a closed form. Thus an empirical corre-lation for the 'ε factor' was determined from numerical re-sults. Table 5.2 shows the various power history trajectories and their corresponding ε factors. Figure 5.5 compares the analytical and DISBURN results for a case of particular interest: constant first cycle reactivity induced through the use of burnable poison.

Superposition of analytical results for the various indi-vidual schemes would, if verified as being sufficiently accu-rate, allow one to compute the discharge burnup resulting from a synthesis of a variety of fuel management strategies.

TABLE 5.2

ANALYTICAL RESULTS FOR COMMON REACTIVITY HISTORIES

Burnable Poison
in Reload Fuel

Shim or Peripheral
Leakage in Cycle j
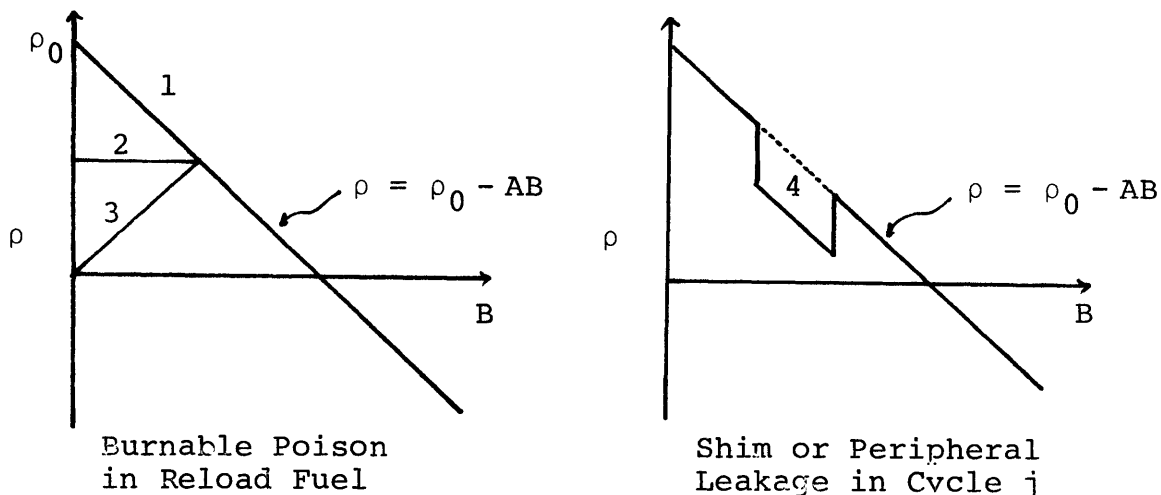
Case*	Prescription for ε
1. (no burnable poison)**	$2(\theta\rho_0)^2 \dfrac{(n-1)}{3(n+1)^2}$
2. (constant ρ in 1st Cycle)	$-(\theta\rho_0)\dfrac{(n-1)}{n(n+1)^2} + (\theta\rho_0)^2 \dfrac{(n-1)^2}{3n(n+1)^2}$
3. (zero ρ at BOL)	$-(\theta\rho_0)\dfrac{(n-1)}{2n(n+1)} + (\theta\rho_0)^2 \dfrac{(n-1)^2}{6n(n+1)^2}$
4. (shim or leakage in Cycle j)	$\dfrac{(15.6-n)(6.8+n)R(\theta\rho_0)}{[(38n-25)+(2n-7)j]}$ $+\ 2(\theta\rho_0)^2 \dfrac{(n-1)}{3(n+1)^2}$

$$\text{where } R = \frac{(\text{shim or leakage reactivity penalty, } \Delta\rho)}{\rho_0}$$

*Case number corresponds to those in the figure.

**Factor of 2 in prescription for ε is an empirical normalization.
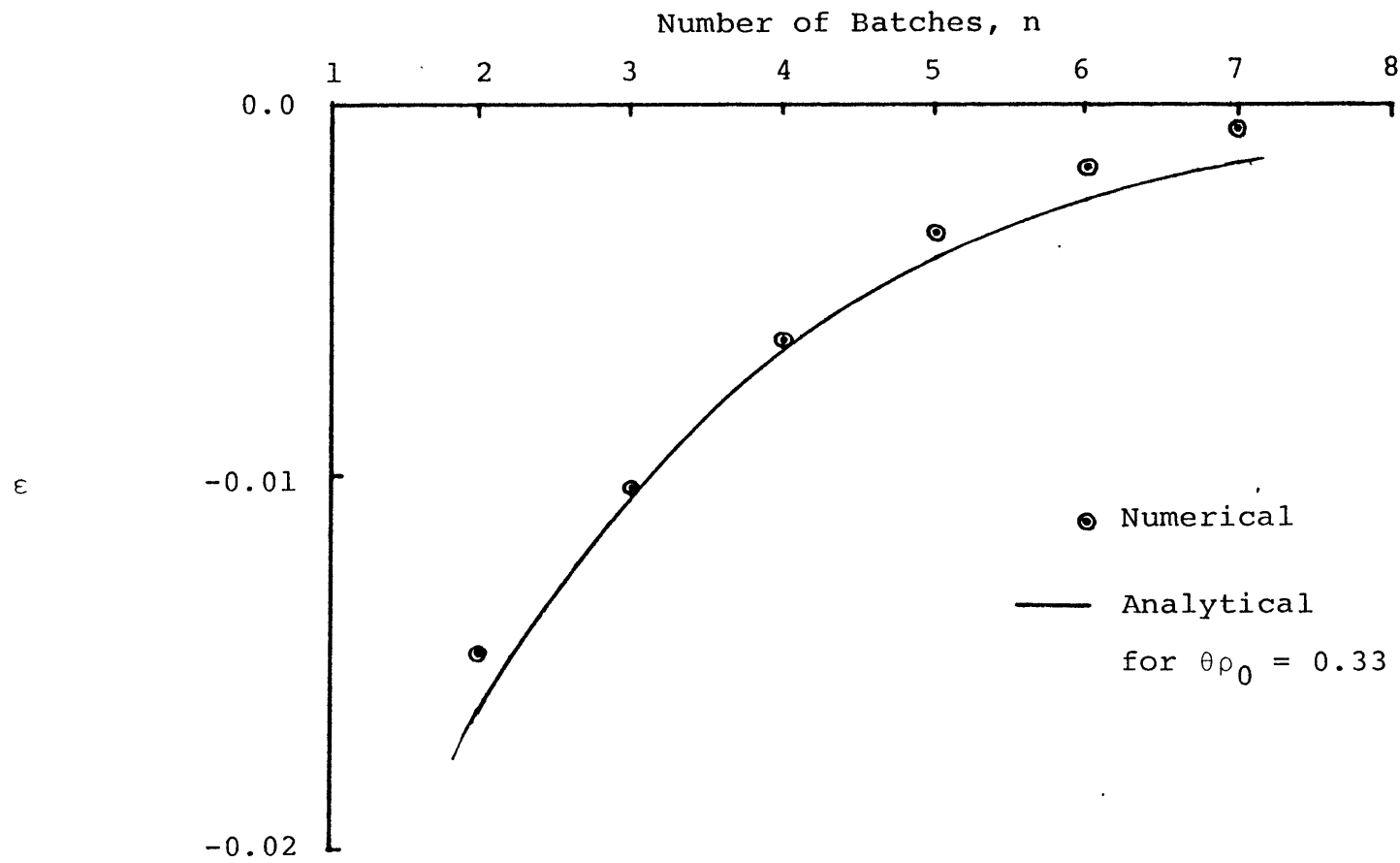
Fig. 5.5 ε as a Function of the Number of Batches, for the case of Constant Reactivity in the First Cycle

The discharge burnup for the synthesis of m of these schemes is given by

$$B_{dis}^m = B_0 \left[1 - \sum_{\ell=1}^{m} \left(\frac{\varepsilon_\ell}{1+\varepsilon_\ell} \right) \right] \tag{5.18}$$

For a number of combinations of individual fuel management strategies, the discharge burnups calculated using the prescription given by Eq. 5.18 were typically biased—running consistently about 1% less than those computed using the DISBURN code. Hence the relative accuracy case-to-case is extremely good—a highly desirable situation because of the projected use of these relations for strategic comparisons. Therefore, fast analyses for scoping purposes can be performed using the analytical expressions for the ε factors developed in the present work.

5.6 CONCLUSIONS

While a considerable investment of time and effort went into model development, the underlying objective of the present work remained the evaluation of the consequences of using burnable poison in PWRs on the uranium utilization. In this regard it was found that the use of burnable poison in conjunction with low-leakage fuel management can increase the discharge burnup by an additional 1%—that is over and above the gain due to the low-leakage nature of the fuel loading scheme. We can therefore conclude that the use of burnable poison does not penalize the discharge burnup (or the conse-

quent uranium utilization) despite nominal amounts of residual poison in the fuel batch.

5.7 RECOMMENDATIONS

The LRM methodology, with the incorporation of features such as the power weighting algorithm and a radial leakage correlation, permits one to compute accurately the discharge burnup of fuel for various cases of fuel management strategies of current interest. It is also capable of evaluating the effects of small changes in core design and fuel management tactics on a consistent basis. Although the present methodology utilizes a power split relation which has a sound theoretical basis (developed from a $1\frac{1}{2}$ group diffusion theory model) and the key features incorporated within it were thoroughly benchmarked against results generated with detailed state-of-the-art computer analyses, further improvements in the model can still be made, as follows:

1) A more detailed treatment of the peripheral fuel assemblies/batches should be investigated. In the present work, only the gross effects of leakage were correlated with the peripheral power fraction; finer effects such as the number of assembly faces exposed to the reflector, and the interaction of the peripheral batch with the next interior ring of fuel should be studied. These 'second order' effects may be important when one has quite different types of fuel on the core periphery, such as reconstituted assemblies having a different lattice pitch than the rest of the core, or thorium fueled blankets in a uranium core, and the like.

2) Although the generalized power split relation (Eq.
5.4) handles the interior and peripheral fuel batches
rigorously in that important constraints were satis-
fied by the relation, the application of the equa-
tion at the core periphery needs to be examined in
more detail, and, if necessary, modified to agree
with the results generated using detailed state-of-
the-art computer analyses. In particular, the most
appropriate value of the parameter θ for peripheral
assemblies may be different from the value applied
to interior assemblies.

3) The relation of the power sharing algorithm used in
the present work to those used in so-called nodal
codes such as FLARE and its successors, should be
further explored.

4) Efforts should be continued to develop a closed form
analytic solution for the case of a fixed shim or
leakage reactivity decrement in cycle j, to either
substantiate or supplant the empirical expression
arrived at by fitting numerical results in the pre-
sent report.

5) The effect of the deliberate retention (or introduc-
tion) of some burnable poison in the second and sub-
sequent burnup cycles should be studied to investigate
the costs and benefits of such operations.

Finally, attention is called to the companion effort by
A. Kamal [K-2], in which further substantiation of the linear
reactivity model is documented, and in which a wide variety of
additional applications of this methodology are discussed.

APPENDIX A

NON-LINEAR REACTIVITY VS. BURNUP DEPENDENCE

Although we have confirmed that reactivity varies very nearly linearly with burnup for PWR lattices, one can introduce even extreme non-linearity without much complication. Let us assume a polynomial curve fit of the form:

$$\rho = \rho_o - A_1 B - A_2 B^2 - A_3 B^3 - A_4 B^4 - \ldots \qquad (A.1)$$

An end-of-cycle reactivity balance can be constructed; consider cycles of length B_c and an n-batch core:

newest batch $\rho_o - A_1 \cdot B_c - A_2 B_c^2 - A_3 B_c^3 - A_4 B_c^4$

next batch $\rho_o - A_1 \cdot 2 B_c - A_2 (2B_c)^2 - A_3 (2B_c)^3 - A_4 (2B_c)^4$

.
.
.

oldest batch $\rho_o - A_1 \cdot n B_c - A_2 (nB_c)^2 - A_3 (nB_c)^3 - A_4 (nB_c)^4$

$$\text{Sum} = 0 = n\rho_o - A_1 B_c \sum_{j=1}^{n} j - A_2 \cdot B_c^2 \sum_{j=1}^{n} j^2 - A_3 \cdot B_c^3 \cdot$$

$$\sum_{j=1}^{n} j^3 - A_4 \cdot B_c^4 \sum_{j=1}^{n} j^4$$

The required sums can be evaluated in closed form [M-4]:

$$\sum_{j=1}^{n} j = \frac{1}{2} n(n+1) \qquad\qquad \sum_{j=1}^{n} j^3 = \frac{1}{4} n^2 (n+1)^2$$

$$\sum_{j=1}^{n} j^2 = \frac{1}{6} n(n+1)(2n+1) \qquad \sum_{j=1}^{n} j^4 = \frac{1}{30} n(n+1)(2n+1)(3n^2+3n+1)$$

Thus our equation for cycle burnup becomes the polynomial:

$$B_c^4 + a\, B_c^3 + b\, B_c^2 + c\, B_c - d = 0 \qquad\qquad\qquad (A.2)$$

where

$$a = \frac{15n(n+1)}{2(2n+1)(3n^2+3n-1)} \left(\frac{A_3}{A_4}\right), \quad c = \frac{15}{(2n+1)(3n^2+3n-1)} \left(\frac{A_1}{A_4}\right)$$

$$b = \frac{5}{(3n^2+3n-1)} \left(\frac{A_2}{A_4}\right), \quad d = \frac{30\rho_o}{n(n+1)(2n+1)(3n^2+3n-1)A_4}$$

This equation can be solved for B_c, and discharge burnup

$n \cdot B_c$, using numerical methods.

Note that the equation correctly reduces to two limiting

cases:

(a) $n = 1$, single batch core, Eq. (A.2) becomes

$\rho(B) = 0$, where $\rho(B)$ is given by Eq. (A.1)

(b) $n = \infty$, Eq. (A.2) yields the same result as would be

obtained by setting the integral of Eq. (A.1) equal

to zero, i.e.:

$$\int_{o}^{B} \rho(B)\, dB = 0$$

Finally, since one can sum <u>any</u> power of sequential integers,

$\sum_{k=0}^{n} k^m$, (Eq. A.6) p. 58, of Ref. [M-4], a polynomial of

arbitrarily high order could be used in lieu of Eq. (A.1), and

therefore any non-pathological $\rho(B)$ curve could be fit and its

implied cycle burnup computed.

Of particular interest here is the use of the above

development to estimate the error in discharge burnup incurred

by use of the linear approximation in the bulk of the present

work.

Consider the reactivity-burnup data of a U-235/UO$_2$

(enrichment $\varepsilon \sim 3.0$w/o) supercell lattice generated by the

LEOPARD program. A linear curve-fit (using the least squares

method) to these data gives the following relation (for burn-

up in MWD/MTHM):

$$\rho = \rho_o - AB \tag{A.3}$$

with $\rho_o = 0.223508$

$\quad A = 9.27205 \times 10^{-6}$

The same data fit to a quadratic yields:

$$\rho = \rho_o' - aB - bB^2 \tag{A.4}$$

with $\rho_o' = 0.222936$

$\quad a = 9.1728106 \times 10^{-6}$

$$b = 2.977847 \times 10^{-12}$$

For an n-batch core at steady state, the discharge burn-up using the linear curve is

$$B_d = \left(\frac{2n}{n+1}\right) \frac{\rho_0}{A} \tag{A.5}$$

Whereas, the discharge burnup employing the quadratic curve is determined as follows. The EOC reactivity balance gives

$$0 = n\rho_0' - aB_c \sum_{j=1}^{n} j - bB_c^2 \sum_{j=1}^{n} j^2 \tag{A.6}$$

Rearranging Eq. (A.5) and substituting the sums by their evaluated forms, we have

$$\alpha B_c^2 + \beta B_c - \rho_0' = 0 \tag{A.7}$$

where $\alpha = \dfrac{b}{6}(n+1)(2n+1)$

and $\beta = \dfrac{a}{2}(n+1)$

Solving Eq. (A.6), and noting that $B_c > 0$, we have

$$B_c = \frac{-\beta + \sqrt{(\beta^2 + 4\alpha \rho_0')}}{2\alpha} \tag{A.8}$$

and the corresponding discharge burnup can then be calculated.

If we assume that the quadratic fit of the data is
"exact," then the error in the discharge burnup incurred by
the use of the linear model is given below (for different n):

n	B_d ("exact")	B_d (linear model)	% error
2	32126	32141	-0.05
3	36126	36158	-0.09
4	38525	38569	-0.11
5	40123	40176	-0.13

From these results, we conclude that the "error" in
using the linear reactivity model is rather insignificant.

The worst case, with regard to the linearity of the
$\rho(B)$ trace, encountered in this work is that of the Pu/ThO_2
system lattice (see Fig. 3.3 and Table 3.2). A third order
polynomial fit to the corresponding data gives

$$\rho = \rho_o'' - a'B + b'B^2 - c'B^3 \tag{A.9}$$

with $\rho_o'' = 0.060659$

$a' = 3.27659 \times 10^{-6}$

$b' = 7.69132 \times 10^{-11}$

$c' = 2.33005 \times 10^{-15}$

Again, performing the EOC reactivity balance, substitut-
ing the appropriate summations and rearranging the resulting

equation yields:

$$\alpha' B_c^3 - \beta' B_c^2 + \gamma' B_c - \rho_o'' = 0 \qquad\qquad (A.10)$$

where $\alpha' = \dfrac{c'n}{4}(n+1)^2$

$$\beta' = \dfrac{b'}{b}(n+1)(2n+1)$$

$$\gamma' = \dfrac{a'}{2}(n+1)$$

Equation A.10 can be solved readily using numerical methods. The results are given below:

n	B_c (MWD/MT)	B_d (MWD/MT)
2	14134	28268
3	10385	31155
4	8215	32860
5	6798	33990

A linear fit to the same set of data for the Pu/ThO$_2$ system lattice gives

$$\rho = \rho_o''' - A''' B$$

with $\rho_o''' = 0.06566$

$$A''' = 3.270 \times 10^{-6}$$

The corresponding discharge burnup can be computed using Eq. (A.5). The error in the discharge burnup incurred by the use of this linear approximation is given below:

n	B_d (3rd order fit), MWD/MT	B_d (linear model), MWD/MT	ΔB %
2	28268	26773	5.3
3	31155	30119	3.3
4	32860	32127	2.2
5	33990	33466	1.5

The results show that for small n, the use of the LRM to evaluate the discharge burnup of the Pu/Th_2O system is not adequate and therefore, a higher order ($\simeq 3$) fit of the reactivity-burnup data and the method of calculating the discharge burnup discussed in this section, must be adopted. However, for higher values of n ($\simeq 5$) the LRM may be employed. The accuracy of the LRM improves with n because as the number of EOC points at which $\rho(B)$ is sampled increases, the more one tends to have compensation between over and under-estimates of the true $\rho(B)$ and its linear approximation. Indeed one could improve the accuracy of the LRM for small n by restricting the curve fit to data points near the estimated EOC $\rho(B)$ values for batches 1, 2, ..., n.

APPENDIX B

REACTIVITY CONTROL USING BURNABLE POISON ONLY

A limiting case has been identified for assessment vis-à-vis burnable poison control, namely a core controlled entirely by burnable poison in the fresh fuel without the need for soluble poison. Although this approach will probably result in over-compensation as regards power suppression in fresh fuel, and may require a faster-than-practicable poison burn, it will serve to define the outer envelope for fuel management strategies.

Using the linear reactivity model of assembly behavior, the conceptual picture of this type of operation can be sketched on a $\rho(B)$ map as shown in Fig. B.1. The assembly without poison would follow the linear trace starting at ρ_o when B=0; with poison it would start at the (negative) reactivity value $\rho_{1,BOC}$, burn out completely and linearly in one cycle to $\rho_{1,EOC}$, then follow the unpoisoned trace to its discharge value at the end of n cycles, $\rho_{n,EOC}$.

One can show that $\rho_{1,BOC} = \rho_{n,EOC}$ as follows. We require that the power-weighted reactivity sum to zero at both BOC and EOC, thus:

$$\sum_{i=1}^{n} f_{i,BOC}\, \rho_{i,EOC} = \sum_{i=1}^{n} f_{i,EOC}\, \rho_{i,EOC} \qquad (B.1)$$
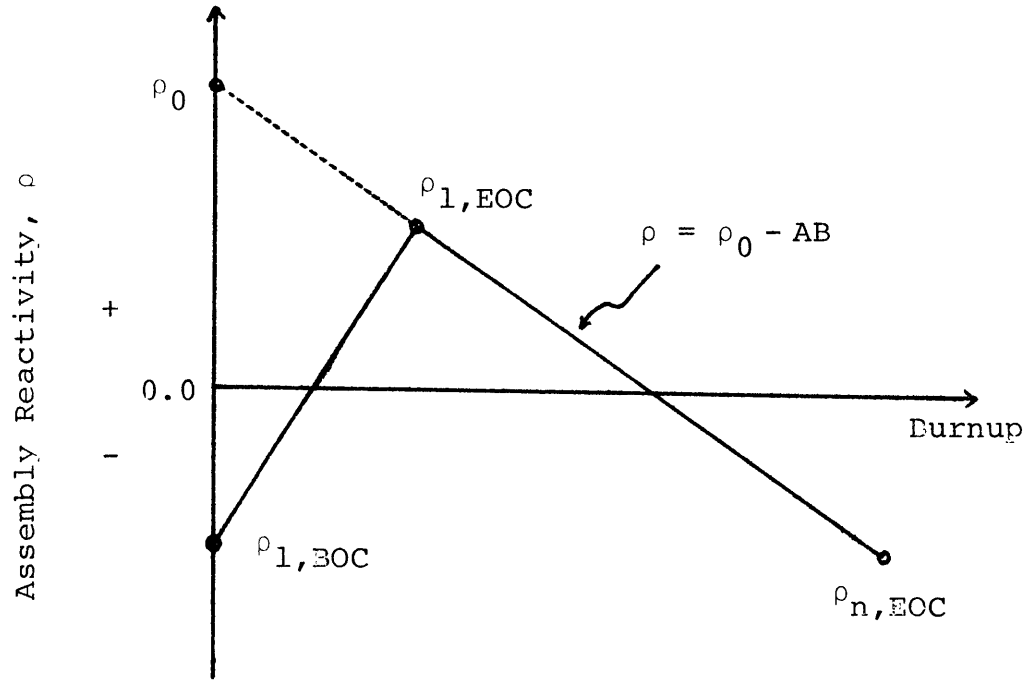
Fig. B.1   The Reactivity versus Burnup Trace for the
           Case of a Core Controlled Entirely by
           Burnable Poison

But since there is no soluble poison,

$$\rho_{i,EOC} = \rho_{i+1,BOC} \qquad\qquad (B.2)$$

The power sharing prescription derived in chapter 3 is given by

$$f_i = \frac{\bar{f}}{1-\theta\,\rho_i} = \frac{1}{n}\left(\frac{1}{1-\theta\,\rho_i}\right) \qquad\qquad (B.3)$$

Or f_i is a function only of ρ_i, since θ is a constant.

This means that in Eq. (B.1) all terms except the first on the LHS and the last on the RHS are identical (by Eq. B.2) and therefore cancel; the remaining terms yield directly;

$$\rho_{1,BOC} = \rho_{n,EOC} \qquad\qquad (B.4)$$

In other words, the reload assembly has the same negative BOL reactivity (as poisoned) as it does when fully burned.

APPENDIX C

DISBURN CODE INPUT DESCRIPTION, LISTING, AND SAMPLE PROBLEM

C.1   CODE DESCRIPTION

The DISBURN (Discharge Burnup) code enables one to compute accurately, the discharge burnup for various cases of fuel management strategies of contemporary interest. The methodology employed in DISBURN is based on the linear reactivity model, and incorporates important features such as power-reactivity weighting and allowance for the effects of neutron leakage. The principal features of the DISBURN code and the algorithms employed in the code have been shown in Table 4.1 and Fig. 4.1 of Chapter 4.

The code is written in FORTRAN (see listing in Table C.2), but can easily be translated into the BASIC language for use with minicomputers. Although the present version of the code is written to be used in an interactive mode at a computer terminal, it can be run in a batch job mode by putting the input data on a separate data file and then appropriately defining the input data file. Table C.1 lists the instructions for input preparation.

The sample problem concerns the evaluation of the low-leakage fuel management scheme for the Maine Yankee reactor system (see Section 4.3.2 of Chapter 4). In this problem, burnable poison was used in the fresh reload fuel to tailor the reactivity in Cycle 1 to increase linearity from a value

of ρ_{BOL} = 0.02, and with no residual poison at the EOC. Table C.3 is a listing of the terminal session for the problem.

TABLE C.1

<u>INPUT SPECIFICATIONS</u>

<u>Card Set 1</u> (one card)

J: number of batches

TSTEP: burnup-step size (MWD/MT)

CONVRG: convergence criterion (MWD/MT)

FORMAT (8x, I2, 2F10.5)

<u>Card Set 2</u> (one card)

THETAI: interior batch θ value

THETAP: peripheral batch θ value

FORMAT (2F10.5)

<u>Card Set 3</u> (one card

RHOINT: extrapolated BOL reactivity value for the linear

$\rho(B)$ curve - ρ_0

A: slope of the linear $\rho(B)$ curve, $(MWD/MT)^{-1}$

FORMAT (F10.5, E10.5)

<u>Card Set 4</u> (one card)

OPTION SPECIFIED BY 'N'

N=1: no burnable poison used

N=2: burnable poison used

FORMAT (3x, I2)

<u>Card Set 5</u> (one card)

(used only when N=2, i.e., case with burnable poison)

TABLE C.1 (continued)

OPTION SPECIFIED BY 'NN'

   NN=1: constant reactivity in Cycle 1

   NN=2: sloping (i.e., ramp) reactivity in Cycle 1

FORMAT (3x, I2)

Card Set 6   (one card)

   (used only when NN=1, i.e., constant reactivity in Cycle 1)

      BI: enter estimated poison burnout point (PBP), MWD/MT,

         for EOC 1

FORMAT (F1.02)

Note: Code will optimize PBP to match EOC point.

Card Set 7   (one card)

   (used only when NN=2, i.e., sloping reactivity in Cycle 1)

  RHOLBOL: BOL reactivity value

      BI: estimated poison burnout point (PBP), MWD/MT, for

         EOC 1

FORMAT (F1.05, F10.2)

Note: Code will optimize PBP to match EOC point.

Card Set 8   (one card)

OPTION SPECIFIED BY 'NNN'

  NNN=1: use fixed poison shim over a cycle or model leak-

       age explicitly

  NNN=2: if neither

FORMAT (x3, I2)

TABLE C.1 (continued-3)

<u>Card Set 9</u> (one card)

    (used only when NNN=1, i.e., using shim or leakage)

      SHIM: amount of shim poison, $\Delta\rho$, or leakage coefficient,

        α.

    FORMAT (F10.5)

<u>Card Set 10</u> (one or more cards)

    (used only when NNN=1)

    APER(I), I = 1 to J: fraction of batch (I) on core peri-

                      phery or

                      fraction of batch (I) with fixed

                      shim poison

    FORMAT (8F10.5)

<u>Card Set 11</u> (one or more cards)

    (used only when NNN=1)

    AINT(I), I = 1 to J: fraction of batch (I) in core

                      interior or

                      fraction of batch (I) without fixed

                      shim poison

    FORMAT (8F10.5)

<u>Card Set 12</u> (one card)

    OPTION SPECIFIED BY 'NNNN'

    NNNN=0: for end of computation

    NNNN=1: for the next case

    FORMAT (x3, I2)

TABLE C.2

DISBURN CODE LISTING

```
CCCCCCCCCCCCCCCCCCCCCCCCCCCCCCCCCCCCCCCCCCCCCCCCCCCCCCCCCCCCCCCCC    LRM00010
C                                                                 C    LRM00020
C                    DISBURN CODE                                 C    LRM00030
C                                              .                  C    LRM00040
CCCCCCCCCCCCCCCCCCCCCCCCCCCCCCCCCCCCCCCCCCCCCCCCCCCCCCCCCCCCCCCCC    LRM00050
       IMPLICIT  REAL*8(A-H, O-Z) , REAL*8(K)                          LRM00060
       DIMENSION DONE(10), B(10), F(10), RHO(10), FA(10),FAVG(10)      LRM00070
       DIMENSION AINT(10), APER(10), PINT(10), PPER(10),RHOP(10)       LRM00080
C                                                                      LRM00090
C                                                                      LRM00100
C                                                                      LRM00110
C      J       NUMBER OF BATCHES                                       LRM00120
C CONVRG       CONVERGENCE CRITERION IN MWD/MT                         LRM00130
C  TSTEP       TIME STEP OR BURNUP INCREMENT IN MWD/MT                 LRM00140
C RHOINI       EXTRAPOLATED BOL REACTIVITY                             LRM00150
C RHOBOL       BOL REACTIVITY VALUE                                    LRM00160
C      A       SLOPE OF THE LINEAR REACTIVITY-BURNUP TRACE, MT/MWD     LRM00170
C     BI       ESTIMATED POISON BURNOUT POINT NEAR EOC 1, MWD/MT       LRM00180
C THETAI       INTERIOR THETA VALUE                                    LRM00190
C THETAP       PERIPHERAL THETA VALUE                                  LRM00200
C   SHIM       FIXED POISON SHIM REACTIVITY PENALTY                    LRM00210
C  ALPHA       LEAKAGE COEFFICIENT                                     LRM00220
C   AINT       FRACTION OF INTERIOR ASSEMBLIES IN EACH BATCH           LRM00230
C   APER       FRACTION OF PERIPHERAL ASSEMBLIES IN EACH BATCH         LRM00240
C                                                                      LRM00250
C                                                                      LRM00260
    10 WRITE(6,4000)                                                   LRM00270
       READ(5,2000) J, TSTEP, CONVRG                                   LRM00280
       WRITE(6,4005)                                                   LRM00290
       READ(5,2050) THETAI, THETAP                                     LRM00300
C                                                                      LRM00310
       ALPHA=0.0                                                       LRM00320
       SHIM=0.0                                                        LRM00330
       NUMB=0                                                          LRM00340
       JLESS=J-1                                                       LRM00350
       STORE=TSTEP                                                     LRM00360
       BI=1000.0                                                       LRM00370
       NN=3                                                            LRM00380
       DO 110 I=1,J                                                    LRM00390
       AINT(I)=1.0                                                     LRM00400
       APER(I)=0.0                                                     LRM00410
   110 CONTINUE                                                        LRM00420
C                                                                      LRM00430
       WRITE(6,4010)                                                   LRM00440
       READ(5,2010) RHOINT, A                                          LRM00450
```

```
        RHOBOL=RHOINT                                            LRM00460
    111 WRITE(6,4020)                                            LRM00470
        READ(5,2020) N                                           LRM00480
C                                                                LRM00490
C   N=1 : OPTION WITHOUT BURNABLE POISON                         LRM00500
C   N=2 : OPTION WITH BURNABLE POISON                            LRM00510
C                                                                LRM00520
        IF (N.EQ.1) GOTO 113                                     LRM00530
        IF (N.EQ.2) GOTO 1110                                    LRM00540
        GOTO 111                                                 LRM00550
C                                                                LRM00560
C                                                                LRM00570
C       CASE WITH BURNABLE POISON                                LRM00580
C                                                                LRM00590
C       NN=1: CONSTAN REACTIVITY IN CYCLE 1                      LRM00600
C       NN=2: SLOPE REACTIVITY IN CYCLE 1                        LRM00610
C                                                                LRM00620
C                                                                LRM00630
   1110 WRITE(6,4035)                                            LRM00640
        READ(5,2020)NN                                           LRM00650
C                                                                LRM00660
        IF (NN.EQ.1) GOTO 1115                                   LRM00670
        IF (NN.EQ.2) GOTO 112                                    LRM00680
        GOTO 1110                                                LRM00690
C                                                                LRM00700
C       CONSTANT REACTIVITY IN CYCLE 1                           LRM00710
C                                                                LRM00720
   1115 WRITE(6,4025)                                            LRM00730
        READ(5,2035) BI                                          LRM00740
        GOTO 113                                                 LRM00750
C                                                                LRM00760
C       SLOPE REACTIVITY IN CYCLE 1                              LRM00770
C                                                                LRM00780
    112 WRITE(6,4030)                                            LRM00790
        READ(5,2030) RHOBOL, BI                                  LRM00800
C                                                                LRM00810
C                                                                LRM00820
C       CASE WITH AND WITHOUT BURNABLE POISON                    LRM00830
C                                                                LRM00840
C       NNN=1: USE FIXED POISON SHIM OR MODEL LEAKAGE            LRM00850
C              EXPLICITLY OVER A CYCLE                           LRM00860
C       NNN=2: IF NEITHER                                        LRM00870
C                                                                LRM00880
C                                                                LRM00890
    113 WRITE(6,4040)                                            LRM00900
```

```
      READ(5,2020) NNN                                          LRM00910
      IF(NNN.EQ.1) GOTO 114                                      LRM00920
      IF(NNN.EQ.2) GOTO 117                                      LRM00930
      GOTO 113                                                   LRM00940
C                                                                LRM00950
  114 WRITE(6,4041)                                              LRM00960
      READ(5,2030) SHIM                                          LRM00970
      GOTO 116                                                   LRM00980
C                                                                LRM00990
  116 WRITE(6,4043)                                              LRM01000
      READ(5,2050) (APER(I), I=1,J)                              LRM01010
      WRITE(5,4044)                                              LRM01020
      READ(5,2050) (AINT(I), I=1,J)                              LRM01030
  117 CONTINUE                                                   LRM01040
      WRITE(6,3000)                                              LRM01050
C                                                                LRM01060
C                                                                LRM01070
  118 DO 119 I=1,J                                               LRM01080
      FA(I)=0.0                                                  LRM01090
  119 CONTINUE                                                   LRM01100
      FAP=0.0                                                    LRM01110
      TSTEP=STORE                                                LRM01120
      ADD=0.0                                                    LRM01130
C                                                                LRM01140
C                                                                LRM01150
C     ESTIMATE CYCLE BURNUP                                      LRM01160
C                                                                LRM01170
      BEST=2.0*RHOINT/((J+1)*A)                                  LRM01180
C                                                                LRM01190
C                                                                LRM01200
C     ESTIMATE BOC POINTS                                        LRM01210
C                                                                LRM01220
C                                                                LRM01230
      DONE(1)=0.0                                                LRM01240
      DO 120 I=1,J                                               LRM01250
      W=I-1                                                      LRM01260
      DONE(I)=W*BEST                                             LRM01270
  120 CONTINUE                                                   LRM01280
C                                                                LRM01290
C                                                                LRM01300
  190 DO 200   I=1,J                                             LRM01310
      B(I)=DONE(I)                                               LRM01320
  200 CONTINUE                                                   LRM01330
C                                                                LRM01340
C                                                                LRM01350
```

```
C       COMPUTE THE REACTIVITY VALUES CORRESPONDING TO THE          LRM01360
C       DIFFERENT BURNUP POINTS FOR DEFFERENT OPTIONS               LRM01370
C                                                                   LRM01380
C                                                                   LRM01390
  330 DO 370 I=1,J                                                  LRM01400
      IF (NN.EQ.1) RHOBOL=RHOINT-A*BI                               LRM01410
      IF (B(I).LE.BI)                                               LRM01420
    $    RHO(I)=RHOBOL+(RHOINT-RHOBOL)*B(I)/BI - A*B(I)             LRM01430
      IF (B(I).GT.BI)                                               LRM01440
    $    RHO(I)=RHOINT-A*B(I)                                       LRM01450
         RHOP(I)=RHOINT-A*B(I)                                      LRM01460
  370 CONTINUE                                                      LRM01470
C                                                                   LRM01480
C                                                                   LRM01490
C       CALCULATE THE BATCH POWER FRACTION                          LRM01500
C                                                                   LRM01510
C                                                                   LRM01520
      FSUM=0.0                                                      LRM01530
      DO 371 I=1,J                                                  LRM01540
      PPER(I)=APER(I)/(J*(1.0-THETAP*(RHOP(I)-SHIM)))               LRM01550
      PINT(I)=AINT(I)/(J*(1.0-THETAI*RHO(I)))                       LRM01560
      F(I)=PPER(I)+PINT(I)                                          LRM01570
      FSUM=FSUM+F(I)                                                LRM01580
  371 CONTINUE                                                      LRM01590
C                                                                   LRM01600
C       CALCULATE PERIPHERAL POWER FRACTION                         LRM01610
C                                                                   LRM01620
      FPER=0.0                                                      LRM01630
      DO 372 I=1,J                                                  LRM01640
      FPER=FPER+PPER(I)/FSUM                                        LRM01650
  372 CONTINUE                                                      LRM01660
C                                                                   LRM01670
C                                                                   LRM01680
C       CALCULATE SYSTEM REACTIVITY                                 LRM01690
C                                                                   LRM01700
C                                                                   LRM01710
      RHOSYS=0.0                                                    LRM01720
      DO 390  I=1,J                                                 LRM01730
      PPER(I)=PPER(I)/FSUM                                          LRM01740
      PINT(I)=PINT(I)/FSUM                                          LRM01750
      RHOSYS=RHOSYS+(PPER(I)*(RHOP(I)-SHIM) + PINT(I)*RHO(I))       LRM01760
  390 CONTINUE                                                      LRM01770
C                                                                   LRM01780
C                                                                   LRM01790
C       IF SYSTEM REACTIVITY HAS NOT CONVERGED, SOLUBLE POISON IS   LRM01800
```

```
C       ADDED UNTIL CONVERGENCE IS ACHIEVED AND THE BATCH BURNUP        LRM01810
C       IS INCREMENTED.                                                 LRM01820
C       IF EOC POINT IS REACHED THE OUTER CONVERGENCE CRITERION         LRM01830
C       IS CHECK                                                        LRM01840
C                                                                       LRM01850
C                                                                       LRM01860
C                                                                       LRM01870
        IF (RHOSYS.GE.0.0)GOTO 391                                      LRM01880
        IF (RHOSYS.LT.0.0)GOTO 410                                      LRM01890
  391 IF (RHOSYS.LE.0.0001)   GOTO 460                                  LRM01900
        IF (RHOSYS.GT.0.0001)   GOTO 392                                LRM01910
C                                                                       LRM01920
C                                                                       LRM01930
  392 DELTA=RHOSYS/J                                                    LRM01940
        FSUM1=0.0                                                       LRM01950
        DO 395 I=1,J                                                    LRM01960
        RHOP(I)=RHOP(I)-DELTA                                           LRM01970
        RHO(I)=RHO(I)-DELTA                                             LRM01980
        PPER(I)=APER(I)/(J*(1.0-THETAP*(RHOP(I)-SHIM)))                 LRM01990
        PINT(I)=AINT(I)/(J*(1.0-THETAI*RHO(I)))                         LRM02000
        F(I)=PPER(I)+PINT(I)                                            LRM02010
        FSUM1=FSUM1+F(I)                                                LRM02020
  395 CONTINUE                                                          LRM02030
C                                                                       LRM02040
C                                                                       LRM02050
        FPER=0.0                                                        LRM02060
        DO 396 I=1,J                                                    LRM02070
        FPER=FPER+PPER(I)/FSUM1                                         LRM02080
  396 CONTINUE                                                          LRM02090
C                                                                       LRM02100
        RHOSYS=0.0                                                      LRM02110
        DO 397 I=1,J                                                    LRM02120
        PPER(I)=PPER(I)/FSUM1                                           LRM02130
        PINT(I)=PINT(I)/FSUM1                                           LRM02140
        RHOSYS=RHOSYS+(PPER(I)*(RHOP(I)-SHIM) + PINT(I)*RHO(I))         LRM02150
  397 CONTINUE                                                          LRM02160
C                                                                       LRM02170
C                                                                       LRM02180
        IF (RHOSYS.LE.0.0001)   GOTO 417                                LRM02190
        IF (RHOSYS.GT.0.0001)   GOTO 392                                LRM02200
C                                                                       LRM02210
C                                                                       LRM02220
C                                                                       LRM02230
  410 DO 415 I=1,J                                                      LRM02240
        B(I)=B(I)-F(I)*TSTEP                                            LRM02250
```

```
      FA(I)=FA(I)-F(I)*TSTEP                          LRM02260
415 CONTINUE                                          LRM02270
      FAP=FAP-FPER*TSTEP                              LRM02280
C                                                     LRM02290
      ADD=ADD-TSTEP                                   LRM02300
      TSTEP=TSTEP/2.0                                 LRM02310
C                                                     LRM02320
C                                                     LRM02330
417 DO 420 I=1,J                                      LRM02340
      B(I)=B(I)+F(I)*TSTEP                            LRM02350
      FA(I)=FA(I)+F(I)*TSTEP                          LRM02360
420 CONTINUE                                          LRM02370
      FAP=FAP+FPER*TSTEP                              LRM02380
      ADD=ADD+TSTEP                                   LRM02390
      GOTO 330                                        LRM02400
C                                                     LRM02410
C                                                     LRM02420
460   CONTINUE                                        LRM02430
540 IF (J.EQ.1)   GO TO 560                           LRM02440
C                                                     LRM02450
C     CHECK FOR CONVERGENCE AT CYCLE END-POINTS       LRM02460
C                                                     LRM02470
550 DO 560 I=1,JLESS                                  LRM02480
      M=I+1                                           LRM02490
      TELL=B(I)-DONE(M)                               LRM02500
      IF (DABS(TELL).GT.CONVRG) GO TO 210             LRM02510
560 CONTINUE                                          LRM02520
C                                                     LRM02530
210 CONTINUE                                          LRM02540
      FAVGS=0.0                                       LRM02550
      FPAVGS=FAP/ADD                                  LRM02560
      DO 211 I=1,J                                    LRM02570
      FAVG(I)=FA(I)/ADD                               LRM02580
      FAVGS=FAVGS+FAVG(I)                             LRM02590
211 CONTINUE                                          LRM02600
      DO 2110 I=1,J                                   LRM02610
      FAVG(I)=FAVG(I)/FAVGS                           LRM02620
2110 CONTINUE                                         LRM02630
      FPAVGS=FPAVGS/FAVGS                             LRM02640
      IF(N.EQ.2) GOTO 212                             LRM02650
      NUMB = NUMB + 1                                 LRM02660
      WRITE(6,3070)NUMB                               LRM02670
      RHOL=SHIM*FPAVGS                                LRM02680
      WRITE(6,3095) FPAVGS,RHOL                       LRM02690
      WRITE(6,3090) (B(I),I=1,J)                      LRM02700
```

```
            WRITE (6,3100) (FAVG(I),I=1,J)                               LRM02710
        212 IF(DABS(TELL).LE.CONVRG) GO TO 990                          LRM02720
      C                                                                  LRM02730
      C                                                                  LRM02740
      C        REINITIALIZE AND UPDATE BOC POINTS                        LRM02750
      C                                                                  LRM02760
      C                                                                  LRM02770
            DO 213 I=1,J                                                 LRM02780
            FA(I)=0.0                                                    LRM02790
        213 CONTINUE                                                     LRM02800
            FAP=0.0                                                      LRM02810
                                                                         LRM02820
            ADD=0.0                                                      LRM02830
            TSTEP = STORE                                                LRM02840
            S=0.0                                                        LRM02850
        220 DO 230    I=1,J                                              LRM02860
            L=I-1                                                        LRM02870
            IF (I.NE.1)   DONE(I)=B(L)                                   LRM02880
        230 CONTINUE                                                     LRM02890
            GO TO 190                                                    LRM02900
      C                                                                  LRM02910
        990 IF (N.EQ.1) GOTO 999                                        LRM02920
            BDELTA=DABS(B(1)-BI)                                         LRM02930
            NUMB=NUMB+1                                                  LRM02940
            WRITE(6,3070) NUMB                                           LRM02950
            WRITE(6,3090) (B(I),I=1,J)                                   LRM02960
            WRITE(6,3100) (FAVG(I),I=1,J)                                LRM02970
            WRITE (6,3090)BI                                             LRM02980
            IF (BDELTA.LE.50.0) GOTO 999                                LRM02990
            BI=BI+BDELTA/5.0                                            LRM03000
            GOTO 118                                                     LRM03010
      C                                                                  LRM03020
        999 WRITE(6,4060)                                               LRM03030
            READ(5,2020)NNNN                                            LRM03040
      C                                                                  LRM03050
      C     NNNN=0: STOP                                                 LRM03060
      C     NNNN=1: NEXT CASE                                            LRM03070
      C                                                                  LRM03080
            IF(NNNN.EQ.0) GOTO 919                                      LRM03090
            IF(NNNN.EQ.1) GOTO 10                                       LRM03100
            GOTO 999                                                     LRM03110
        919 STOP                                                         LRM03120
      CCCCCCCCCCCCCCCCCCCCCCCCCCCCCCCCCCCCCCCCCCCCCCCCCCCCCCCCCCCCCCCCCCC  LRM03130
      C                                                               C   LRM03140
      C        FORMATS FOR INPUT AND OUTPUT STATEMENTS                C   LRM03150
```

```
C                                                                       LRM03160
CCCCCCCCCCCCCCCCCCCCCCCCCCCCCCCCCCCCCCCCCCCCCCCCCCCCCCCCCCCCCCCCCCCCCCC  LRM03170
2000 FORMAT(8X,I2,2F10.5)                                                LRM03180
2010 FORMAT(F10.5,E10.5)                                                 LRM03190
2020 FORMAT(3X,I2)                                                       LRM03200
2030 FORMAT(F10.5,E10.2)                                                 LRM03210
2035 FORMAT(F10.2)                                                       LRM03220
2040 FORMAT(8X,I2,F10.5)                                                 LRM03230
2050 FORMAT(8F10.5)                                                      LRM03240
3000 FORMAT(1X///4X,' THE VALUES OF BATCH BURNUP B(I) IN MWD/MT,'/       LRM03250
     $      4X,' THE POISON BURNOUT POINT BI (EOC POINT),'/              LRM03260
     $      4X,' PERIPHERAL POWER REACTION, LEAKAGE REACTIVITY AND'/     LRM03270
     $      4X,' BATCH POWER FRACTION F(I) ARE ARRANGED IN'/             LRM03280
     $      4X,' THE FOLLOWING ORDER AFTER EACH ITERATION'///            LRM03290
     $      13X,4HPER,9X,4HRHO/                                          LRM03300
     $      13X,4HB(1),9X,4HB(2),9X,4HB(3),9X,4HB(4),9X,4HB(5),          LRM03310
     $      6X,3HETC/13X,4HF(1),9X,4HF(2),9X,                            LRM03320
     $      4HF(4),9X,4HF(5),6X,3HETC/13X,3HB1////                       LRM03330
3070 FORMAT(/3X,I3,2X,F10.4                                              LRM03340
3080 FORMAT(5X,F10.2,5X)                                                 LRM03350
3090 FORMAT(5X,8(3X,F10.1))                                             LRM03360
3095 FORMAT(5X,2(3X,F10.5))                                             LRM03370
3100 FORMAT(5X,8(3X,F10.4)/1H )                                          LRM03380
4000 FORMAT(1X//,' INPUT NUMBER OF BATCHES, BURNUP INCREMENT(MWD/MT),'/  LRM03390
     $      ' AND CONVERGENCE CRITERION.'/                              LRM03400
     $      ' FORMAT(8X,I2,2F10.4)'/)                                    LRM03410
4005 FORMAT(1X//,' INPUT INTERIOR THETA AND PERIPHERAL THETA'/           LRM03420
     $      ' FORMAT(2F10.5)'/)                                          LRM03430
4010 FORMAT(1X//,' INPUT RHO INTERCEPT AND SLOPE OF TRACE.'/             LRM03440
     $      ' FORMAT(F10.5,E10.5)'/)                                     LRM03450
4020 FORMAT(1X//,' WITH SOLUBLE POISON ONLY: INPUT 1'/                   LRM03460
     $      ' WITH BURNABLE POISON  :  INPUT 2'/                         LRM03470
     $      ' FORMAT(3X,I2)'/)                                           LRM03480
4025 FORMAT(1X//,' CONSTANT REACTIVITY IN CYCLE 1 : '/                   LRM03490
     $      ' INPUT POISON BURNOUT POINT(PBP)'/                          LRM03500
     $      ' CODE WILL OPTIMIZE PBP TO MATCH EOC POINT'/                LRM03510
     $      ' FORMAT(10.2)'/)                                            LRM03520
4030 FORMAT(1X//,' SLOPE REACTIVITY IN CYCLE 1 : '/                      LRM03530
     $      ' INPUT BOL RHO AND POISON BURNOUT POINT(PBP)'/              LRM03540
     $      ' CODE WILL OPTIMIZE PBP TO MATCH EOC POINT'/                LRM03550
     $      ' FORMAT(F10.5,F10.2)'/)                                     LRM03560
4035 FORMAT(1X//,' BURNABLE POISON CASE:'/                               LRM03570
     $      ' FOR CONSTANT REACTIVITY IN CYCLE 1, INPUT 1'/              LRM03580
     $      ' FOR SLOPE REACTIVITY IN CYCLE 1, INPUT 2'/                 LRM03590
     $      ' FORMAT(3X,I2)'/)                                           LRM03600
```

```
4040 FORMAT(1X//' USING FIXED POISON SHIM OVER A CYCLE OR'/                    LRM03610
     $          ' MODEL LEAKAGE EXPLICITLY: INPUT 1'/                           LRM03620
     $          ' IF NEITHER: INPUT 2'/                                         LRM03630
     $          ' FORMAT(3X,I2)'/)                                              LRM03640
4041 FORMAT(1X//' INPUT AMOUNT OF SHIM POISON OR LEAKAGE'/                      LRM03650
     $          ' COEFFICIENT: ALPHA'/                                          LRM03660
     $          ' FORMAT(F10.5)'/)                                              LRM03670
4043 FORMAT(1X//' INPUT FRACTION OF BATCH (I) IN PERIPHERY OR'/                 LRM03680
     $          ' FRACTION OF BATCH WITH SHIM POISON: I=1,2,..,N '/             LRM03690
     $          ' FORMAT(8F10.5)'/)                                             LRM03700
4044 FORMAT(1X//' INPUT FRACTION OF BATCH (I) IN INTERIOR OR'/                  LRM03710
     $          ' FRACTION OF BATCH WITHOUT SHIM: I=1,2,...,N '/                LRM03720
     $          ' FORMAT(8F10.5)'/)                                             LRM03730
4060 FORMAT(1X//' END OF COMPUTATION'////                                       LRM03740
     $          ' FOR THE NEXT CASE, INPUT 1'/                                  LRM03750
     $          ' FOR END OF COMPUTATION, INPUT 0'/                             LRM03760
     $          ' FORMAT(3X,I2)'/)                                              LRM03770
     END                                                                        LRM03780
```

TABLE C.3

SAMPLE PROBLEM

```
 FORTGI DISBURN
G1 COMPILER ENTERED
 ISOURCE ANALYZED
PROGRAM NAME = MAIN
*  NO DIAGNOSTICS GENERATED
R; T=1.29/1.65 15:26:24

.GLOBAL TXTLIB FORTMOD2
R; T=0.01/0.02 15:26:35

.LOAD DISBURN
R; T=0.09/0.20 15:26:47

.START
EXECUTION BEGINS...


INPUT NUMBER_OF_BATCHES, BURNUP_INCREMENT(MWD/MT),
AND CONVERGENCE CRITERION.
FORMAT(8X,I2,2F10.4)

.         3      100.0       20.0


INPUT INTERIOR THETA AND PERIPHERAL THETA
FORMAT(2F10.5)

.         1.5         1.5
```

```
INPUT RHO_INTERCEPT AND SLOPE OF TRACE.
FORMAT(F10.5,E10.5)


.     0.2235 0.9272E-5



WITH SOLUBLE POISON ONLY: INPUT 1
WITH BURNABLE POISON     : INPUT 2
FORMAT(3X,I2)


.     2



BURNABLE POISON CASE:
FOR CONSTANT REACTIVITY IN CYCLE 1, INPUT 1
FOR SLOPE REACTIVITY IN CYCLE 1, INPUT 2
FORMAT(3X,I2)


.     2



SLOPE REACTIVITY IN CYCLE 1 :
INPUT BOL_RHO AND POISON BURNOUT POINT(PBP)
CODE WILL OPTIMIZE PBP TO MATCH EOC POINT
FORMAT(F10.5,F10.2)


.     0.0200    11000.0



USING FIXED POISON SHIM OVER A CYCLE OR
MODEL LEAKAGE EXPLICITLY: INPUT 1
IF NEITHER: INPUT 2
FORMAT(3X,I2)


.     1
```

INPUT AMOUNT OF SHIM POISON OR LEAKAGE
COEFFICIENT: ALPHA
FORMAT(F10.5)

.   0.1640

INPUT FRACTION OF BATCH (I) IN PERIPHERY OR
FRACTION OF BATCH WITH SHIM POISON: I=1,2,..,N
FORMAT(8F10.5)

.   0.0   0.0   0.667

INPUT FRACTION OF BATCH (I) IN INTERIOR OR
FRACTION OF BATCH WITHOUT SHIM: I=1,2,...,N
FORMAT(8F10.5)

.   1.0   1.0   0.333

THE VALUES OF BATCH BURNUP B(I) IN MWD/MT,
THE POISON BURNOUT POINT BI (EOC POINT) ,
PERIPHERAL POWER FRACTION, LEAKAGE REACTIVITY AND
BATCH POWER FRACTION F(I) ARE ARRANGED IN
THE FOLLOWING ORDER AFTER EACH ITERATION

B(1)	B(2)	B(3)	B(4)	B(5)	ETC
F(1)	F(2)	F(3)	F(4)	F(5)	ETC
BI					

1

11935.2	23554.1	32379.8
0.3683	0.3591	0.2726 .
11000.0		

2

11916.3	23557.9	32396.8
0.3677	0.3595	0.2728
11187.0		

3

11910.7	23562.1	32412.4
0.3673	0.3598	0.2729
11332.9		

4

11899.2	23567.7	32421.9
0.3669	0.3600	0.2730
11448.5		

5

11899.7	23573.9	32437.1
0.3667	0.3602	0.2731
11538.6		

6

11891.9	23571.8	32438.4
0.3664	0.3604	0.2732
11610.8		

7

11885.7	23569.7	32438.4
0.3662	0.3605	0.2732
11667.1		

8

11881.9	23577.4	32446.6
0.3661	0.3606	0.2733
11710.8		

9

11878.5	23583.6	32440.7
0.3660	0.3606	0.2733
11745.0		

10

11885.3	23583.5	32454.8
0.3659	0.3607	0.2733
11771.7		

11

11873.8	23583.3	32455.9
0.3659	0.3608	0.2734
11794.4		

```
12
        11872.1         23581.6         32460.9
         0.3658          0.3608          0.2734
        11810.3

13
        11871.1         23582.1         32467.4
         0.3658          0.3608          0.2734
        11822.7


END OF COMPUTATION



FOR THE NEXT CASE, INPUT 1
FOR END OF COMPUTATION, INPUT 0
FORMAT(3X,I2)

.     0
R; T=51.83/56.18 15:33:14

.
```

APPENDIX D

RESULTS OF 3 X 3 - FUEL BUNDLE PDQ-7 CALCULATIONS

The power split relation (derived from a $1\frac{1}{2}$ group diffusion theory model) for a two-region problem such as that shown in Fig. 3.8 of Chapter 3, can be written as

$$f_1 = \frac{(\frac{V_1}{V_2})\,(\frac{\overline{f}}{k_\infty})_2}{1 - \theta\rho_1} \tag{D.1}$$

where subscripts '1' and '2' correspond to the interior test assembly and the surrounding assemblies, respectively. Equation D.1 can be rearranged into a form through which the power split relation can be easily tested:

$$\frac{(\frac{V_1}{V_2})\,(\frac{\overline{f}}{k_\infty})_2}{f_1} = 1 - \theta\rho_1 \tag{D.2}$$

A series of two-group PDQ-7 calculations were performed for the assembly arrangement given in Fig. 3.8 of Chapter 3. Three successive constant values of k_2 (0.9, 1.0, 1.2) were employed, and the values of k_1 ($= \frac{1}{1-\rho_1}$) were varied over a wide range of enrichments, burnups, fuel-to-moderator ratios and boron concentrations. The basic assembly and pincell composition and configuration were those of the Maine Yankee Reactor (see Tables 2.3 and 2.4 of Chapter 2), and all cross sections were prepared using LEOPARD supercell computations.

Table D.1 lists the results of the analyses. These data
points were plotted in Fig. 3.10 of Chapter 3.

TABLE D.1

RESULTS OF PDQ-7 CALCULATIONS FOR 3 X 3 ROD BUNDLES

$$y = \frac{(\frac{V_1}{V_2})(\frac{\overline{f}}{k_\infty})_2}{f_2}$$

Variables	$x = \rho_1$	$k_2=1.2$	$k_2=1.0$	$k_2=0.9$
1a) Variation in Burnup, MWD/MT				
$(\varepsilon = 4.3$ w/o$)$				
150	0.2892	0.6870	0.6141	0.5631
10000	0.2295	0.7385	0.6619	0.6078
25000	0.1261	0.9126	0.8229	0.7584
1b) Variation in Burnup, MWD/MT				
$(\varepsilon = 3.0$ w/o$)$				
15000	0.0875	1.0313	0.9111	0.8638
25000	-0.0021	1.1970	1.0812	1.0033
35000	-0.0929	1.3532	1.2384	1.1531
2) Variation in Boron Concentration, PPM				
0	0.2515	0.7948	0.7139	0.6564
100	0.2425	0.8039	—	—
200	0.2335	0.8131	0.7309	0.6724
400	0.2157	0.8312	0.7479	0.6884
500	0.2068	0.8402	—	—
600	0.1979	—	0.7766	0.7044
800	0.1802	—	0.7817	0.7204
900	0.1714	0.8762	—	—

TABLE D.1 (continued

$$y = \frac{(\frac{V_1}{V_2}) \, (\overline{\frac{f}{k_\infty}})_2}{f_2}$$

Variables	$x = \rho_1$	$k_2 = 1.2$	$k_2 = 1.0$	$k_2 = 0.9$
3) Variation in Enrichment, w/o U-235				
4.3	0.2884	0.6893	0.6162	0.5650
4.0	0.2821	—	0.6333	0.5810
3.5	0.2684	0.7486	—	0.6162
3.0	0.2515	0.7948	0.7139	0.6564
2.5	0.2269	—	—	0.7157
2.0	0.1900	0.9610	0.8698	0.8036
4) Variation in Pitch, in.				
0.500	0.1922	0.8757	0.7903	0.7278
0.575	0.2494	0.7898	0.7160	0.6583
0.580	0.2515	—	—	0.6566
0.600	0.2680	0.7873	0.7074	—

*Unless stated, otherwise: fuel enrichment $\varepsilon = 3.0$ w/o U-235,

burnup point = 0 MWD/MT,

boron concentration = 0 PPM,

pitch = 0.580 in

APPENDIX E

RELATION OF POWER SHARING ALGORITHM TO NODAL METHODS

We have developed a power sharing prescription using the differential form of the neutron balance equation as a starting point. There has been considerable work in the past along similar lines starting from integral equation formulations— the classical 'nodal' approach (FLARE and its successors). Since both deal with the same phenomena, it should be possible to manipulate both into similar forms.

The general approach in FLARE-type calculations is as follows:

The neutron production rate, S_j, and absorption rate, A_j, in node j (part-of, or an entire assembly) are coupled by the multiplication factor, $k_{\infty j}$,:

$$S_j = \lambda^{-1} k_{\infty j} A_j \tag{E.1}$$

where λ is the eigenvalue needed to achieve system criticality.

Nodes are coupled by the kernel:

$$A_j = \sum_m W_{mj} S_m$$

$$\equiv \sum_{m \neq j} W_{mj} S_m + W_{jj} S_j \tag{E.2}$$

where W_{mj} is the probability that a neutron born at node m is

ultimately absorbed at node j.

Substituting A_j of Eq. E.2 into Eq. E.1, the source in node j is then

$$S_j = \lambda^{-1} k_{\infty j} \sum_{m \neq j} W_{mj} S_m + \lambda^{-1} k_{\infty j} W_{jj} S_j \qquad (E.3)$$

or

$$S_j = \frac{\lambda^{-1} k_{\infty j} \sum_{m \neq j} W_{mj} S_m}{1 - \lambda^{-1} k_{\infty j} W_{jj}} \qquad (E.4)$$

This is the basic FLARE equation.

Starting with Eq. E.4, consider a critical system, $\lambda \equiv 1.0$, and normalizing by total power, we obtain

$$f_j = \frac{k_{\infty j} \sum_{m \neq j} W_{mj} f_m}{1 - k_{\infty j} W_{jj}} \qquad (E.5)$$

But $k = 1/(1-\rho)$; thus

$$f_j = \frac{\sum_{m \neq j} W_{mj} f_m}{1 - W_{jj} - \rho_j} \qquad (E.6)$$

or

$$f_j = \frac{\sum_{m \neq j} \left(\frac{W_{mj}}{1 - W_{jj}} \right) f_m}{1 - \left(\frac{1}{1 - W_{jj}} \right) \rho_j} \qquad (E.7)$$

which has a numerator characterizing the "surroundings" and a denominator of the form "$(1 - \theta \rho_j)$". Equation E.7 is, there-

fore, similar in structure to the power split relation derived from the $1\frac{1}{2}$ group diffusion theory model in the present work: Eq. 3.46 of Chapter 3.

APPENDIX F

DATA FOR THE CASE OF FIXED POISON SHIM IN CYCLE J

An empirical expression for the ε factor for the case of fixed poison shim in cycle j has been formulated based on the results generated using the DISBURN code (see Table F.1). The formula is given by Eq. 4.12 in Chapter 4, and the plots for the data are shown in Figs. 4.12 through 4.16 in the same chapter. The following values were used in the computations:

extrapolated BOL reactivity, $\rho_0 = 0.22$

slope of the linear $\rho(B)$ curve $= 0.912 \times 10^{-5}$, MT/MWD

theta value $(\theta) = 1.5$

TABLE F.1

VALUES OF THE ε FACTOR FOR THE CASE OF FIXED POISON SHIM IN CYCLE J

Poison Shim Reactivity, $\Delta\rho$	ε Factor (DISBURN)					
	j = 1	j = 2	j = 3	j = 4	j = 5	j = 6
n = 2						
0.02	0.0574	0.0511	—	—	—	—
0.04	0.1113	0.0975	—	—	—	—
0.08	0.2315	0.1995	—	—	—	—
0.10	0.2986	0.2555	—	—	—	—
0.12	0.3706	0.3166	—	—	—	—
n = 3						
0.04	0.0777	0.0699	0.0638	—	—	—
0.08	0.1512	0.1347	0.1213	—	—	—
0.10	0.1894	0.1679	0.1508	—	—	—
0.12	0.2287	0.2023	0.1811	—	—	—
0.16	0.3080	0.2718	0.2440	—	—	—
n = 4						
0.04	0.0611	0.0557	0.0515	0.0482	—	—
0.08	0.1145	0.1027	0.0944	0.0874	—	—
0.10	0.1409	0.1269	0.1156	0.1068	—	—
0.12	0.1676	0.1509	0.1372	0.1269	—	—
0.16	0.2209	0.1992	0.1810	0.1668	—	—

Poison Shim Reactivity, $\Delta\rho$	ε Factor (DISBURN)					
	$j = 1$	$j = 2$	$j = 3$	$j = 4$	$j = 5$	$j = 6$
$n = 5$						
0.04	0.0509	0.0468	0.0438	0.0409	0.0389	—
0.10	0.1139	0.1027	0.0953	0.0886	0.0838	—
0.15	0.1632	0.1489	0.1372	0.1276	0.1196	—
0.20	0.2115	0.1933	0.1776	0.1653	0.1555	—
0.25	0.2575	0.2359	0.2177	0.2029	0.1905	—
$n = 6$						
0.04	0.0438	0.0404	0.0378	0.0358	0.0341	0.0327
0.10	0.0953	0.0872	0.0812	0.0759	0.0719	0.0686
0.15	0.1347	0.1238	0.1153	0.1075	0.1024	0.0972
0.20	0.1730	0.1591	0.1485	0.1390	0.1313	0.1251
0.25	0.2087	0.1929	0.1796	0.1683	0.1591	0.1515

REFERENCES

A-1   Andrews, J. B., et al., "Development of an Extended Burnup Mark B Design, First Semi-Annual Progress Report: July-December 1978," BAW-1546-1,(1979).

A-2   Adamsam, E. G., et al., "Computer Methods for Utility Reactor Physics Analysis," Reactor and Fuel-Processing Technology, Vol. 12, No. 2,(Spring 1969).

A-3   Amster, H. and Suarez, R., "The Calculation of Thermal Constants Averaged over a Wigner-Wilkins Flux Spectrum: Description of the SOFOCATE Code," WAPD-TM-39, (January 1957).

A-4   Atefi. B., "A Two-Lumped Fission Product Model for Fast Reactor Analysis," Trans. Am. Nucl. Soc., 38, 659-660, (June 1981)

B-1   Bowling, M. L. and Miller, J. G., "Core Design, Operation and Economics of 18-Month Fuel Cycles," Trans. Am. Nucl. Soc., 30, 279-280, (November 1978).

B-2   Bowling, M. L., Smith, M. L. and Franklin, C. B., "Development of a Fuel Management Scheme for Extended Burnup at VEPCO," Trans. Am. Nucl. Soc., 33, 392-393, (November 1979).

B-3   Barry, R. F., "LEOPARD—A Spectrum Dependent Non-Spatial Depletion Code," WCAP-3269-26, (September 1973).

B-4   Bohl, H., Gelbard, E. and Ryan, G., "MUFT-4-Fast Neutron Spectrum Code for the IBM-704," WAPD-TM-72, (July 1957).

B-5   Breen, R. J., "A One-Group Model for Thermal Activation Calculations," Nucl. Sci. Eng., 9, 91, (1961).

C-1   Correa, F., Driscoll, M. J. and Lanning, D. D., "An Evaluation of Tight-Pitch PWR Cores," MIT Energy Laboratory Report No. MIT-EL-79-022, (August 1979).

C-2   Coleman, T. A., et al., "Qualification of the B & W Mark B Fuel Assembly for High Burnup, First Semi-Annual Progress Report: July-December 1978," BAW-1546-1, (1979).

C-3   Chang, Y. I., et al., "Alternative Fuel Cycle Options: Performance Characteristics and Impact on Nuclear Power Growth Potential," RSS-TM-4, Argonne National Laboratory, Argonne, Illinois, (January 1977).

C-4 Chernick, J., "Status of Reactor Physics Calculations for U.S. Power Reactors," Reactor Technology, Vol. 13, No. 4, (Winter 1970-1971).

C-5 Cadwell, W. R., "PDQ-7 Reference Manual," WAPD-TM-678, (January 1967).

D-1 Driscoll, M. J., Fujta, E. K. and Lanning, D. D., "Improvement in PWRs on the Once-Through Fuel Cycle," Trans. Am. Nucl. Soc., 30, 280-281, (November 1978).

D-2 Driscoll, M. J., Lecture Notes, Subject 22.35: Nuclear Fuel Mangement, Dept. of Nucl. Eng., M.I.T., 1981.

D-3 Driscoll, M. J., Pilat, E. E. and Correa, F., "Routine Coastdown in LWRs as an Ore Conservation Measure," Trans. Am. Nucl. Soc., 33, 399, (November 1979).

E-1 Eich, W. J., "LWR Assembly Reaction Rate Representation," Presented at Conf. Nuclear Data Problems for Thermal Reactor Applications, Brookhaven National Laboratory, (May 22-24, 1978).

F-1 Fujita, E. K., Driscoll, M. J. and Lanning, D. D., "Design and Fuel Management of PWR Cores to Optimize the Once-Through Fuel Cycle," M.I.T. Energy Laboratory Report No. MIT-EL-78-017, (August 1978).

F-2 Flipot, A. J., et al., "Burnable Poison Dispersion in UO_2 Fuel," Nuclear Engineering International, Vol. 15, No. 167, (April 1970).

G-1 Garel, K. C., et al., "A Comparative Assessment of the PWR, SSCR, and PHWR Concepts," Trans. Am. Nucl. Soc., 30, 301, (November 1978).

G-2 Ghahramani, K. and Driscoll, M. J., "Ore Price Escalation in Fuel Cycle Economic Analyses," Trans. Am. Nucl. Soc., 28, 383-384, (June 1978).

G-3 Graves, H. W., Nuclear Fuel Management, John Wiley & Sons, Inc., (1979).

H-1 Hove, C. M., Robichaud, G. C. and Tulenko, J. S., "PWR Once-Through Fuel Cycle Improvements," Trans. Am. Nucl. Soc., 30, 275-276, (November 1978).

H-2 Hofman, P. L., Busselman, G. J. and Holeman, R. H., "Nuclear Characteristics of Some Compact, Water Moderated Plutonium Burners," HW-79977, (April 1964).

H-3   Harris, R. P., "Use of Gadolinium in PWR Extended Burnup
      Fuel Cycles," Interim Report, CEND-391, Combustion Engi-
      neering Power Systems, Windsor, Connecticut, (September
      1981).

H-4   Ho, A., "Design Evaluation of Westinghouse 15 x 15 Fuel
      Lumped Burnable Poison," PNE-FM-M-81-1, School of Nucl.
      Eng., Purdue University, (May 23, 1981).

J-1   Jonsson, A., Rec., J. R. and Singh, U. N., "Verification
      of a Fuel Assembly Spectrum Code Based on Integral Trans-
      port Theory," TIS-5815, Combustion Engineering Power Sys-
      tems, Windsor, Connecticut, (June 1978).

K-1   Kamal, A., "The Effect of Axial Power Shaping on Ore
      Utilization in Pressurized Water Reactors," S.M. Thesis,
      Dept. of Nucl. Eng., M.I.T., (January 1980).

K-2   Kamal, A., "The Selective Use of Thorium and Heteroge-
      neity in Uranium-Efficient Pressurized Water Reactors,"
      Ph.D. Thesis, Dept. of Nucl. Eng., M.I.T., (Expected,
      June 1982).

L-1   Lang, P. M., "Development of Improvements to the Light
      Water Reactor Fuel Cycle," Paper Presented at the ANS
      Fuel Cycle and Waste Management Division Topical Meeting
      on 'Technical Bases for Nuclear Fuel Cycle Policy,' at
      Newport, Rhode Island, (September 1981).

L-2   Lan, J. S., "Assessment of the Prevailing Physics Codes:
      LEOPARD, LASER, and EPRI-CELL," Trans. Am. Nucl. Soc.,
      38, 685-687, (June 1981).

L-3   Littlechild, J. E., Buttler, G. G. and Lester, G. W.,
      "The Production of Burnable Poison Oxide Fuel," Proc.
      Int. Conf. on Nuclear Fuel Performance, BSNE, No. 65,
      (October 1973).

M-1   Matzie, R. A., et al., "Uranium Resource Utilization Im-
      provements in the Once-Through PWR Fuel Cycle," CEND-
      380, Combustion Engineering Power Systems, Windsor,
      Connecticut, (April 1980).

M-2   MacNabb, W. V., "Two Near-Term Alternatives for Improved
      Nuclear Fuel Utilization," Trans. Am. Nucl. Soc., 33,
      398, (November 1979).

M-3   Momsen, B. F., "An Analysis of Plutonium Recycle Fuel
      Elements in San Onofre-1," Nucl. Eng. Thesis, Dept. of
      Nucl. Eng., M.I.T., (May 1974).

M-4   Mangulis, V., *Handbook of Series for Scientists and Engineers*, Academic Press, New York, (1965).

Q-1   Quan, B. L., Malone, J. P. and Pilat, E. E., "Yankee Atomic Experience with Coastdown," YAEC-1270, (May 1981).

R-1   Robbins, T., "Preliminary Evaluation of a Variable Lattice Fuel Assembly and Reactor Design Concept," Draft Report Under Subcontract No. 11Y13576V for Oak Ridge National Laboratory, Pickard, Lowe and Garrick, Inc., Washington, D.C., (February 1979).

S-1   Shapiro, N. L. and Lin, Y., "Improvement of Fuel Utilization for Once-Through PWR Cycles," *Trans. Am. Nucl. Soc.*, 30, 276-277, (November 1978).

S-2   Sefcik, J. A., Driscoll, M. J. and Lanning, D. D., "Analysis of Strategies for Improving Uranium Utilization in Pressurized Water Reactors," M.I.T. Energy Laboratory Report No. MIT-EL-80-132, (January 1981).

S-3   Sider, F. M., "An Improved Once-Through Fuel Cycle for Pressurized Water Reactors," TIS-6529, Combustion Engineering Power Systems, Windsor, Connecticut, (June 1980).

S-4   Smith, M. L., Franklin, C. B. and Schleicher, T. W., "Extended Burnup and Extended Cycle Design," *Trans. Am. Nucl. Soc.*, 34, 389-390, (June 1980).

S-5   Schweiger, R. G., "Managing Nuclear Fuel, A Special Report," POWER, (December 1969).

S-6   Spierling, H., "The Value of Recycle Plutonium in Pressurized Water Reactors," Ph.D. Thesis, Dept. of Nucl. Eng., M.I.T., (February 1972).

S-7   Solan, G. M., Handschuh, J. A. and Bergeron, P. A., "Maine Yankee Cycle 4 Design Report," YAEC-1171, (January 1979).

T-1   Turner, S. E., Elgin, W. J. and Mowery, A. L., "Historical Survey of U.S. LWR Fuel Utilization," *Trans. Am. Nucl. Soc.*, 33, 390-391, (November 1979).

W-1   Williamson, E. A., Terney, W. B. and Huber, D. J., "Interactive Fuel Management Using a CRT," *Trans. Am. Nucl. Soc.*, 30, 341, (November 1978).